MEDICAL UNIVERSITY OF VIENNA

Insights into mutant calreticulin driven MPN targeted therapies – Assessing monoclonal antibody immunotherapies and mapping cancer dependencies

Doctoral thesis at the Medical University of Vienna for obtaining the academic degree

Doctor of Philosophy (PhD)

Submitted by

Naga Sarada Achyutuni

Supervisor:
Robert Kralovics, PhD
CeMM Research Center for Molecular Medicine
of the Austrian Academy of Sciences
Lazarettgasse 14, AKH BT25.3
1090 Vienna, Austria

Vienna, 05/2021

Declaration

The following doctoral thesis is compiled in a cumulative format. It contains work that is in print in the American journal of hematology, which is Chapter 3.1 and an unpublished project that constitutes Chapter 3.2. The author of the thesis Sarada Achyutuni is a co-first author on the first manuscript and the work described in the thesis has been performed by the author in the research group of Dr. Robert Kralovics at CeMM Research Center for Molecular Medicine of the Austrian Academy of Sciences in Vienna, Austria.

Chapter 3.1 contains the manuscript published in *American Journal of Hematology*. Sarada Achyutuni*, Harini Nivarthi*#, Andrea Majoros, Eva Hug, Christina Schueller, Ruochen Jia, Cecilia Varga, Michael Schuster, Martin Senekowitsch, Dimitris Tsiantoulas, Anoop Kavirayani, Christoph J Binder, Christoph Bock, Oleh Zagrijtschuk and Robert Kralovics# (2021) Hematopoietic expression of a chimeric murine-human CALR oncoprotein allows the assessment of anti-CALR antibody immunotherapies *in vivo. American Journal of Hematology*
*Equal Contribution, #Corresponding authors

R.K. and H.N. conceived and designed the study, interpreted the data, and contributed to the manuscript writing. H.N. (mouse model generation, phenotyping, and bone marrow transplantation) and S.A. (transcriptome analysis, antibody treatment and ELISA) designed and performed the experiments, analyzed the data, and wrote the manuscript. A.M., R.J., C.S. and C.V. conducted specific experiments and analyzed the data. A. K. coordinated the histology processing and analyzed and interpreted the histopathology data. E.H. designed the ELISA assay. M.Sc. and M.Se contributed in processing the NGS samples and in analyzing the sequencing files. D.M., C.Bo. and C.Bi contributed to the intellectual input.

Chapter 3.2 contains unpublished data of genome-wide genetic perturbation screen in murine cell lines, sgRNA validation results and drug-based inhibition studies. The work was carried out by the author at CeMM – Research center for molecular medicine in the lab of Dr. Robert Kralovics.

"Still I Rise"

"You may write me down in history
With your bitter, twisted lies,
You may trod me in the very dirt
But still, like dust, I'll rise.

Just like moons and like suns,
With the certainty of tides,
Just like hopes springing high,
Still I'll rise.

You may shoot me with your words,
You may cut me with your eyes,
You may kill me with your hatefulness,
But still, like air, I'll rise"

- Maya Angelou

Table of Contents

ACKNOWLEDGEMENTS

I would like to thank my supervisor Dr. Robert Kralovics for providing me with the opportunity to do my doctoral studies in his laboratory at CeMM. I learned and profited a lot from his feedback, ideas, and thoughts on project direction. His enthusiastic and inquisitive morale plus a humane approach towards people was a pivotal driving force throughout my PhD. I would like to thank the members of my PhD committee Dr. Stefan Kubicek and Dr. Veronika Sexl for following my progress and providing me with valuable guidance.

I would also like to thank Harini Nivarthi who has been a constant support and a great mentor throughout my PhD journey. I am grateful for the scientific and intellectual input that she has provided over the last three years. She has been a kind and valuable guide through some tough times. I would also like to take a moment to thank my colleagues who made my transition into an international environment easier. Roland Jager, Ruochen Jia, Elisabeth Fuchs, Fiorella Schillick for the help, the feedback and wonderful atmosphere. I would like to thank Eva Hug, Erica Xu, Illaria Casetti and Felix Rosebrock from the Myelopro team. They brought in a kind energy to the lab meeting discussions.

I would like to thank the entire CeMM community for creating an incredible place to work and a great PhD program.

To my closest friends, Sneha Patibanda, Deepti Kundur & Divya Vani who have been my truest comrades, you have kept me grounded to my roots and thank you for being my constant cheerleaders. To my scientific alter-ego, Madhura Ketkar for being humble and awesome. To Soundarya and Susheel Ravinuthala, for timely invoking the Uchiha. To my new family in Vienna, Jana Block, Lennart Enders, Sejla Salic, Asma Farhat, Thorina Boenke, Martin Senekowitsch, Yiota Tsokkou and Cecilia Varga. Thank you for all the incredible experiences. I owe my gratitude to Solly Puthur, Lalita Gupta and Priya Srinivas, my teachers who have been an epitome of resilient force and inspiring many young girls like me to pursue their dreams.

To the two most important people in my life, my parents – Mahesh Kumar Achyutuni and Sreedevi Achyutuni. I owe my biggest gratitude, from being an amazing support system to fostering the ideology of living a life with purpose, to believing that my voice mattered and always encouraging to seek a sense of individuality in every goal, I dreamt and achieved so far. My brother – Varun Achyutuni for supporting and pushing me constantly to step out of my comfort zone. Thank you for encouraging me and making me feel loved.

ABBREVIATIONS

AA	Amino Acid
ADCC	Antibody Dependent Cell Mediated Cytotoxicity
ADCP	Antibody Dependent Cell Mediated Phagocytosis
AML	Acute Myeloid Leukemia
ATP	Adenosine Triphosphate
BM	Bone Marrow
BiTEs	Bi-specific T-cell Engager
BMT	Bone Marrow Transplant
BSA	Bovine Serum Albumin
Cas9	SpCas9/Streptococcus pyogenes
CDC	Complement Mediated Cytotoxicity
CLP	Common Lymphoid Progenitor
CMP	Common Myeloid Progenitor
CRISPR	Clustered regularly interspaced short palindromic repeats
CALR	Calreticulin
DNA	Deoxyribonucleic Acid
EPO	Erythropoietin
ET	Essential Thrombocythemia
ELISA	Enzyme Linked Immunosorbent Assay
ER	Endoplasmic Reticulum
FDA	Food and Drug Administration
FBS	Fetal Bovine Serum
GFP	Green Fluorescent Protein
GMP	Granulocyte Macrophage Progenitor
GO	Gene Ontology
GSEA	Gene-set Enrichment Analysis
GTP	Guanosine triphosphate
HSC	Hematopoietic Stem Cell
IFN	Interferon
IL	Interleukin
LSK	Lineage Negative c-Kit Positive Sca-1 Positive
LT-HSC	Long Term Hematopoietic Stem Cell
JAK2	Janus Kinase 2
K/O	Knock-out
mAb	Monoclonal Antibody

MEP	Megakaryocyte Erythroid Progenitor
MF	Myelofibrosis
MPN	Myeloproliferative Neoplasm
MPL	Thrombopoietin Receptor
mRNA	Messenger RNA
mTOR	Mechanistic Target of Rapamycin
mTORC1	Mechanistic Target of Rapamycin Complex 1
mTORC2	Mechanistic Target of Rapamycin Complex 2
mutCALR	mutant CALR
NGS	Next Generation Sequencing
NFKB	Nuclear Factor Kappa-Light-Chain Enhancer of Activated B cells
PB	Peripheral Blood
PBS	Phosphate Buffered Saline
Ph	Philadelphia Chromosome
PMF	Primary Myelofibrosis
PV	Polycythemia Vera
RA	Rheumatoid Arthritis
RBC	Red Blood Cell
Rheb	Ras Homolog enriched in Brain
RNA	Ribonucleic Acid
ROS	Reactive Oxygen Species
STAT	Signal Transducer and Activator of Transcription
sCALR	Secreted CALR
scFv	Single chain variable fragments
scRNA	single cell RNA
seq	Sequencing
sgRNA	single guide RNA
ST-HSC	Short Term Hematopoietic Stem Cell
TPO	Thrombopoietin
TPO-R	Thrombopoietin Receptor
TNF	Tumor Necrosis Factor
WBC	White Blood Cell
WHO	World Health Organization

ABSTRACT

Myeloproliferative Neoplasms (MPN) are characterized by an abnormal expansion of different myeloid lineages. Somatic mutations in JAK2, CALR and MPL predominantly drive the oncogenic program of the three classical MPN subtypes – Polycythemia vera (PV), essential thrombocythemia (ET) and primary myelofibrosis (PMF). Hyperactive JAK-STAT signaling is central to the molecular pathogenesis of MPN. In 2013, frameshift mutations were identified in the exon 9 region of the calreticulin gene and they contribute to 30-35% of the patients diagnosed with ET and PMF. These mutations result in the generation of a novel amino acid sequence at the C-terminal end of the oncoprotein (mutCALR). MutCALR associates with the thrombopoietin receptor and is presented on the cell surface as a complex. The presence of a novel peptide at the C-terminal end of all CALR mutations represents a *'bona fide'* tumor antigen, thereby presenting unique opportunities for immunotherapy. Currently, the treatment mode for MPN patients is focused on cytoreduction and improving survival outcomes. There aren't any curative therapeutic regimes.

In this thesis, we provide a proof of principle of an antibody-based immunotherapy approach to target CALR positive MPN in mice. We also map mutCALR gene dependencies that would provide insights into the development of small molecule-based inhibitors for treating CALR positive MPN.

To assess the success of potential immunotherapy approaches, we generated a hybrid murine-human oncoprotein mouse model expressing human del52 mutCALR exon 9 sequence under the endogenous mouse promoter. The CALR-del52 transgenic mice recapitulate the MPN phenotype and allowed us to use it for modeling potential immunotherapy regimens. mutCALR homozygous mice that were treated with a mAb targeted against the human mutant calreticulin showed reduced levels of platelets six hours post treatment. We observed that the stem cells were effectively targeted by the anti-mutCALR mAb in both spleen and bone-marrow compartment.

In a second project, we performed a genome-wide genetic perturbation screen using CRISPR-Cas9 in murine homozygous and heterozygous mutant CALR cell lines. We identified potential synthetic lethal interactions and tumor suppressor genes associated with mutCALR MPN disease progression. The major hits from the tumor suppressor gene (TSG) cohort were associated with negatively regulating the mTOR signaling pathway and positively regulating erythroid progression. The genes from the TSG cohort were individually knocked-out with sgRNA using CRISPR-Cas9 technology. The effect of loss-of-function (LOF) of these genes

in the murine cell lines was individually validated in a competition assay setup. Further, we explored the efficacy of mTOR inhibitors against positive regulators of mTOR and performed drug inhibition assays. We show that mTOR inhibitors diminish the proliferative potential of mutCALR cell lines.

We have contributed to the understanding of two key avenues that would aid in the development of targeted therapies against mutCALR. The immunotherapy approach using a monoclonal antibody targeting mutCALR reveals key challenges that the therapy would need to address in the clinics. The gene-dependency arc dissects the potential interconnection of a network that exists between mutCALR and mTOR pathway. Finally, both approaches would enable getting a better understanding of the disease plus establishing better therapeutic regimes for mutCALR positive patients.

ZUSSAMMENFASSUNG

Myeloproliferative Neoplasien (MPN) sind gekennzeichnet durch die krankhafte Vermehrung myeloischer Zellen. Die drei klassischen Subtypen umfassen die Polyzythämia vera (PV), die Essentielle Thrombozythämie (ET) und die Primäre Myelofibrose (PMF). Ihnen liegen zumeist Driver-Mutationen in den Genen JAK2, CALR und MPL zugrunde, die das maligne Wachstum der Tumorzellen vorantreiben. Ein hyperaktiver JAK-STAT Signalweg gilt als zentraler Pathomechanismus der MPN. Im Jahr 2013 wurden bei 30-35 % der Patienten mit ET und PMF Frameshift-Mutationen in Exon 9 des Calreticulin-Gens identifiziert. Diese Mutationen führen zur Bildung einer neuen Aminosäuresequenz am C-terminalen Ende des Onkoproteins (mutCALR). MutCALR assoziiert mit dem Thrombopoietin-Rezeptor und wird als Komplex auf der Zelloberfläche präsentiert. Das Vorhandensein eines neuartigen Peptids am C-terminalen Ende aller CALR-Mutationen stellt ein Bona-fide-Tumorantigen dar und bietet damit einzigartige Möglichkeiten für eine Immuntherapie.

Derzeit konzentriert sich die Behandlung von MPN auf die Zytoreduktion und die Verbesserung der Überlebenschancen der Patienten. Bisher ist keine Heilbehandlung verfügbar. In dieser Doktorarbeit erbringen wir den Grundsatzbeweis für einen Antikörper-basierten Immuntherapie-Ansatz zur Bekämpfung von CALR-positiven MPN in Mäusen. Außerdem kartieren wir mutCALR-Genabhängigkeiten, die Einblicke in die Entwicklung von niedermolekularen Inhibitoren zur Behandlung von CALR-positiven MPN geben.

Um den Erfolg potenzieller Immuntherapieansätze zu beurteilen, haben wir ein hybrides murin-humanes Onkoprotein-Mausmodell generiert, das die humane del52 mutCALR Exon 9 Sequenz unter dem endogenen Mauspromotor exprimiert. Die CALR-del52 transgenen Mäuse rekapitulieren den MPN-Phänotyp und ermöglichen somit die Verwendung als Modell potenzieller Immuntherapien. MutCALR homozygote Mäuse, die mit einem gegen den humanes mutCALR gerichteten mAb behandelt wurden, zeigten sechs Stunden nach der Behandlung reduzierte Thrombozytenwerte. Es wurde beobachtet, dass die Stammzellen sowohl in der Milz als auch im Knochenmark durch den anti-mutCALR-mAb wirksam angegriffen werden.

In einem zweiten Projekt , wir führten einen genomweiten genetischen Perturbationsscreen mit CRISPR-Cas9 in murinen Zellinien mit homozygoter oder heterozygoter CALR-Mutation durch. Wir identifizierten mögliche synthetische letale Wechselwirkungen und Tumorsuppressorgene, die mit dem Fortschreiten der mutCALR MPN-Krankheit assoziiert sind. Die wichtigsten Treffer aus der Gruppe der Tumorsuppressorgene (TSG) sind mit der negativen Regulierung des mTOR-Signalwegs und der positiven Regulierung der erythroiden Progression verbunden. Die identifizierten TSG wurden einzeln mit sgRNA unter Verwendung

der CRISPR-Cas9-Technologie ausgeknockt. Der Effekt des Funktionsverlustes dieser Gene in den murinen Zelllinien wurde individuell in einem Kompetitionsassay validiert. Weiterhin untersuchten wir die Wirksamkeit von Inhibitoren von positiven Regulatoren des mTOR Signalweges führten Inhibitionsassays durch. Wir konnten zeigen, dass mTOR-Inhibitoren das proliferative Potenzial von mutCALR-Zelllinien vermindern.

Diese Arbeit trägt zum Verständinis zweier wichtiger Wege bei, die bei der Entwicklung von gezielten Therapien gegen mutCALR helfen. Der Immuntherapie-Ansatz mit einem gegen mutCALR gerichteten mAb offenbahrt wichtige Herausforderungen in der Therapie. Die Untersuchung von Genabhängigkeiten zeigt die mögliche Verbindung zwischen mutCALR und dem mTOR-Signalweg. Letztlich tragen beide Ansätze zu einem besseren Verständnis der Krankheit bei und ermöglichen die Etablierung besserer Therapieschemata für mutCALR-positive Patienten.

1. INTRODUCTION

1.1 Myeloproliferative Neoplasms

Myeloproliferative Neoplasms (MPN) are a heterogenous group of clonal hematological disorders that are characterized by an abnormal hyperproliferation and accumulation of terminally differentiated myeloid cells. The term “Myeloproliferative neoplasm” was coined by Dameshek in 1951. According to WHO classification, MPN can be categorized into nine diagnostic units and polycythemia vera (PV), essential thrombocythemia (ET), primary myelofibrosis (PMF) are considered as the classical MPN subtypes (Tefferi and Vardiman, 2008). The three main subtypes are distinguished on variable parameters that are associated with the pathogenesis of the disease. Patients diagnosed with polycythemia vera have increased red cell mass, hematocrit and hemoglobin values which is a representative of involvement of the erythroid lineage. Megakaryocytic lineage hyperproliferation and high platelet counts in the peripheral blood are pathological features of patients diagnosed with essential thrombocythemia. Primary myelofibrosis is defined by the presence of fibrosis in the bone marrow that is further marked by the occurrence of extramedullary hematopoiesis. Both PV and ET can progress to PMF and all three can also transform into secondary acute myeloid leukemia (Nangalia *et al.*, 2019).

The identification of somatic disease driver mutations in JAK2, CALR and MPL became an important milestone in understanding MPN pathogenesis. These mutations constitutively activate the JAK-STAT signaling pathway which plays a central role in regulating hematopoiesis and expansion of various blood lineages. Moreover, in MPN, the hyperactivation of JAK-STAT signaling pathway occurs in a ligand-independent manner. In 2013, frameshift mutations were identified in the exon 9 region of the calreticulin gene (Klampfl *et al.*, 2013; Nangalia *et al.*, 2013). The exon 9 mutations result in the generation of a novel sequence at the C-terminus of the mutant protein (mutCALR) and this makes it a unique *bona fide* tumor antigen (M. O. Holmström *et al.*, 2018).

The research focus of this thesis is assessing and dissecting mutant CALR driven MPN targeted therapies. We explore two approaches – immunotherapy and mapping mutCALR gene dependencies. We assess the applicability and challenges of naked-antibody therapeutics targeted against mutCALR MPN in a murine transgenic model. We also dissect the different pathway networks that mutCALR MPN is dependent on and possibly expose a vulnerability that can be targeted. The first part of the introduction discusses an overview of the clonal evolution of PV, ET and PMF, further emphasizing on the disease driver mutations and the existing first line treatment regimes in clinics. The second part focuses on the CALR

mutations, their pathophysiology, hallmarks, and development of effective targeted therapies against the mutant protein. The last part enlists the existing transgenic models that can be used for mutCALR MPN disease-modeling.

1.2 Clonal Evolution of MPN

Hematopoiesis is a tightly regulated process that controls the expansion of distinctive blood cell lineages. The hematopoietic stem cell (HSC) populating the bone marrow surface during embryogenesis. Long term HSCs (LT-HSCs), short-term HSCs (ST-HSCs) and multipotent progenitors (MPPs) are precursor cell types of the bone marrow microenvironment. LT-HSCs are cells with high self-renewing properties that reconstitute the blood cells of an animal for its entire lifespan and ST-HSCs, which reconstitute the blood cells for a limited period. ST-HSCs differentiate into MPPs that differentiate into oligolineage-restricted progenitors. These progenitors mature and become committed to a distinctive blood lineage type. The blood cells either differentiate towards lymphoid or myeloid lineage, depending on the microenvironment cues. The common lymphoid progenitor gives rise to B cells, T cells and NK cells. The common myeloid progenitor (CMP) gives rise to GMPs, which in turn differentiate into monocytes, macrophages, and granulocytes. The CMP also differentiates to MEPs (megakaryocyte or erythroid progenitors) that eventually produce megakaryocytes and erythrocytes. While CMPs and CLPs can give rise to dendritic cells (Figure 1).

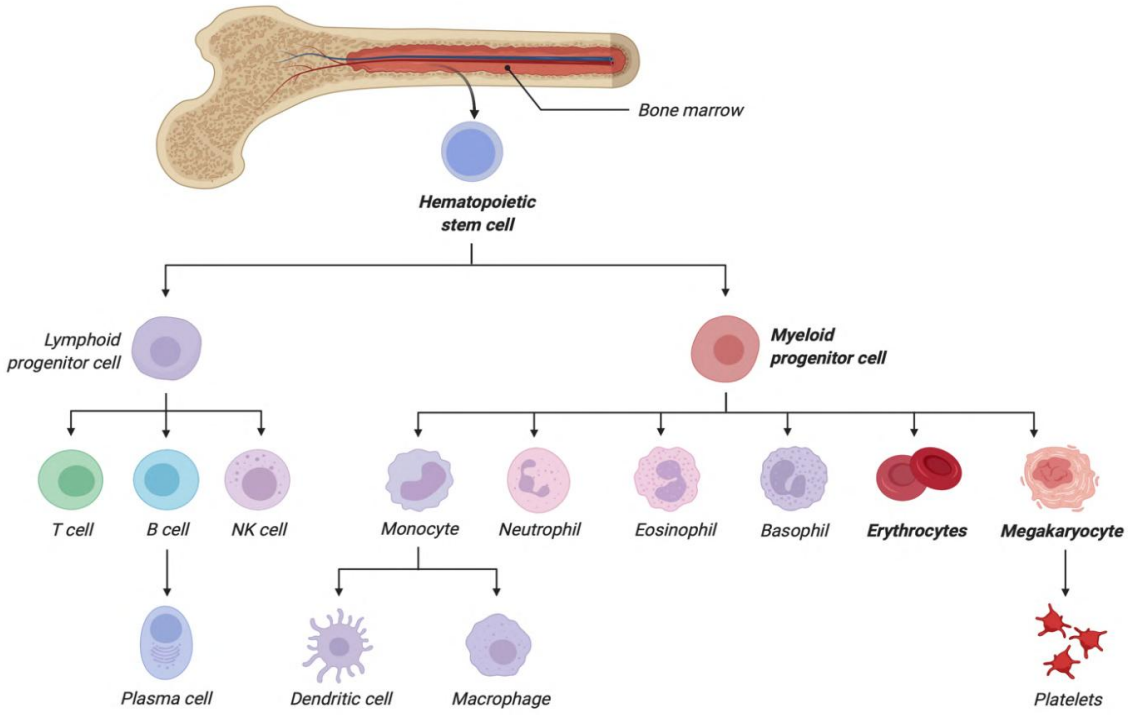

Figure 1: Clonal hematopoiesis in a healthy individual.

These various populations have distinctive cell surface markers, that makes them distinguishable. The bone marrow stroma plays a crucial role in the process of hematopoiesis where cytokines, chemokines and stromal cells support the cell maintenance and development (Rieger and Schroeder, 2012).

Bone marrow niche is governed by cues from major signaling pathways such as hedgehog, notch, Wnt and BMP along with matrix metalloproteases and multitude of adhesion molecules. There is an interplay between these components that maintains the hematopoietic stem cell pool in quiescent state and aids in blood production to supplement the loss of blood during infection or injury.

Mutations in the progenitor cells can provide them with a clonal advantage further contributing to an expansion of a subset of cells that promote clonal hematopoiesis. These mutations provide a proliferative advantage and lead to an excessive production of terminally differentiated cells.

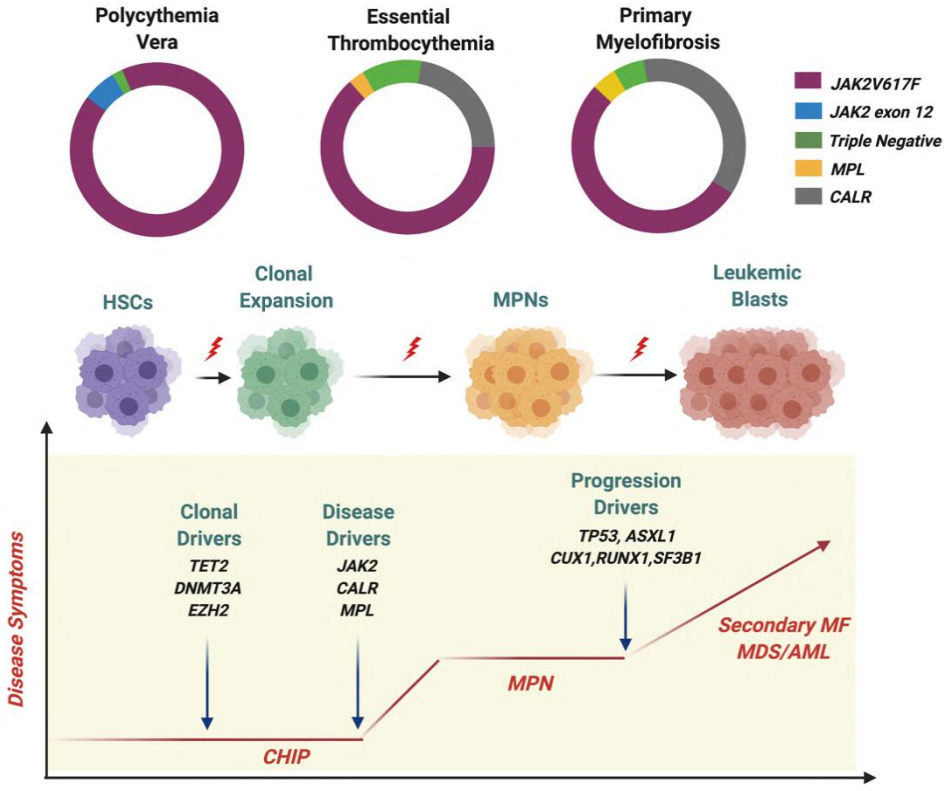

Figure 2: Clonal Evolution of MPN.

These mutations, particularly affecting the myeloid progenitors, give rise to the onset of myeloproliferative neoplasms (MPN) (Figure 2). Mutations can be categorized into three groups: 1) Clonal drivers: Mutations that lead to clonal hematopoiesis and not show a disease phenotype 2) Disease drivers: mutations that lead to clonal hematopoiesis and contribute to

disease development 3) Progression drivers: Mutations that lead to disease progression and further lead to transformation into leukemia or secondary myelofibrosis (Bowman, Busque and Levine, 2018).

MPNs are heterogeneously clonal and the sequence of acquisition of mutations can be inferred from the genotypes of detectable subclones. Clonal driver mutations in TET2, DNMT3A, EZH2 genes in HSCs result in clonal expansion of a subset of hematopoietic cells that carry a pre-disposed somatic mutation. The prevalence or acquisition of disease driver mutations in JAK2, CALR and MPL triggers the onset of MPNs. The accumulation of progression drivers in genes TP53, ASXL1, CUX1, RUNX1 and SF3B1 can lead to the transformation of MPNs to secondary PMF or acute myeloid leukemia (AML).

Classical MPN subtypes are classified into PV, ET and PMF (Figure 3). The very first case of myelofibrosis was reported in 1879, polycythemia vera in 1892 and essential thrombocythemia in 1934. Thrombocytosis is the prominent feature of patients diagnosed with essential thrombocythemia (ET). ET patients can also have either a normal or increased number of leukocytes at the diagnosis stage. Patients with polycythemia vera (PV) have an increased amount of red cell volume that is marked by the increased number of red blood cells.

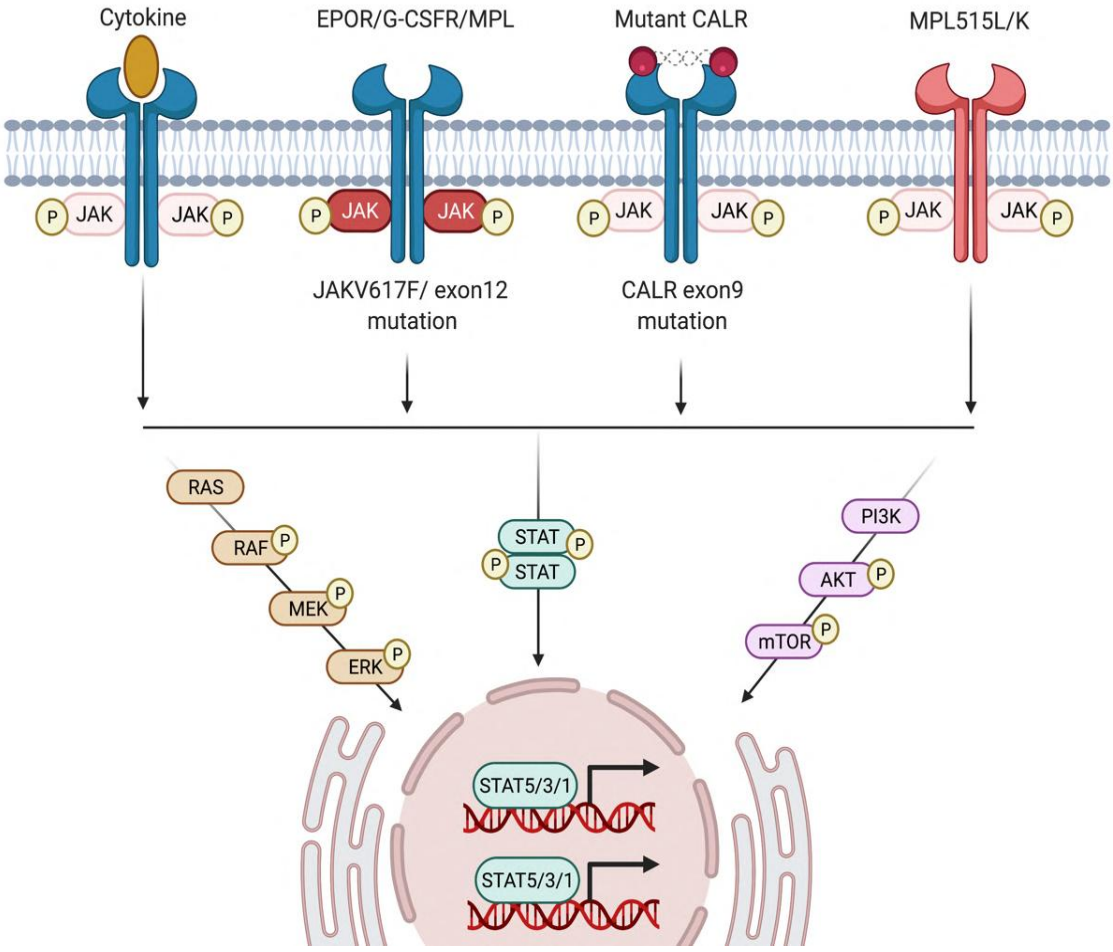

Figure 3: Central role of JAK kinases in the pathogenesis of MPNs.

These patients can also have either a normal or increased number of platelets or leukocytes. Cytopenia is often associated with patients diagnosed with Myelofibrosis (MF). These patients can also have an increased number of platelets and leukocytes. There is a significant scarring of bone marrow tissue because of reticulin fiber disposition leading to fibrosis.

Constitutional symptoms, chronic inflammation and splenomegaly are common among the three classical subtypes (Tefferi and Vardiman, 2008). The identification of point mutation in the JAK2 gene opened a new paradigm of understanding MPN disease progression. The point mutation leads to the substitution of phenylalanine for valine at position 617 - JAK2 V617F and results in the loss-of-function of the pseudokinase domain. JAK2 receptor is constitutively activated in a ligand independent manner.

The JAK2 V617F mutation is the most common, occurring in 97% of PV patients, 60% of both ET and MF patients. The discovery of JAK2 exon 12 mutations, MPL and CALR mutations filled the missing gap of mutations contributing to the disease pathogenesis. JAK2 exon 12 mutations occur in 2% of PV patients. Thrombopoietin receptor, MPL mutations occur in 5-10% of ET and MF patients. The calreticulin mutations contribute to 25-30% of ET and MF. Calreticulin is a chaperone that is known to be crucial in protein folding machinery and for maintaining calcium homeostasis in ER. Mutant calreticulin (mutCALR) can activate the MPL receptor directly, thus leading to a ligand independent constitutive activation of the JAK-STAT signaling pathway. As such, patients represent a gene expression profile that is associated with JAK/STAT signaling, further proving the pathway to be the major driver in MPN pathogenesis (Klampfl *et al.*, 2013; Nangalia *et al.*, 2013).

Either of the clonal driver mutation is necessary for the disease initiation and progression, but they never occur simultaneously in the same clone. However, they are acquired in a mutually exclusive manner. The timeline of acquisition of clonal, driver and progression driver mutations define the onset of MPN development and clinical outcome in patients. (Tefferi, 2010; De Roeck *et al.*, 2018; Reap *et al.*, 2020).

1.3 Mutations in CALR gene

In 2013, frameshift mutations were identified in the exon 9 region of the CALR gene. These mutations lead to the generation of a novel sequence at the C-terminal end of mutCALR protein. All mutations were categorized as insertions and/or deletions and exist largely in a heterozygous state. The two prominent ones that were identified are Type 1 (ins5) and Type 2 (del52). The frameshift mutations generate an alternate reading frame and in comparison, to wildtype CALR, mutCALR has a unique positive charge because of amino acid compositions, mainly substituted with arginine and methionine (Figure 4). The C-terminal end of the wildtype

protein comprises the ER retention signal (KDEL) which is crucial for the recycling of the chaperone in and out of ER. The mutations in the C-terminal end results in the loss of KDEL sequences which in turn, impacts the chaperone's shuttling ability and impairment of subcellular localization and calcium binding capacity. CALR mutations contribute to 20-25% in ET and 25-30% in PMF (Klampfl *et al.*, 2013; Nangalia *et al.*, 2013). In a study, BaF/3 cells with overexpression of the 52-bp deletion CALR mutant can proliferate in a cytokine-independent fashion. When these cells were treated with JAK2 inhibitor, it hindered their growth, implying that the JAK-STAT signaling is necessary for the ligand-independent proliferation of the cells. The mutant cells have also shown increased levels of STAT5 phosphorylation at protein level, as validated by western blotting. These results suggest the central dependency of mutCALR cells on the JAK-STAT signaling. The stratification of patients based on driver mutations revealed that mutCALR driven MPN patients have a more benign clinical outcome in comparison to MPN disorders driven by JAK2 or MPL mutations. Patients with CALR mutations have better overall survival with a reduced risk for thrombosis. These patients also have lower RBC and WBC counts than those of patients with JAK2 mutations (Klampfl *et al.*, 2013; Nangalia *et al.*, 2013).

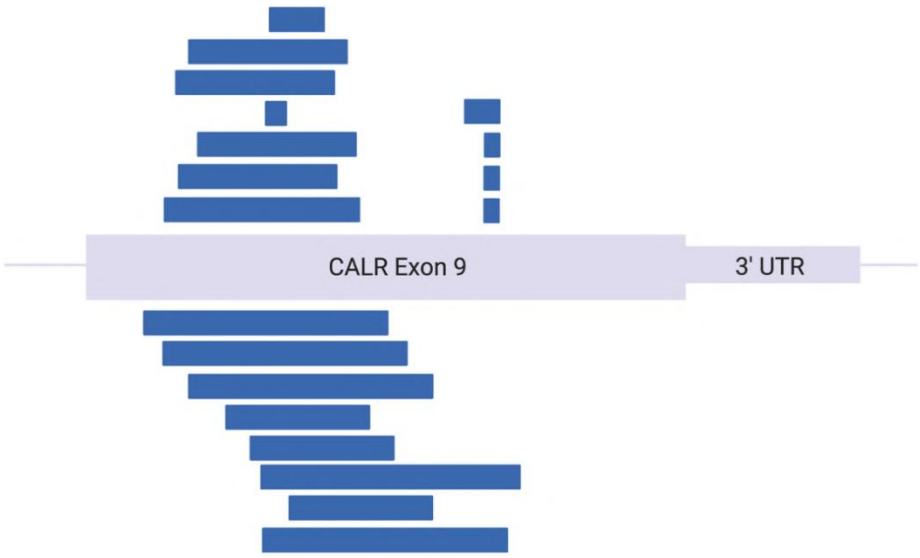

Figure 4: CALR exon9 mutations in MPN.

1.4 Molecular Pathophysiology of Mutant CALR driven MPN

Mutant calreticulin depends on the thrombopoietin receptor (MPL) for driving disease pathogenesis. In fact, both mutCALR and MPL activate STAT5 and BaF/3 cells are known to depend on MPL signaling for their growth. Further, MPL is mainly expressed in megakaryocyte lineage and this also confirms why CALR mutations are present in ET and PMF but not in PV

patients. Several studies have shed a light on understanding the molecular mechanism of mutCALR driven MPN pathophysiology. Mutant CALR associates with the thrombopoietin receptor via the partially N-glycosylated residues on the receptor, forming a complex. A glycan-deficient CALR del52 can impair this interaction and further the oncogenic signaling network, signifying the importance of this association. mutCALR is also known to undergo homo-multimerization through its mutant C-terminal end and binds to the thrombopoietin receptor as multimers. This interaction brings the homodimers of the thrombopoietin receptor in proximity, thereby activating the downstream transduction machinery in the absence of a ligand. There is a hyperactive JAK-STAT signaling pathway that drives the mutCALR driven MPN disease pathogenesis (Figure 5). This signal transduction in mutCALR cells initiates before the complex makes it to the cell surface. The overexpression of mutCALR del52 in BaF/3 cells is also known to make them growth-independent (Elf *et al.*, 2015; Araki *et al.*, 2016; Chachoua *et al.*, 2016; Marty *et al.*, 2016; Nivarthi *et al.*, 2016).

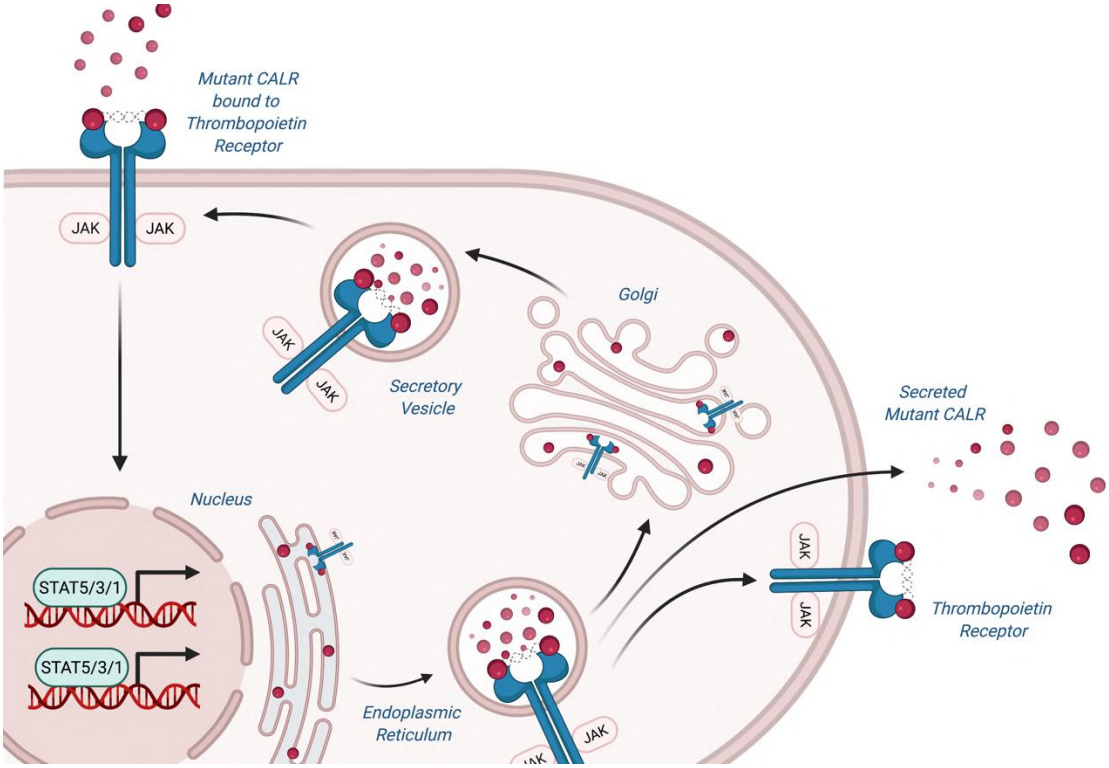

Figure 5: Mechanism of association of mutant chaperone with the thrombopoietin receptor and its cycling as a complex.

1.5 Hallmarks of mutant CALR driven MPN

The hallmarks of mutCALR driven MPN can be distinguished into five main categories. Hyperactive JAK-STAT signaling pathway and cytokine-independent growth of mutCALR cells

is one of the important hallmarks. Patients diagnosed with MPN have an increased number of platelets and megakaryocytes in their periphery (Andrikovics *et al.*, 2014). mutCALR is present in ET and PMF patients and association of the oncoprotein with the MPL receptor drives the abnormal expansion of the myeloid lineage. Another important characteristic is the presence of a secretory mutCALR epitope in the extracellular milieu. CALR exon 9 mutations lead to the generation of a novel sequence at the C-terminus and loss of the KDEL sequence. This loss of the retention signal leads to an impairment in the shuttling and recycling of the chaperone. Recent studies have quantified the presence of the secreted oncoprotein in patient plasma through immunological assays and western blotting (Han *et al.*, 2016; Pecquet *et al.*, 2019). Splenomegaly is another attribute of patients diagnosed with MPN with a persistent presence of reticulin deposition in the bone marrow – a sign of fibrosis (Curto-Garcia, Harrison and McLornan, 2020). Chronic inflammation is another hallmark of MPN phenotype.

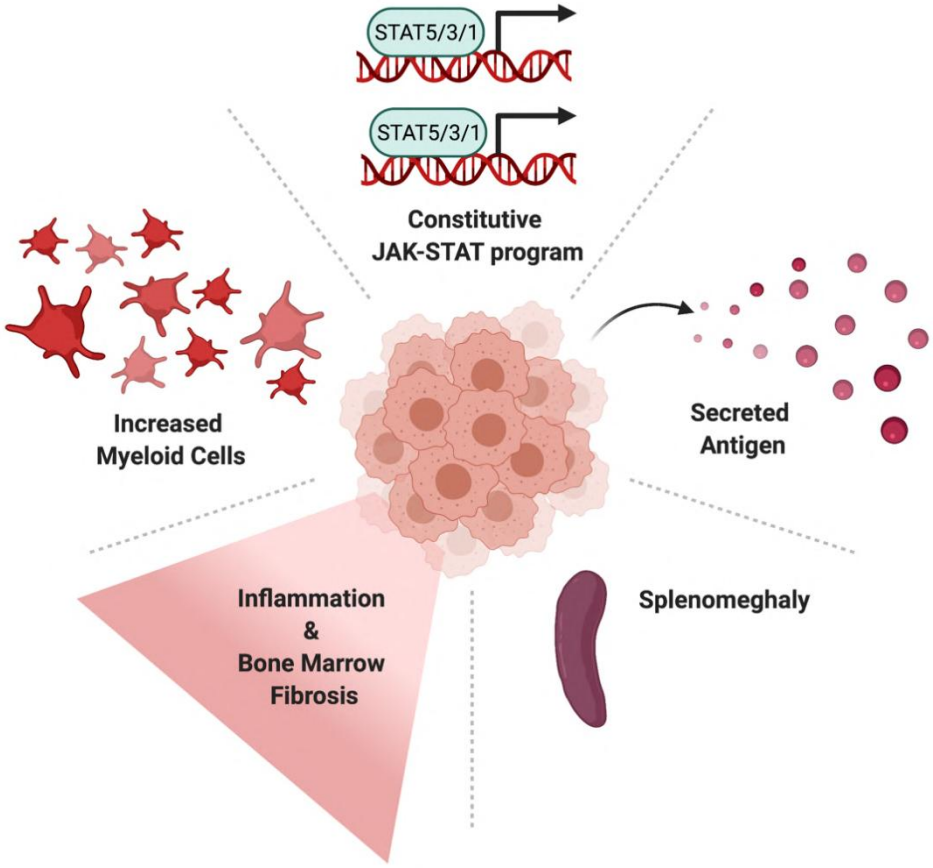

Figure 6: Hallmarks characteristics of MPN.

Most importantly, in the context of inflammation, there is substantial evidence of alteration of neutrophil ROS generation and alteration in serum inflammatory cytokine levels. JAKV617F mutated HSCs have a distinctive gene expression profile (Uras *et al.*, 2019). Constitutively active JAK-STAT signaling in mutant clone drives gene transduction recapitulating an

inflammatory signature. Recent studies highlight the secretion of TNF-α in the bone marrow microenvironment. It is known to reduce the proliferative activity of normal HSCs, but mutant HSCs are resistant to it. This inflammatory microenvironment can provide a proliferative advantage to the mutant clones and further contribute to remodeling the bone marrow microenvironment. There is a correlation between the implication of chronic inflammation on thrombosis and progression of MPN to secondary MF or AML (Fleischman *et al.*, 2011). Chronic inflammation coupled with hyperviscosity from elevated levels of RBC and WBC, along with altered vessel architecture combine all together to make thrombosis an issue for patients. The chronic inflammation also leads to the erosion of bone marrow, further depleting HSC numbers. This could also lead to the development of AML in these patients (Iurlo, Cattaneo and Gianelli, 2019) (Figure 6).

1.6 mutCALR MPN targeted therapies

The existing treatment management for MPN is focused on reducing the complications and there is a need for the development of better curative therapies. JAK-STAT signaling pathway plays a crucial role in molecular pathogenesis and the development of efficacious JAK2 inhibitors has been a major focus in the field of MPN treatment. Ruxolitinib, JAK1/2 inhibitor has been approved as a first line of therapy in MF patients. The drug targets the kinase domain of JAK1 and JAK2 but is not particularly against JAKV617F. The treatment with ruxolitinib is more focused on managing the symptoms and isn't curative.

It has been proven to reduce splenomegaly and constitutional symptoms in patients (Stein, Crispino and Moliterno, 2011; Soret and Kiladjian, 2016; M.H. *et al.*, 2017).

In some patients, long-term follow up studies have shown that ruxolitinib treatment mildly reduced mutant allelic burden and significantly contributed to better disease prognosis. Interferon-α is another candidate that has shown better response rates of hematological response and molecular remission in MPN patients. The toxicity and administration mode have been major bottlenecks as a first line treatment option. It also led to the development of ropeginterferon. This treatment is another alternative to cytoreductive treatment options for MPN (M.H. *et al.*, 2017; Kallam *et al.*, 2019).

There are still many challenges that are faced by the current line of treatments and there is a need to develop better regimes to treat mutCALR driven MPN. The main objective of the targeted therapy is to not only increase the overall survival but also reduce the allelic burden and effectively eliminate the mutant clone thriving in the niche. There are many ways by which this can be achieved: 1) Immunotherapy 2) Mapping cancer dependencies and 3) Mapping drug vulnerabilities (Li, Rampal and Xiao, 2019) (Figure 7).

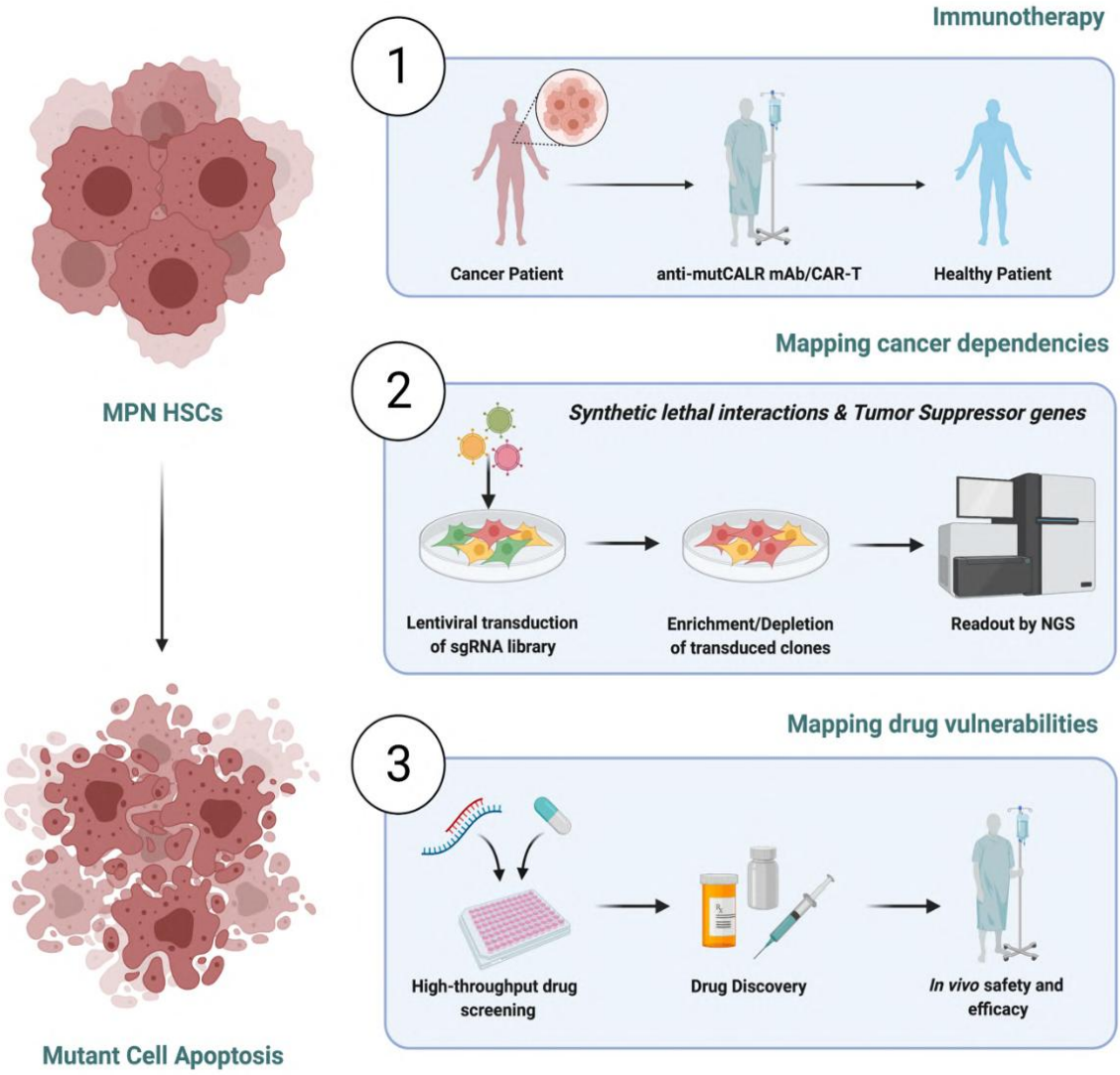

Figure 7: Insights into developing mutCALR MPN targeted therapies

1.6.1 Immunotherapy

CALR mutations are found in approximately 60% in patients with ET and PMF. There are more than 60 mutations that have been identified so far and all these mutations share a 34-AA consensus sequence in the C-terminus. The mutant protein via its C-terminus associates with the thrombopoietin receptor and sits on the cell surface as a complex. This C-terminus is a potential tumor-associated antigen that can be targeted with antibodies (Figure 8). Tumor-specific immune responses can be enhanced via targeted immunotherapy using monoclonal antibodies, therapeutic vaccines, CAR-T and BiTEs (Masarova, Bose and Verstovsek, 2019; Braun and Zeiser, 2020; Holmström, Hasselbalch and Andersen, 2020).

Immune surveillance systems usually profile and identify such rouge proteins, only to clear them out via several immunodepletion mechanisms. Cancer cells can evade the body's innate

immune system. This is another important hallmark of cancer (Hanahan and Weinberg, 2011; Fouad and Aanei, 2017).

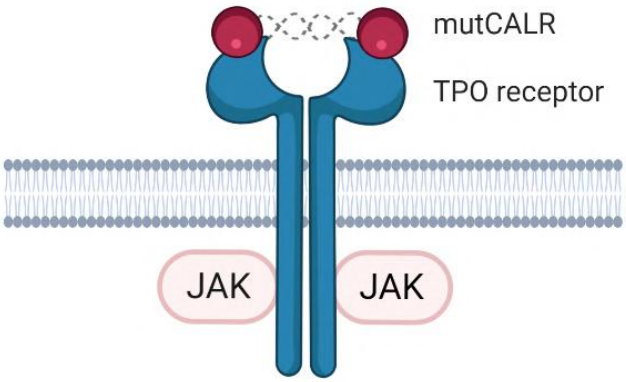

Figure 8: mutCALR associates with the TPO receptor

Antibodies induce broad effector mechanisms and are an important component of humoral immune response (Figure 9). They serve as a bridge between innate and adaptive immune systems. Antibodies are composed of two structural entities: 1) a variable fragment (Fab) that facilitates the interaction with the antigen or mutant epitope and 2) a constant region (Fc) that interacts with the Fc receptors on immune cells and initiates downstream effector mechanisms.

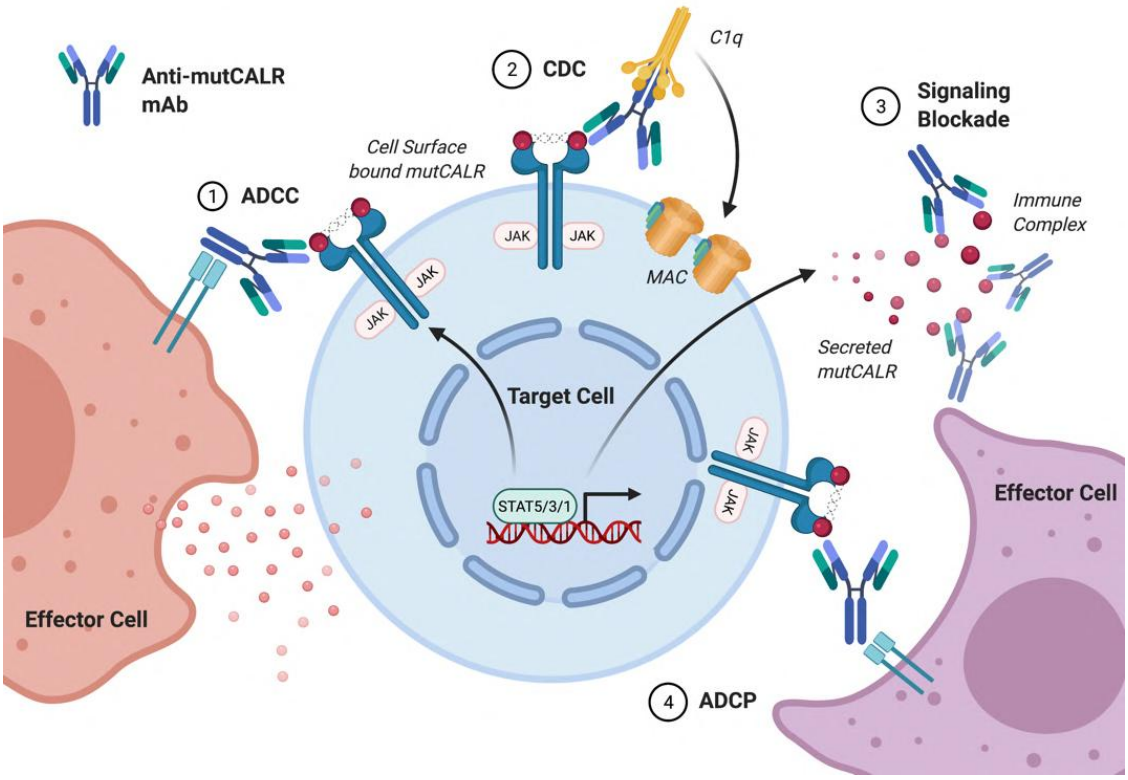

Figure 9: Antibody effector function mechanisms

The interaction with Fc receptors on immune cells is crucial as it mediates the killing of cancer cells or pathogen infected cells through various immune effector mechanisms (Van Erp *et al.*, 2019).

The constant Fc region of the antibody acts as a bridge in interacting with complement proteins in extracellular space or Fc receptors on many effector cell types. There are four known Fc-mediated antibody effector functions are antibody-dependent cell-mediated cytotoxicity (ADCC), antibody-dependent cellular phagocytosis (ADCP), complement-dependent cytotoxicity (CDC) or mediate the neutralizing effect on secreted antigen that acts as a decoy receptor. The last mechanism also helps the target cell evade immune system clearance (Lu *et al.*, 2018; Van Erp *et al.*, 2019).

1.6.2 Mapping cancer dependencies

There isn't much information regarding the regulatory networks that govern the mutCALR MPN progression. Another effective way is to map gene-gene dependencies that aid in driving the disease. The discovery of CRISPR-Cas9 has led to the development of genome-wide perturbation screens where one can potentially identify synthetic lethal interactions that are detrimental for tumor cell survival or tumor suppressor genes that further worsen the disease progression (Ran *et al.*, 2013; Zhou *et al.*, 2014; Hartenian and Doench, 2015). This can also aid in developing potential small molecule inhibitors that can be used for targeting downstream or upstream of identified targets. A cancer dependency map would give us deeper insights into specific gene axis that could impact the viability of mutant clones and how safe it would be to target this gene in MPN patients (McDonald *et al.*, 2017; Tutuncuoglu and Krogan, 2019).

1.6.3 Mapping drug vulnerabilities

High-throughput drug screening platforms can also be used to potentially identify and screen for potential small molecule inhibitors that target mutCALR cells. The identification of potential hits can be used to synthesize analogues that have increased potency against the mutant clones. These drugs or analogues can be further assessed for *in vivo* modeling and be scaled up for clinics (Scanlon, Dostal and Griswold, 2014; Menden *et al.*, 2017)

1.7 Modeling mutCALR driven MPN *in vivo*

With the discovery of CALR mutations in 2013, the focus has been shifted to the establishment of transgenic models that can be used to study the disease progression *in vivo*. To date, there have been four models that have been established.

A conditional Knock-in mouse expressing the mutant CALR del52 CDNA sequence was generated that develops a phenotype that resembles essential thrombocythemia. The heterozygous mice are characterized by an increased number of megakaryocytes with

morphologically distinct features, extramedullary hematopoiesis and but no reticulin fiber staining in either BM or spleen. Further, these mice also show signs of increased megakaryopoiesis and compromised erythropoiesis in the BM. Mice transplanted with heterozygous mutant bone marrow develop thrombocytosis with 60% mutant chimerism in myeloid and lymphoid lineages. The homozygous mice have a more penetrant phenotype that closely recapitulates PMF. Spleen and Bone Marrow compartments of these homozygous mice showed a positive staining for reticulin fibers, further confirming PMF like features. Both homozygous and heterozygous mice didn't show a competitive HSC advantage in serial transplantations. scRNA-seq of LSKs also revealed very little gene signature pattern as the analysis of the transcriptome was performed at the single cell level. Prominent gene-sets included pathways that were associated with cholesterol homeostasis and TNF-α signaling (Li *et al.*, 2018; Prins *et al.*, 2020).

Another group generated a knock-in model using CRISPR-Cas9 technology to modify the endogenous mouse locus, with two mutations del61 and del52. These mice exhibit essential thrombocythemia like phenotype and are characterized by elevated circulating platelets. The del52 mouse model is more penetrant than del61, with a significant and more elevated STAT5 activation. The del52 HSCs show a mild proliferative advantage over WT HSCs. These mice have an increased number of megakaryocytes in the bone marrow and the disease is transplantable. The phenotype is considered mild when compared to other existing models, because the human CALR mutant C-terminus is more oncogenic than that of mice CALR mutant C-terminus. Homozygous status of both mutations is embryonically lethal highlighting the functional role of CALR C-terminus crucial for the development of heart during embryogenesis (Balligand *et al.*, 2020).

A third plasmid-based transgenic model under the expression of MHC1 promoter which dissects the necessity of CALR in erythroid and megakaryocyte differentiation, further describes how CALR haplo-insufficiency augments stem cell activity and acts as a precursor for the development of MPN. The CALR deficient mice showed extramedullary hematopoiesis in the spleen and elevated platelet count. The mutant cells from these mice also have a clonal advantage over WT cells in a competitive BMT setup. The presence of haplo-insufficiency doesn't affect the severity of the disease, further restoring the functions of HSCs that were impaired by the CALRdel52 mutation. Gene expression analysis revealed pathways that are necessary for stem cell renewal, to be impaired in the LSKs of the haplo-insufficient mice and pathways that are crucial for MPN progression were enriched (Shide *et al.*, 2020).

In the fourth model, the mice generated are a conditional Knock-in with human mutant C-terminus expressing del52 and ins5 in a murine model. The phenotypic changes are more prominent for the del52 model over the ins5 model. These mice show splenomegaly, have

increased platelet and WBC counts, with significant decrease of number of cells in the bone marrow and increased numbers of megakaryocytes. Upon competitive bone marrow transplants, the mutant cells show a proliferative advantage. Homozygous mice show more enhanced phenotype with MF like phenotype with reticulin staining and presence of extramedullary hematopoiesis (Benlabiod *et al.*, 2020).

However, none of these mice have been used for the exploration or assessment of potential therapeutic targets against mutant CALR driven MPN.

2. AIMS

The main aim of this thesis is to develop novel mutCALR MPN targeted therapies. To generate a murine-human chimeric transgenic mouse model that provides a proof of concept for modeling and applicability of potential immunotherapeutic interventions. This will aid in gaining a deeper knowledge to understand mutCALR driven MPN disease mechanisms plus to identify potential challenges faced by immunotherapy regimes and further, in identifying regulatory networks aiding mutCALR driven MPN progression.

The specific aims were:

1) To generate a transgenic murine model that can recapitulate MPN phenotype
2) Develop and assess the success of anti-mutCALR mAb therapy *in vivo*
3) Identify the factors affecting naked-antibody immunotherapeutics
4) Perform a genome-wide genetic perturbation screen *in vitro* in murine mutant CALR cell lines
5) Identify list of synthetic lethal interactions and tumor suppressor genes

3. RESULTS

3.1 Manuscript #1: Hematopoietic expression of a chimeric murine-human CALR oncoprotein allows the assessment of anti-CALR antibody immunotherapies *in vivo*

Sarada Achyutuni, Harini Nivarthi, et al.

Published in ***American Journal of Hematology, 2021***

Somatic mutations in JAK2, MPL and CALR predominantly drive the pathological expansion of myeloid lineages contributing to the development of Myeloproliferative neoplasms (MPNs). Frameshift mutations in the exon 9 region of the calreticulin gene lead to the generation of a novel mutant C-terminus. This unique sequence is a *bona fide* tumor antigen and represents an attractive therapeutic target. Mutant CALR (mutCALR) associates with the thrombopoietin receptor and activates the JAK-STAT signaling pathway constitutively.

In this study, we generated a hybrid murine-human oncoprotein mouse model expressing human del52 mutCALR exon 9 sequence under the endogenous mouse promoter. These mice recapitulate human MPN marked by prominent thrombocytosis and megakaryocytosis. The mice also develop splenomegaly and the disease progression worsens with age. In a competitive bone marrow transplant setup, the mutCALR stem cells outgrow the wildtype stem cells showing a proliferative advantage. Differential gene expression profile of mutCALR stem cells revealed a gene-expression pattern concomitant with human MPN. mutCALR homozygous mice also have a significant amount of secreted CALR (sCALR) in plasma of their periphery.

To test our hypothesis that mutCALR mice can be used for modelling immunotherapeutic regimes, we treated mutCALR homozygous mice with a mAb targeted against the human mutant calreticulin. The treatment with ant-mutCALR mAb showed reduced levels of platelets six hours post treatment in the mice periphery. We observed that the stem cells were effectively targeted by the anti-mutCALR mAb in both spleen and bone-marrow compartment. We detected sCALR in the periphery and we also quantified immune complexes that are formed with the interaction of sCALR and anti-mutCALR mAb. Herein, we describe a murine model that reiterates MPN phenotype and provides a proof of concept that the mutCALR mice can be used for assessing anti-mutCALR immunotherapies *in vivo* (Achyutuni *et al.*, 2021).

Received: 1 February 2021 | Revised: 18 March 2021 | Accepted: 21 March 2021

DOI: 10.1002/ajh.26171

RESEARCH ARTICLE

AJH WILEY

Hematopoietic expression of a chimeric murine-human CALR oncoprotein allows the assessment of anti-CALR antibody immunotherapies in vivo

Sarada Achyutuni[1,2] | Harini Nivarthi[2] | Andrea Majoros[3] | Eva Hug[3] | Christina Schueller[1,2] | Ruochen Jia[1,2,3] | Cecilia Varga[1] | Michael Schuster[2] | Martin Senekowitsch[2] | Dimitris Tsiantoulas[1] | Anoop Kavirayani[4] | Christoph J Binder[1,2] | Christoph Bock[2] | Oleh Zagrijtschuk[3] | Robert Kralovics[1,2]

[1]Department of Laboratory Medicine, Medical University of Vienna, Vienna, Austria

[2]CeMM Research Centre for Molecular Medicine of the Austrian Academy of Sciences, Vienna, Austria

[3]MyeloPro Diagnostics and Research GmbH, Vienna, Austria

[4]Vienna Biocenter Core Facilities, Vienna, Austria

Correspondence
Robert Kralovics, Department of Laboratory Medicine, Medical University of Vienna, Währinger Gürtel 18-20, 1090 Vienna, Austria.
Email: robert.kralovics@meduniwien.ac.at

Harini Nivarthi, Adam-Betz-Gasse 22A/1, 1220, Vienna, Austria.
Email: niv.hari@gmail.com

Abstract

Myeloproliferative neoplasms (MPNs) are characterized by a pathologic expansion of myeloid lineages. Mutations in *JAK2*, *CALR* and *MPL* genes are known to be three prominent MPN disease drivers. Mutant CALR (mutCALR) is an oncoprotein that interacts with and activates the thrombopoietin receptor (MPL) and represents an attractive target for targeted therapy of CALR mutated MPN. We generated a transgenic murine model with conditional expression of the human mutant exon 9 (del52) from the murine endogenous *Calr* locus. These mice develop essential thrombocythemia like phenotype with marked thrombocytosis and megakaryocytosis. The disease exacerbates with age showing prominent signs of splenomegaly and anemia. The disease is transplantable and mutCALR stem cells show proliferative advantage when compared to wild type stem cells. Transcriptome profiling of hematopoietic stem cells revealed oncogenic and inflammatory gene expression signatures. To demonstrate the applicability of the transgenic animals for immunotherapy, we treated mice with monoclonal antibody raised against the human mutCALR. The antibody treatment lowered platelet and stem cell counts in mutant mice. Secretion of mutCALR did not constitute a significant antibody sink. This animal model not only recapitulates human MPN but also serves as a relevant model for testing immunotherapeutic strategies targeting epitopes of the human mutCALR.

1 | INTRODUCTION

The identification of *CALR* gene mutations has been a breakthrough towards understanding the molecular basis and diagnosis of patients with MPN. Type 1 (del52) and type 2 (ins5) mutations are the most recurrent mutations in MPN patients.[1,2] Mutant CALR (mutCALR) proteins induce ligand-independent activation of the thrombopoietin receptor (encoded by the *MPL* gene).[3-7] The mutCALR protein acts as a rogue chaperone and is known to stabilize the dimeric form of MPL.[8] Also, mutCALR cannot be recycled in endoplasmic reticulum (ER) as its wild type counterpart because of the absence of the KDEL residues at the C-terminus. Notably, mutCALR physically interacts

Sarada Achyutuni and Harini Nivarthi contributed equally to this study.

with the MPL receptor and is presented on the cell surface as a complex with MPL and it was also shown to be secreted into the extracellular milieu.[4,9] The mutant C-terminus of the protein serves as a bona fide neo-antigen, offering the possibility of developing immunotherapeutic strategies to target the oncoprotein.[10]

The alternative reading frame used by the human mutCALR oncoprotein displays a 60–70% homology to the murine *Calr* exon 9 alternative reading frame. Thus, potential therapeutic antibodies raised against the mutant C-terminus of human mutCALR may not necessarily recognize the mouse frameshifted sequence. Therefore, we aimed to generate a chimeric murine-human transgenic model that can be used for studying immunotherapeutic interventions targeting human mutCALR. To preserve the epitope composition of the mutant C terminus, we conditionally knocked-in the human exon 9 carrying the del52 mutation into the endogenous locus of the mouse *Calr* gene. The resulting mouse-human CALR-del52 chimeric oncogene recapitulated the MPN phenotype *in vivo*. Here in, we provide a proof of concept that the mutCALR murine transgenic model can be used to assess the *in vivo* efficacy of immunotherapeutic interventions using antibodies or their derivatives.

2 | MATERIAL AND METHODS

2.1 | Generation of conditional knock-in *CALR*-del52 transgenic mice

The *CALR*-del52 transgenic mice were generated by homologous recombination of embryonic stem cells in C57BL/6 mice (Ozgene, Perth, Australia). The targeting vector consisted of two *loxP* sites flanking the murine endogenous exons 8 and 9 with a poly A sequence, a PGK-neomycin selection cassette (flanked by Flp recombinase target FRT sequences) and a cDNA sequence of murine exon 8 ligated with the human exon 9 del52 with the endogenous murine 3' UTR. Embryonic stem cells were transfected with the targeting construct, selected with neomycin and the cells with homologous recombination were identified by Southern blotting. The targeted stem cells were then microinjected into C57BL/6 blastocysts to obtain chimeras that were bred with C57BL/6 mice to generate germline transmitting *CALR*-del52 conditional knock-in mice. The PGK-neo cassette was deleted using the OzFlp: Ubic-Flpe mice (Figure 1A). The conditional transgenic mice were bred with OZCre mice (PGK-cre in *ROSA26* locus) to generate germline heterozygous *CALR*-del52 mice. The germline knock-in mice did not survive past embryogenesis in the homozygous state. The mice were bred with *Vav*-iCre transgenic mice[11] for hematopoietic specific expression of *CALR*-del52.

2.2 | Animal experiments

The mice were housed and maintained under standard conditions and all experiments were performed in accordance with Austrian law under the animal experimentation license number BMWFW-66.015/0004-WF/V/3b/2016. The genotyping primers are listed in Table S1. Blood was obtained from *Vena facialis* and at end point by heart puncture. Blood parameters were measured using the animal blood counter scil Vet abc. The sternum and a part of the spleen were processed for histopathology. Single cell suspensions were made from the rest of the spleen and the bone marrow from the femurs and tibia and analyzed by flow cytometry.

2.3 | Enzyme-linked immunosorbent assay (ELISA) for quantification of secreted mutCALR

To quantify secreted mutCALR (sCALR) in murine and human sera, two antibodies against mutCALR were used – polyclonal antibodies against a 22-mer peptide derived from the mutCALR C-terminus in rabbits (capture antibody) and polyclonal antibodies against the recombinant CALR-ins5 protein in chicken (detection antibody). The rabbit anti-mutCALR specific polyclonal antibody (anti-mutCALRab - SAT601) was diluted in PBS at a concentration of 2 μg/mL and 50 μL was used to coat each well of a 96-well plate. The assay plates were incubated overnight at 4°C and later washed with wash buffer (0.05% Tween20 in PBS). Plasma samples from *vav*Cre, CALRdel52$^{fl/+}$;*vav*Cre (mutCALR^{het}), CALRdel52$^{fl/fl}$;*vav*Cre (mutCALR^{hom}), *CALR* mutated patients and healthy control were diluted 1:4 in the blocking buffer (2% BSA, 0.05% Tween20 in 1xPBS) and were added to the plates. The samples were incubated for 2 h at 30°C and later washed with wash buffer. Chicken anti-mutCALR polyclonal antibody was added to all the wells at a concentration of 0.5 μg/mL for 1 h at 30°C. Following washing of the plates, secondary antibody anti-chicken IgY-HRP was used in the assay (1:50 000) for 1 h at room temperature. The plates were then washed and developed with TMB for 5 min at room temperature. The absorbance was read at 450 and 620 nm using Spectra-Max i3 (Molecular Devices). Recombinant CALRdel52 and CALRins5 proteins (MyeloPro) were used as a standard to calculate the concentration of the samples.

2.4 | Anti-mutCALR antibody treatment of mice

The mice (3n) were injected intraperitoneally with 3 mg/kg of mouse IgG2a anti-mutCALR monoclonal antibody twice a day, for 2.5 days. The control group received an equal volume of the vehicle (PBS). Blood was obtained from *Vena facialis*. The end point analysis was performed as described above.

3 | RESULTS

3.1 | *CALR*-del52 transgenic mice express the mutant CALR protein and develop myeloproliferative disease

In the presence of Cre recombinase, the endogenous murine exon 9 of *Calr* is replaced by human del52 mutated exon 9 (Figure 1A). This

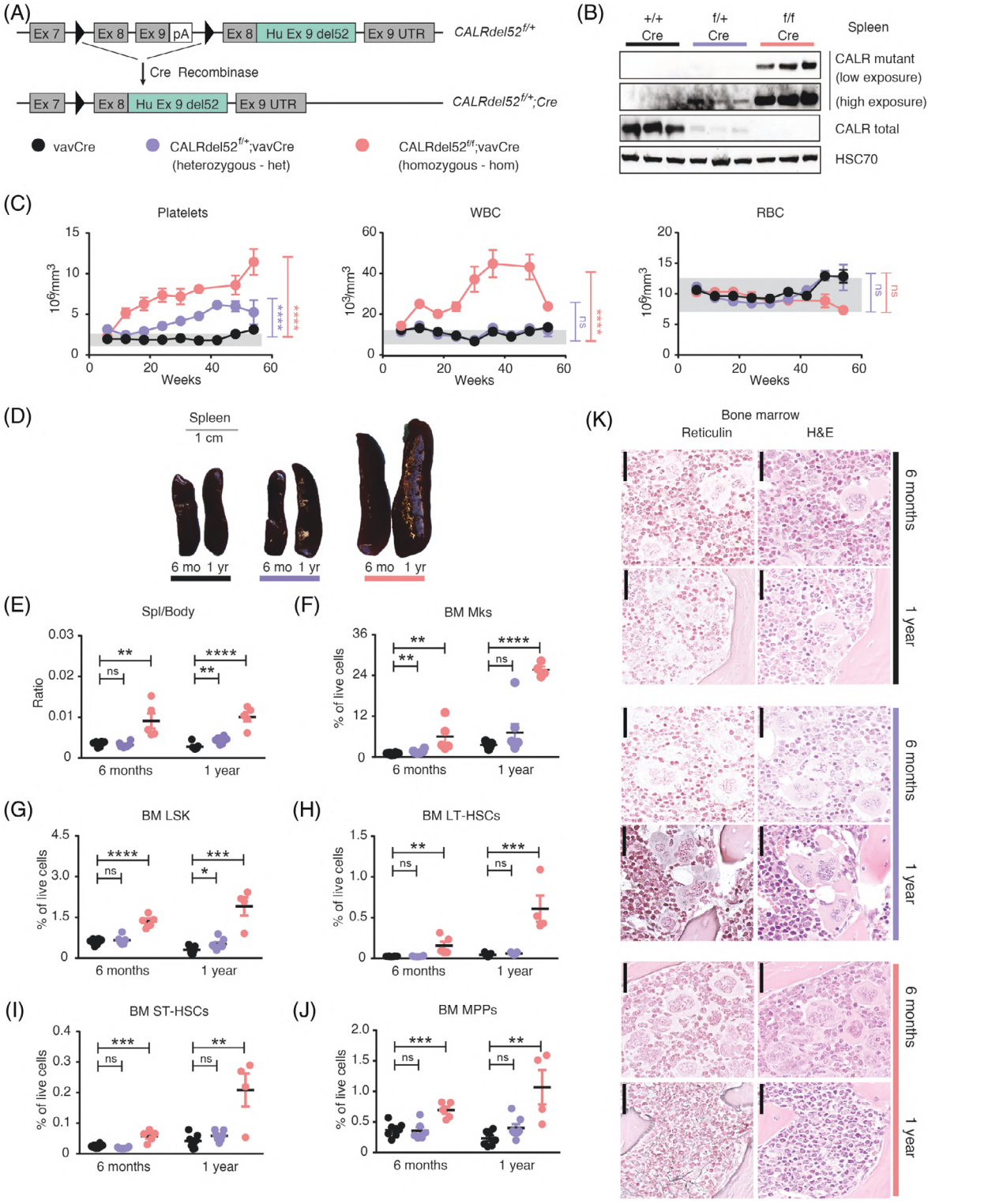

FIGURE 1 CALR mutant mice develop myeloproliferative disease. (A) Schematic representation of the transgenic *Calr* locus. (B) Western blot analysis of wild type and mutant CALR proteins (high and low exposure) from splenocytes of transgenic mice. (C) Peripheral blood counts of platelets, WBC and RBC from transgenic mice over time. (D) Representative images of spleens from transgenic mice at 6 months and 1 year of age. (E) Spleen to body weight ratio. Percentage of different populations in the bone marrow of transgenic mice at 6 months and 1 year of age (F), Megakaryocytes (G), LSK cells (H), LT-HSCs (I), ST-HSCs and (J) MPPs. (K) Histopathological analyses of sterna of transgenic mice at 6 months and 1 year of age, by H&E and reticulin staining. Black bars correspond to 50 μm

results in the generation of a mouse-human chimeric *CALR*-del52 (murine Calr with human mutant C-terminal end), under the control of the endogenous murine *Calr* promoter. We generated the conditional *CALR*-del52 mice by breeding with *vav*Cre transgenic animals to restrict the expression of *CALR*-del52 to the hematopoietic system. To confirm the expression of the mutant CALR protein, Western blot analysis was performed with the whole cell extracts of splenocytes and probed using antibodies against total CALR and mutant CALR. The expression level of mutant CALR were higher in mutCALR homozygous (mutCALR^{hom}) mice for the *CALR*-del52 transgene compared to mutCALR heterozygous (mutCALR^{het}) mice. The expression level of total CALR is significantly lower in the mutCALR^{hom} mice compared to that in the wild type mice due to the increased degradation and secretion of the mutCALR protein (Figure 1B).[9] We followed the peripheral blood values of a cohort of mutCALR^{het} and mutCALR^{hom} mice and *vav*-Cre control mice (Figure 1C). Compared to wild type controls, mutCALR^{het} mice had elevated platelet counts from 6 weeks of age without any significant change in total white blood count (WBC) and red blood count (RBC). However, in the mutCALR^{hom} mice, the platelet counts were significantly higher. In older mice, leukocytosis and erythropenia were evident along with thrombocytosis. We analyzed the mice in more detail at 6 months and 1 year of age and made similar observations in the peripheral blood (Figure S1A).

The mutCALR^{hom} mice manifested splenomegaly at 6 months of age with high spleen to body weight ratio (2.25-fold) that increased at 1 year of age (3.3-fold). The mutCALR^{het} mice developed mild splenomegaly only at 1 year (1.3-fold) (Figure 1D,E). The total number of cells in the bone marrow (BM) was significantly reduced in 6 months (4-fold) and 1 year (6-fold) old mutCALR^{hom} mice (Figure S1C). We saw a significant increase in the percentage of megakaryocytes (Mks) in the bone marrow of mutCALR^{het} (1.7-fold) and mutCALR^{hom} (6-fold) mice at 6 months. The percentage of Mks increased further in mutCALR^{hom} mice at 1 year (7-fold) (Figure 1F). The percentage of hematopoietic stem cells (HSCs, LSK, lineage$^-$ sca1$^+$ kit$^+$) was also significantly increased in the mutCALR^{hom} mice at 6 months (2-fold), which further increased at 1 year (6-fold) of age. However, the mutCALR^{het} mice showed increased LSK cells only at 1 year (1.7-fold) of age (Figure 1G). In mutCALR^{hom} mice this increase in LSK cells was due to increase in all three sub-populations of the stem cells - long term HSCs (LT-HSCs, Lineage$^-$ SCA1$^+$ CD117/c-KIT$^+$ CD150$^+$ CD48$^-$), short term HSCs (ST-HSCs, Lineage$^-$ SCA1$^+$ c-KIT$^+$ CD150$^-$ CD48$^-$) and multipotent progenitor cells (MPPs, Lineage$^-$ SCA1$^+$ c-KIT$^+$ CD48$^+$) (Figure 1H–J). Similar to the bone marrow, we observed increased percentage of progenitor populations in the spleen of mutCALR^{hom} mice at both time points and in mutCALR^{het} mice at 1 year of age (Figure S1D–G).

Histopathological analysis of the bone marrow confirmed a myeloproliferative phenotype with prominent megakaryocytosis and megakaryocytic dyspoiesis in the bone marrow mutCALR^{hom} mice (Figure 1K, Figure S1B). These features were milder in the mutCALR^{het} mice and in 6 months old mice. The one-year-old mutCALR^{hom} mice had mild to moderate trabecular osteosclerosis and minimal to mild increase in reticulin positive fibers. Overt myelofibrosis was not a prominent feature in these mice (Figure 1K). In the spleen, the splenic red pulp was significantly expanded by the myeloproliferative process with marked megakaryocytosis and megakaryocytic dyspoeisis in 6 month- and 1 year-old mutCALR^{hom} mice. Lymphoid follicles were significantly attenuated in the spleens of these mice. In the mutCALR^{het} mice, these features were much less prominent at 1 year of age, and insignificant to marginal at 6 months (Figure S1H).

The conditional *CALR*-del52 mice were bred with Oz-Cre transgenic animals (which express Cre in germ line cells) to generate mice with germ line expression of CALR-del52 (*CALR*$^{del52/+}$). Germline homozygous mice are not present in these litters suggesting embryonic lethality as previously reported.[12] Germline heterozygous mice are viable and develop a phenotype similar to the mutCALR^{het} mice (Figure S2). Taken together, the *CALR-del52* transgenic animals develop a disease reminiscent of human essential thrombocythemia.

3.2 | CALR mutant stem cells have increased proliferation capacity in a competitive bone marrow transplant

We performed a competitive bone marrow transplant assay by transplanting a mixture of total bone marrow cells from mutCALR^{hom} mice (CD45.2) and *vav*Cre mice (F1:CD45.1/45.2), in a ratio of 10:90; into lethally irradiated wild type recipient mice (CD45.1) (Figure 2A). The recipient mice were bled regularly, and the blood parameters and percentage of mutant cells (by FACS) were determined (gating strategies have been shown in Figure S4). There was a steady increase in the number of platelets and WBC in the recipient mice, while the number of RBC remained unchanged (Figure 2B). The percentage of CALR mutant cells kept steadily increasing with time, in all lineages (Figure S3A). Five months after the transplant, the mice were euthanized, and the hematological organs were analyzed by FACS. A majority of myeloid cells (around 60%) in the blood were derived from the CALR mutant cells (Figure 2C). In the bone marrow, 75% of LSK cells and nearly 100% of LT-HSCs were of the mutant cell origin (Figure 2D).

We then performed a competitive bone marrow transplant wherein sorted LSK cells from mutCALR^{het} and mutCALR^{hom} mice (CD45.2) and *vav*Cre mice (F1 CD45.1/45.2), were transplanted into lethally irradiated wild type recipient mice (CD45.1); in a ratio of 20:80 (Figure 2E). The mice were euthanized and analyzed after 20 weeks by assessing blood parameters and by flow cytometry. We did not find any significant differences in the percentage of different populations in the blood or bone marrow among the four groups (Figure S3C,D). We also did not see a significant increase in the percentage of mutant cells in the myeloid lineage, in the blood; although the percentage of chimerism was significantly reduced in the T-cells, in mice that received LSK cells from mutCALR^{hom} mice. In the bone marrow, we saw a significant increase in the mutant chimerism in LSK cells only in mice that received mutCALR^{hom} transplants. Within the LSK cells, all the three progenitor populations (LT-HSCs, ST-HSCs and MPPs) showed significant increase of the mutant chimerism

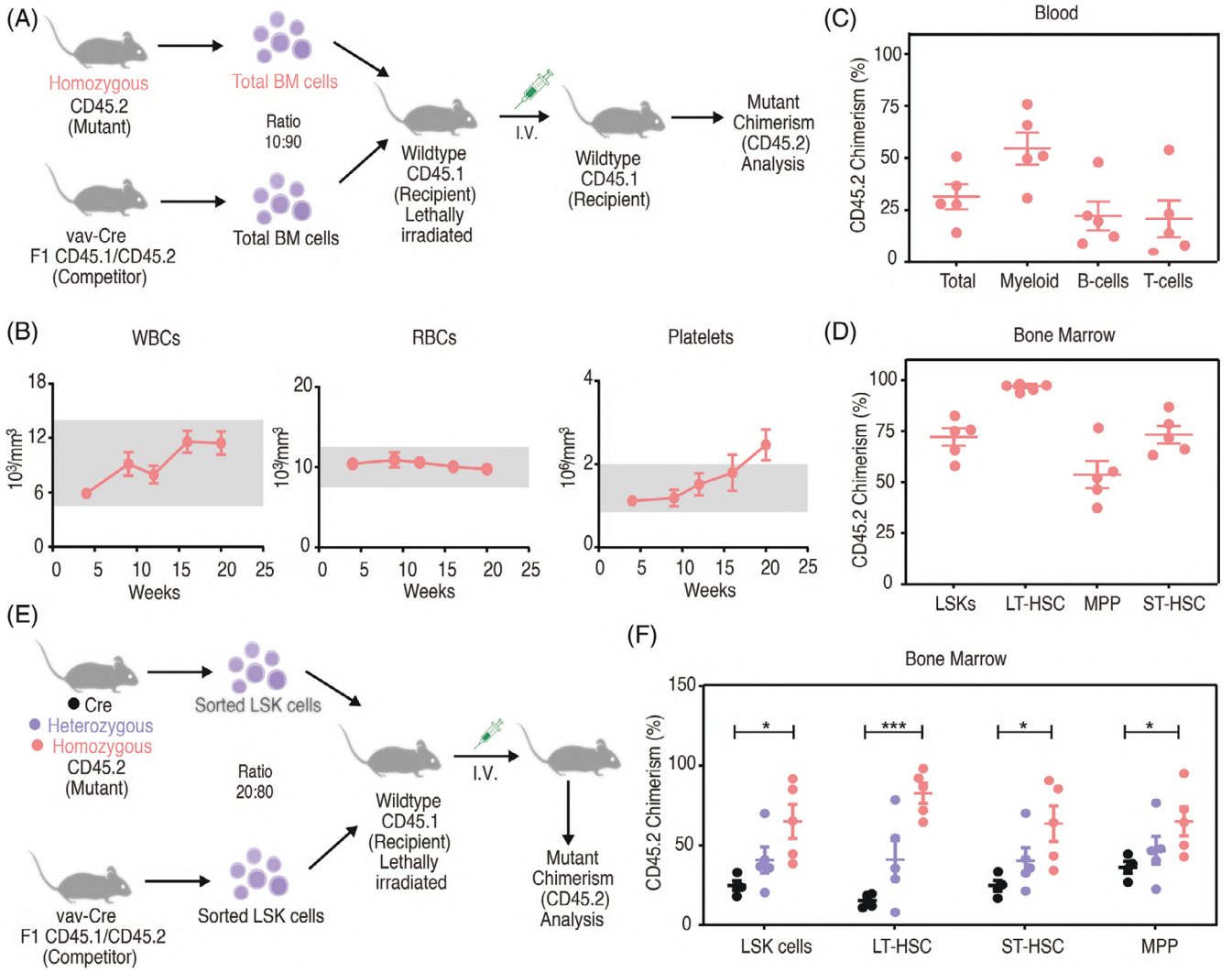

FIGURE 2 CALR mutant stem cells have a proliferative advantage. (A) Schematic representation of experimental plan of total bone marrow transplant. (B) Peripheral blood parameters of WBCs, RBCs and platelets from chimeric mice over time. Percentage of CALR mutant cells (CD45.2) in the donor graft in different populations in (C), blood and (D) bone marrow. (E) Schematic representation of experimental plan for competitive proliferation of LSK cells. (F) Percentage of CD45.2 cells in the donor graft in different populations in bone marrow

percentage in mutCALR^{hom} transplanted mice (Figure 2G). In conclusion, the stem cells from the CALR-del52 homozygous mice have an increased proliferative advantage compared to those from wildtype and heterozygous mice.

3.3 | Transcriptome profiling reveals a distinctive gene signature pattern in murine hematopoietic stem cells

To understand the effect of mutCALR, we determined the transcriptome of bone marrow LSK (Lin-Sca+Kit+) cells (Figure 3A). Principal Component Analysis reveals hierarchical clustering of samples based on genotype (Figure 3B). We identified 460 differentially expressed genes between wild type and mutCALR LSK cells (Figure S5B) and the top 25 upregulated and downregulated genes are shown (Figure 3C). Gene set enrichment analysis (GSEA) against hallmarks cohort revealed 12 gene-sets that are significantly enriched, and six gene sets significantly depleted in mutCALR LSKs. We saw upregulation of genes in the IL-6 JAK–STAT signaling pathway, including the bona fide STAT5 targets such as *Mycn*, *Socs1*, and *Junb* (Figures 3D). Components of the cholesterol homeostasis (*Clu*, *Trib3*, *Plscr1*, *Aldoc*, *Jag*) were ranked significantly high in the GSEA. Interferon alpha response, TNFA signaling via NFKB, bile acid metabolism, MTORC1 signaling, P53 pathway, interferon gamma response and hypoxia are few other gene-sets that are significantly upregulated in the mutCALR LSK cells. We see a significant downregulation in gene-sets associated with E2F targets, G2M checkpoint, mitotic spindle, epithelial to mesenchymal transition, Kras signaling and coagulation in mutCALR LSK cells (Figure 3E,F). The transcriptome analysis identified

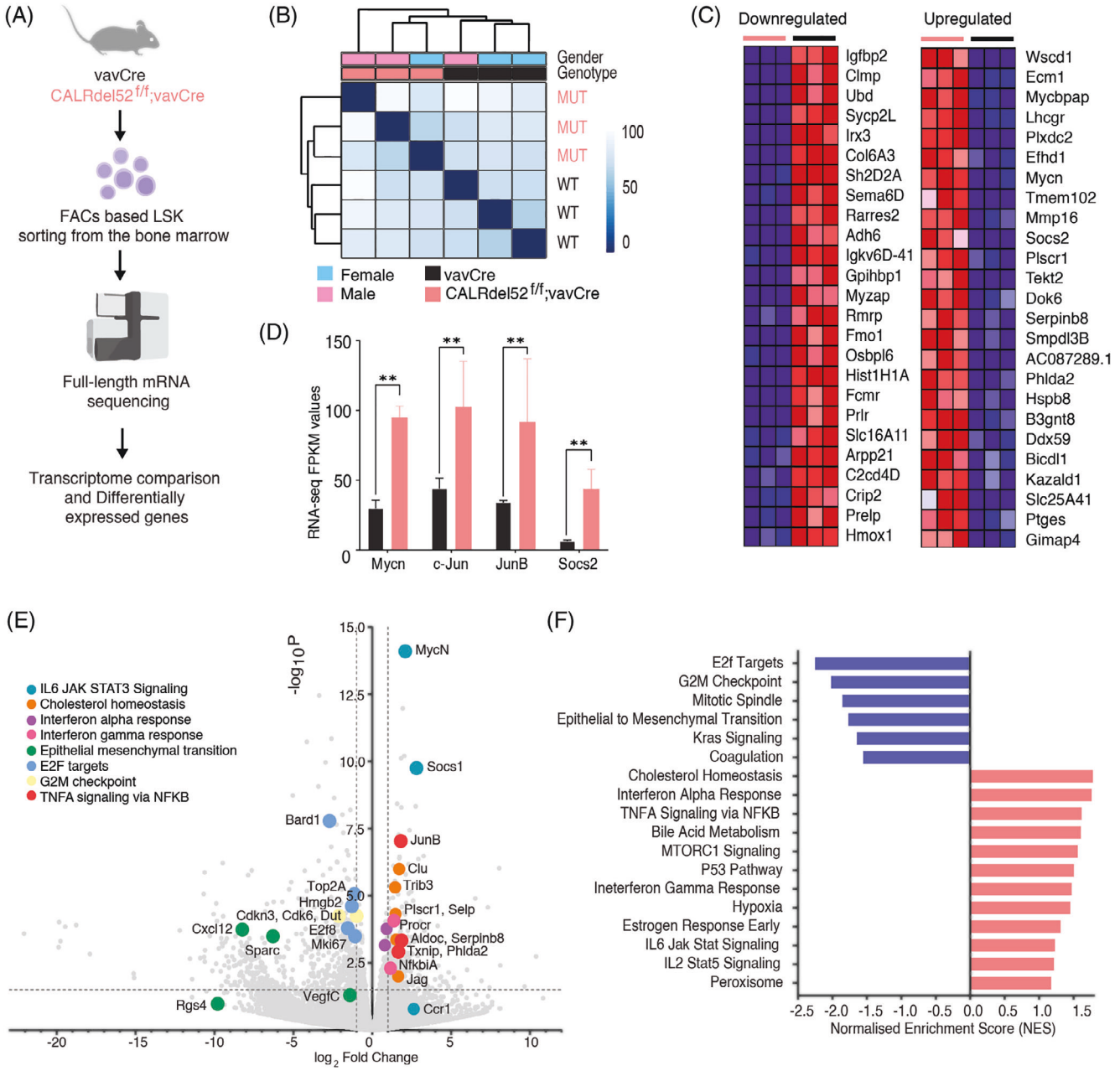

FIGURE 3 Transcriptome analysis of stem cells with CALR mutations. (A) Schematic representation of the RNA-seq pipeline (B) Hierarchical clustering of the reads according to genotype of the samples: *vav*Cre vs CALRdel52$^{fl/fl}$;*vav*Cre (C) Heatmap annotation of top 25 upregulated and downregulated genes in mutCALR LSK cells (D) FPKM values of STAT5 target genes (E) Volcano plot representing differentially regulated gene-sets (Hallmark GSEA) in mutCALR LSK cells (F) Bar plot representing statistically significant gene-sets upregulated and downregulated in mutCALR LSK cells. (* - show statistical significance, which has been explained in the supplementary methods)

specific pathways associated with the oncogenic functions of mutCALR and reveals the inflammatory gene expression signature in the bone marrow stem cells.

3.4 | Treatment with anti-mutCALR monoclonal antibody reduces platelet and LSK counts

The mutant CALR protein represents a bona fide tumor antigen that is a target for immunotherapeutic strategies. We were able to detect the presence of the mutCALR protein on the surface of the total cells, lineage negative cells, LSK cells and megakaryocytes in the bone marrow of mutCALR^{hom} mice, by FACS (Figure 4A). Since, the expression of the protein was higher in the homozygous mice and the homozygous mice best represent the human MPN phenotype, we chose to use these mice for immunotherapy experiments. We treated the mice with a monoclonal antibody targeting the human mutant C-terminus.

The mutCALR^{hom} mice were injected with anti-mutCALR mAb, intraperitoneally 3 mg/kg, twice a day for a period of 2.5 days (Figure 4B). After treatment, only platelet counts were significantly

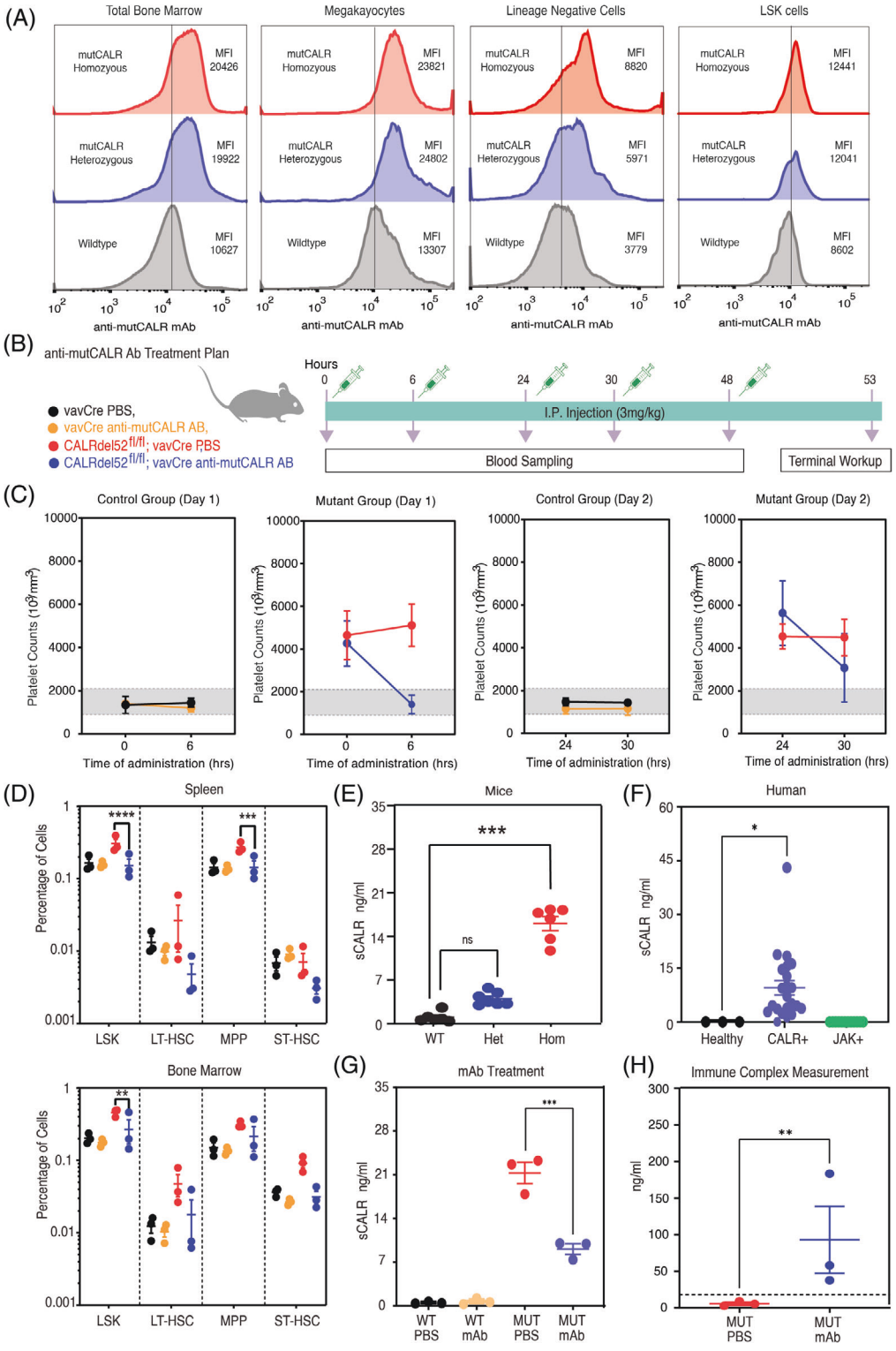

FIGURE 4 Immunodepletion of platelets and stem cells by anti-mutCALR antibody. (A) FACS analysis of different lineages in bone marrow for expression of mutCALR on the cell surface. (B) Schematic representation of anti-mutCALR mAb treatment plan (C) Peripheral blood parameters of platelets over 2 day time-period (D) Percentage of different populations in bone marrow and spleen of treatment and control groups (E) sCALR quantification in 1 year old transgenic mice and (F) patient samples and healthy donors (Kruskal-Wallis test), (G) sCALR quantification in 8-month old mice treated with antibody (H) ELISA assay to detect presence of mutCALR-Ab immune complexes in plasma of mice treated with anti-mutCALR antibody

altered in the peripheral blood. Platelet values normalized 6 h post antibody treatment. The platelet counts returned to thrombocythemic levels in 24 h after treatment in the mutCALR^{hom} mice. This fluctuation persisted on day 2. We did not observe any effects of the treatment on blood parameters in wild type mice (Figures 4C, S6A).

At terminal workup, the antibody treated mice had a significant reduction in the percentage of LSKs and MPPs in the spleen of mutCALR^{hom} mice. There was no change in the levels of ST-HSCs, ~~and~~ LT-HSCs and megakaryocytes (Figure S6B). The mutCALR LSK cells in the bone-marrow were also significantly reduced in the antibody treated mice, while the other cell populations remained unchanged (Figure 4D). In conclusion, anti-mutCALR antibody treatment of mice resulted in immunodepletion of platelets and hematopoietic stem cells *in vivo* in mutCALR-dependent manner.

Since shedding and secretion of antigen constitutes a potential antibody sink, we examined the soluble mutCALR (sCALR) levels in the plasma of transgenic mice. The mutCALR^{hom} mice had a significantly increased amount of sCALR compared to the wild type and mutCALR^{het} mice (Figure 4E, ELISA setup in Figure S6C,D). This is consistent with the levels of sCALR detected in MPN patients with CALR mutations, using the same ELISA assay (Figure 4F). Notably, the mutCALR^{hom} mice treated with anti-mutCALR antibody have significantly reduced levels of sCALR in the plasma in comparison to PBS treated mice (Figure 4G). We ruled out any competition between the two antibodies by performing a competitive ELISA (data not shown). Therefore, immunological depletion of the antigen (by formation of antigen–antibody complexes) could be a possible reason for the reduction of ELISA signal. Accordingly, we were able to detect antigen–antibody complexes of the monoclonal antibody bound to sCALR in the plasma of the treated mice (Figures 4H, S6D). These data indicate that sCALR was reduced in the plasma due to immunodepletion.

4 | DISCUSSION

A relevant transgenic mouse model is required for screening and understanding the molecular mechanisms of therapeutic interventions in a pre-clinical setting. We have developed a murine model that expresses the mutCALR oncoprotein with human mutant C-terminal peptide (del52) under the control of the endogenous murine *Calr* promoter.

The use of *vav*Cre transgenic mice restricted the expression of the mutCALR protein to the hematopoietic tissue. We were able to detect the expression of the mutCALR protein in the splenocytes of transgenic mice. Notably, the mutCALR^{hom} mice expressed higher levels of the CALR-del52 protein than the mutCALR^{het} mice. Transgenic mice expressing human CALR-del52 under MHC-I promoter[13] or murine mutant CALR protein[12] have a relatively mild increase in platelets. However, transgenic mice expressing mouse-human hybrid CALR mutant proteins generated by" knock-in" strategy similar to ours,[14,15] developed a myeloproliferative disease which was more severe in homozygous mice. Similarly, the phenotype in the mutCALR^{hom} mice was characterized by increased platelets and WBC and reduced RBC in the peripheral blood. The mutCALR^{hom} mice also developed splenomegaly and increased percentage of megakaryocytes and stem cells in the bone marrow (Figure 1). The LSK cells from mutCALR^{hom} mice also showed proliferative advantage in a competitive bone marrow transplantation assay, as previously reported by Benlabiod et al.[15] Using transgenic mice with the expression of Cre in germ line tissue, we generated mice with systemic CALR-del52 expression (*Calr*$^{del52/+}$). The mice do not survive past embryogenesis when they are homozygous for CALR-del52, similar to the Calr knockout mice and CRISPR/Cas9 knock-in mice.[12,16]

To dissect the signature pattern associated with the mutant CALR, we performed transcriptome profiling of the LSK cells sorted from the mutCALR^{hom} mice. The pathways revealed by GSEA, fall into four major categories: oncogenic signaling (K-ras signaling, mTORC1, P53 and JAK–STAT signaling pathways), cell cycle control (E2F targets, G2M checkpoint), inflammation (TNFα, IFNα and IFNγ signaling) and metabolism (bile acid, cholesterol homeostasis). Constitutive JAK–STAT signaling is one of the hallmarks of classical MPNs. We see an enrichment of genes that are known to be bona fide STAT5 targets. Major signaling networks are also known to feed into the JAK–STAT signaling.[17] The prominent ones that have emerged in the transcriptome data are categorized into oncogenic signaling list. One of the hallmarks of cancer is deregulation of cell cycle. Interestingly, we see that the components of G2M checkpoints and E2F targets are downregulated in mutCALR LSKs. The crucial role of CDK6 in stem cell quiescence, cytokine secretion and cell proliferation has already been demonstrated, in the context of JAKV617F.[18] It would be interesting to investigate the role of cell cycle control associated genes in CALR-positive MPN progression. A chronic state of inflammation is another hallmark of MPN.[19] NFKB is known to be the master regulator in promoting inflammation. We see that the components of TNFα signaling via NFKB, IFNα and IFNγ are upregulated in mutCALR LSKs. We also see that cholesterol homeostasis is significantly upregulated in mutCALR LSKs. As the ER luminal calcium plays an important role in sensing cholesterol,[20] the perturbation of cholesterol homeostasis may be due to the loss of calcium binding capacity in the del52-homozygous cells. Compared to the report of Prins et al.[21] we identified several other pathways in the GSEA analysis. This is likely because we performed transcriptome analysis from 1000 LSK cells rather than single cells. While single cell RNA-seq has the advantages of identifying transcriptional signature of individual cells, information of low-expressed genes can be lost in the process, which can be accessed in conventional transcriptome analysis.

MutCALR associates with the thrombopoietin receptor and is trafficked onto the cell surface as a complex.[4] We were able detect the presence of the mutCALR protein on the surface of the target cells in the bone marrow of mutCALR mice. The cell-surface residing protein can act as a neoantigen and, therefore, be targeted by antibody-based immunotherapy. To test this hypothesis, we administered a murine anti-mutCALR IgG2a raised against the human oncoprotein to the mutCALR^{hom} mice. During antibody treatment, we observed a short-term platelet immunodepletion in the mutCALR^{hom}

mice. At the end of treatment, we detected a significant reduction in the percentage of LSK cells in both the spleen and the bone marrow, in the monoclonal antibody treated mutCALR mice. The control *vav*Cre mice were not affected by the antibody treatment, demonstrating the specificity of the antibody against mutCALR. Interestingly, the platelet values were replenished within the 18-h gap between two injections. The amount of antibody used here may not be sufficient to combat the very high rate at which the mutCALR megakaryocytes shed platelets.

Secretion of mutCALR has been shown in cell culture supernatants.[4,9] However, the biologic effects of the secreted neoantigen has not yet been investigated in mice or patients.[22] To test if the transgenic mice could be used to model the pathophysiologic role of secreted mutCALR, we measured the soluble mutCALR (sCALR) in the transgenic mice and in MPN patients. The plasma levels in patients with CALR mutations and in mutCALR mice were comparable suggesting that the mutCALR mice also recapitulate this aspect of the MPN phenotype. The sCALR in plasma may act as a "sink" for the anti-mutCALR monoclonal antibody and lead to dampening of the antibody therapeutic effects. Although we detected the presence of immunocomplexes of the anti-mutCALR antibody and the sCALR in the plasma of treated mice, this did not prevent the immunodepletion of LSK cells in both spleen and bone marrow (Figure 4). These data suggest that the secreted mutCALR and the abundant platelets in the peripheral blood do not constitute a significant antibody sink. The mechanisms of how the antibody treatment leads to platelet and LSK cell depletion is unclear at the moment and further studies are needed to clarify the mode of action.

In summary, we have generated transgenic mice that recapitulate the MPN phenotype and provide proof of concept that an antibody raised against the mutant C-terminus can be effectively used to target the platelets and mutant LSK cells. The mutCALR mice serve as a modeling platform to study the molecular mechanisms and immunotherapeutic strategies to target the disease.

ACKNOWLEDGMENTS

This study was supported by the Austrian Science Fund, FWF SFB F4702, P29018-B30, granted to RK and P30041-B26 granted to HN. We thank Raimund Holly, Felix Rosebrock, Erica Xu, Faith Hall-Glenn, Nevena Milosavljavic, Beatrice Grabner and David Stuecklschwaiger for their technical assistance. We also thank Agnieszka Piszczek, Tamara Engelmaier, Julia Klughofer, and Mihaela Zeba for tissue processing and histochemical staining.

AUTHOR CONTRIBUTIONS

Robert Kralovics and Harini Nivarthi conceived and designed the study, interpreted the data and contributed to the manuscript writing. Harini Nivarthi (mouse model generation, phenotyping and bone marrow transplantation) and Sarada Achyutuni (transcriptome analysis, antibody treatment and ELISA) designed and performed the experiments, analyzed the data and wrote the manuscript. Andrea Majoros, Ruochen Jia, Christina Schueller and Cecilia Varga conducted specific experiments and analyzed the data. Anoop Kavirayani coordinated the histology processing and analyzed and interpreted the histopathology data. Eva Hug designed the ELISA assay. Michael Schuster and Martin Senekowitsch contributed in processing the NGS samples and in analyzing the sequencing files. Oleh Zagrijtschuk, Dimitrios Tsiantoulas, Christoph Bock and Christoph Binder contributed to the intellectual input.

CONFLICT OF INTEREST

The authors declare no conflict of interest.

DATA AVAILABILITY STATEMENT

The data that support the findings of this study are available on request from the corresponding author.

ORCID

Sarada Achyutuni https://orcid.org/0000-0002-0907-3308
Harini Nivarthi https://orcid.org/0000-0002-5545-5673
Christina Schueller https://orcid.org/0000-0001-7618-6815
Robert Kralovics https://orcid.org/0000-0002-6997-8539

REFERENCES

1. Klampfl T, Gisslinger H, Harutyunyan AS, et al. Somatic mutations of calreticulin in myeloproliferative neoplasms. *N Engl J Med*. 2013;369:2379-2390. https://doi.org/10.1056/nejmoa1311347.
2. Nangalia J, Massie CE, Baxter EJ, et al. Somatic CALR mutations in myeloproliferative neoplasms with nonmutated JAK2. *N Engl J Med*. 2013;369:2391-2405. https://doi.org/10.1056/nejmoa1312542.
3. Marty C, Pecquet C, Nivarthi H, et al. Calreticulin mutants in mice induce an MPL-dependent thrombocytosis with frequent progression to myelofibrosis. *Blood*. 2016;127:1317-1324. https://doi.org/10.1182/blood-2015-11-679571.
4. Chachoua I, Pecquet C, El-Khoury M, et al. Thrombopoietin receptor activation by myeloproliferative neoplasm associated calreticulin mutants. *Blood*. 2016;127:1325-1335.
5. Nivarthi H, Chen D, Cleary C, et al. Thrombopoietin receptor is required for the oncogenic function of CALR mutants. *Leukemia*. 2016;30:1759-1763. https://doi.org/10.1038/leu.2016.32.
6. Araki M, Yang Y, Masubuchi N, et al. Activation of the thrombopoietin receptor by mutant calreticulin in CALR-mutant myeloproliferative neoplasms. *Blood*. 2016;127:1307-1316. https://doi.org/10.1182/blood-2015-09-671172.
7. Elf S, Abdelfattah N, Chen E, et al. Physical interaction between mutant calreticulin and the thrombopoietin receptor is required for hematopoietic transformation. *Blood*. 2015;126:LBA-4. https://doi.org/10.1182/blood.v126.23.lba-4.lba-4.
8. Pecquet C, Chachoua I, Roy A, et al. Calreticulin mutants as oncogenic rogue chaperones for TpoR and traffic-defective pathogenic TpoR mutants. *Blood*. 2019;133:2669-2681. https://doi.org/10.1182/blood-2018-09-874578.
9. Han L, Schubert C, Köhler J, et al. Calreticulin-mutant proteins induce megakaryocytic signaling to transform hematopoietic cells and undergo accelerated degradation and Golgi-mediated secretion. *J Hematol Oncol*. 2016;9:45. https://doi.org/10.1186/s13045-016-0275-0.
10. Schischlik F, Jäger R, Rosebrock F, et al. Mutational landscape of the Transcriptome offers a rich Neoantigen resource for immunotherapy of Myeloproliferative neoplasms. *Blood*. 2018;132:3058. https://doi.org/10.1182/blood-2018-99-118049.
11. de Boer J, Williams A, Skavdis G, et al. Transgenic mice with hematopoietic and lymphoid specific expression of Cre. *Eur J Immunol*. 2003;33:314-325. https://doi.org/10.1002/immu.200310005.

12. Balligand T, Achouri Y, Pecquet C, et al. Knock-in of murine Calr del52 induces essential thrombocythemia with slow-rising dominance in mice and reveals key role of Calr exon 9 in cardiac development. *Leukemia*. 2020;34:510-521. https://doi.org/10.1038/s41375-019-0538-1.
13. Shide K, Kameda T, Yamaji T, et al. Calreticulin mutant mice develop essential thrombocythemia that is ameliorated by the JAK inhibitor ruxolitinib. *Leukemia*. 2017;31:1136-1144.
14. Li J, Prins D, Park HJ, et al. Mutant calreticulin knockin mice develop thrombocytosis andmyelofibrosis without a stemcell self-renewal advantage. *Blood*. 2018;131:649-661. https://doi.org/10.1182/blood-2017-09-806356.
15. Benlabiod C, da Cacemiro MC, Nédélec A, et al. Calreticulin del52 and ins5 knock-in mice recapitulate different myeloproliferative phenotypes observed in patients with MPN. *Nat Commun*. 2020;11(1):4886–4900. https://doi.org/10.1038/s41467-020-18691-3.
16. Mesaeli N, Nakamura K, Zvaritch E, et al. Calreticulin is essential for cardiac development. *J Cell Biol*. 1999;144:857-868. https://doi.org/10.1083/jcb.144.5.857.
17. Jia R, Kralovics R. Progress in elucidation of molecular pathophysiology of myeloproliferative neoplasms and its application to therapeutic decisions. *Int J Hematol*. 2020;111:182-191. https://doi.org/10.1007/s12185-019-02778-9.
18. Uras IZ, Maurer B, Nivarthi H, et al. CDK6 coordinates JAK2V617F mutant MPN via NF-kB and apoptotic networks. *Blood*. 2019;133:1677-1690. https://doi.org/10.1182/blood-2018-08-872648.
19. Rai S, Hansen N, Hao-Shen H, Dirnhofer S, Tata NR, Skoda RC. IL-1β secreted from mutant cells carrying JAK2-V617Ffavors early clonal expansion and promotes MPN disease initiation and progression. *Blood*. 2019;134:307. https://doi.org/10.1182/blood-2019-129800.
20. Wang WA, Liu WX, Durnaoglu S, et al. Loss of calreticulin uncovers a critical role for calcium in regulating cellular lipid homeostasis. *Sci Rep*. 2017;7:5941. https://doi.org/10.1038/s41598-017-05734-x.
21. Prins D, Park HJ, Watcham S, et al. The stem/progenitor landscape is reshaped in a mouse model of essential thrombocythemia and causes excess megakaryocyte production. *Sci Adv*. 2020;6:1-13.
22. Pecquet C, Balligand T, Chachoua I, et al. Secreted mutant calreticulins as rogue cytokines trigger thrombopoietin receptor activation specifically in CALR mutated cells: perspectives for MPN therapy. *Blood*. 2018;132:4.

SUPPORTING INFORMATION

Additional supporting information may be found online in the Supporting Information section at the end of this article.

How to cite this article: Achyutuni S, Nivarthi H, Majoros A, et al. Hematopoietic expression of a chimeric murine-human CALR oncoprotein allows the assessment of anti-CALR antibody immunotherapies in vivo. *Am J Hematol*. 2021;96:698–707. https://doi.org/10.1002/ajh.26171

3.1.1 Epitope Mapping of the anti-mutCALR mAb

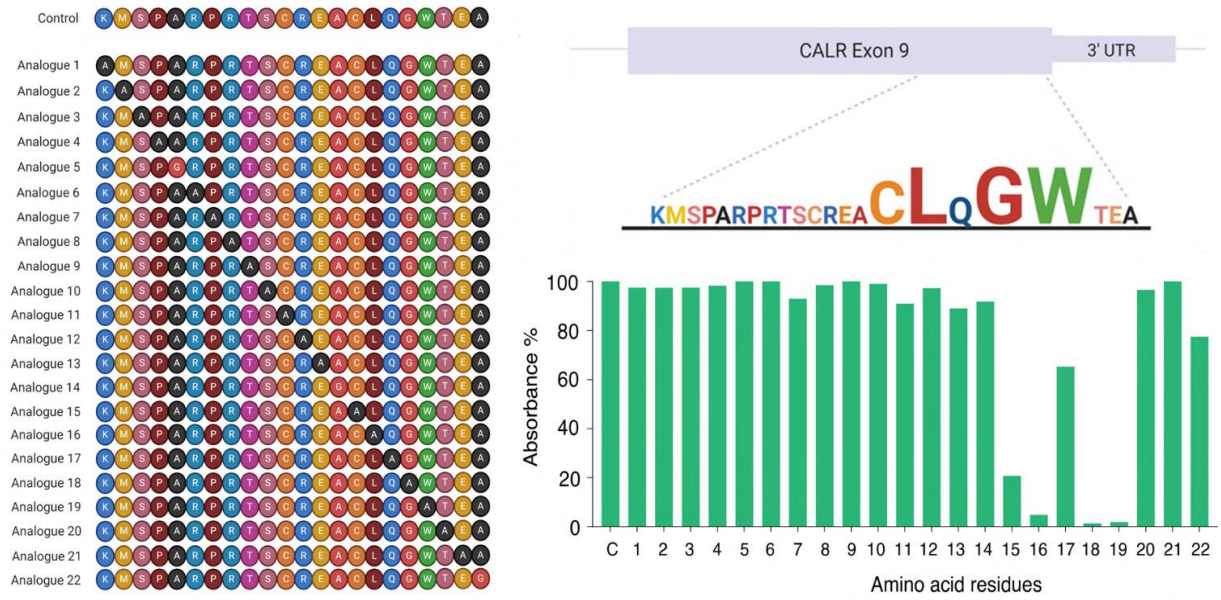

Figure 10: Peptide library and immunological assay identifying the epitope that is crucial for anti-mutCALR mAb binding

Epitope mapping is crucial for the development of vaccines and patents. The identification of an epitope for a particular therapeutic monoclonal antibody sheds light on the probable mechanism of action accountable for illicting the respective immune response. We performed the epitope characterization of the anti-mutCALR mAb used in the study and mapped it to the mutCALR peptide sequence (Figure 10). For this purpose, we generated a library of peptides of the last 22-AA residues of human mutCALR del52. The library consists of a control peptide and a collection of peptides wherein consecutives residues of each peptide sequence were mutated using alanine walking (Analogue 1-22). We performed an ELISA where we coated the wells individually with the control and mutated peptides. The wells were incubated with anti-mutCALR mAb used in our study. We measured the absorbance of the signal from all the wells. The control well (C) had the highest absorbance and in five mutated peptide wells there was a significant decrease in absorbance (15-19). Hence, we conclude that the ‘CLQGW’ residues are crucial for the interaction of the antibody with the mutant epitope.

3.2 Identification of vulnerabilities of mutCALR driven MPN

Myeloproliferative neoplasms are clonal hematological disorders. They are characterized by an abnormal expression of different myeloid lineages. A constitutive JAK-STAT signaling pathway is one of the hallmark features of the three classical MPNs – PV, ET and PMF. Somatic mutations in three disease driver genes – *JAK2*, *MPL* and *CALR* lead to onset of the disease. Mutations in *CALR* are insertions and/or deletions that lead to a 'frameshift' generating a very specific alternative reading frame. Our lab has shown that CALR mutant proteins specifically induce the activation of thrombopoietin receptor (MPL) (Marty *et al.*, 2016). To further clarify the mechanism of CALR mutants, we also developed a conditional knock-in mouse model with CALR mutant (del52) (Achyutuni *et al.*, 2021).

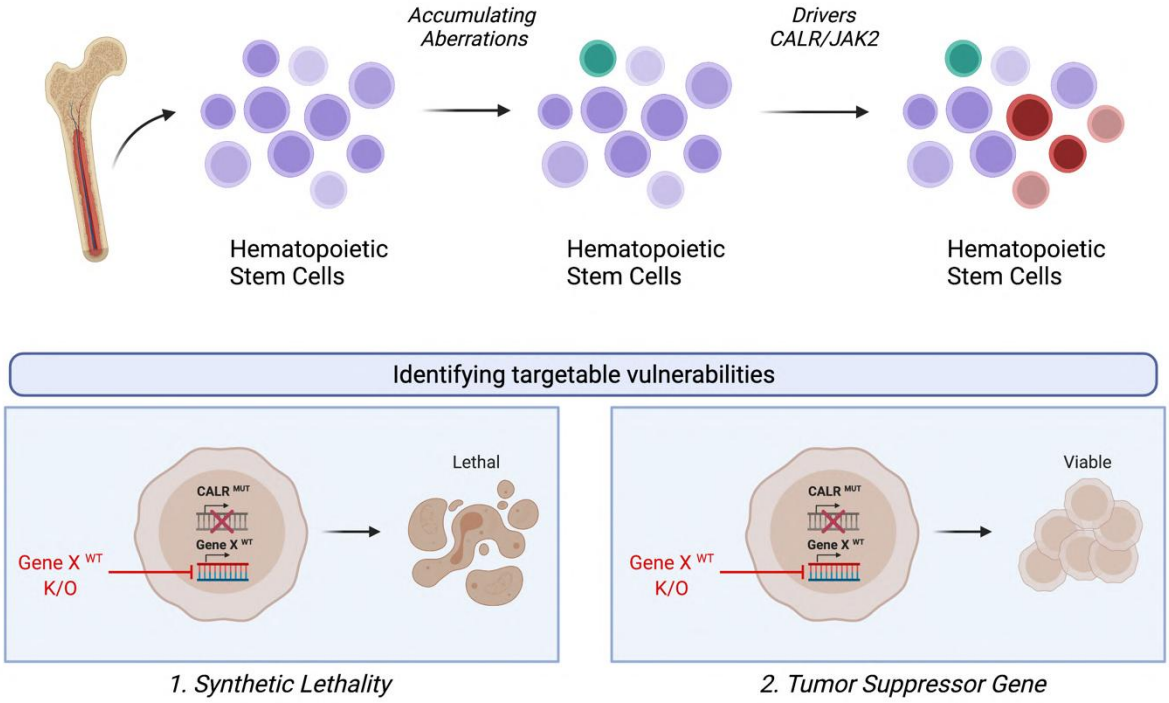

Figure 11: Rationale behind identifying targetable vulnerabilities

In a hematopoietic stem cell niche, cells undergo divisions and accumulate aberrations. Many of these mutations are passenger mutations that pass from one generation to other letting the clone thrive normally in a healthy population of cells. A few of these mutations are clonal drivers such as JAK2, CALR and MPL in human MPN. These mutations give the clone a proliferative advantage over the inherent population, thereby allowing it to outgrow the general cell populations. The driver mutations do so by inducing signaling pathways and altering the gene expression profile of the mutant cells. This usually includes co-opting various genes involved in the pathways regulating proliferation and cell cycle control. Identification of important gene-

gene dependencies in the context to mutCALR is of significant interest. For example, the knock-down of a particular gene could either be detrimental or advantageous to the mutant clone. The identification of such gene dependencies reveals a vulnerability that can be targeted by genetic perturbation systems or small molecule inhibitors.

The principal aim of this experiment is to perform an *in vitro* CRISPR-Cas9 screen to identify the group of essential genes in Wild-type, Heterozygous & Homozygous mutCALR murine cell lines. We aim to identify a dependency map that is a signature of mutCALR driven MPN regulatory network and further validate them *in vitro*. However, the validation of these hits *in vivo* is essential to assess their functional relevance in CALR-del52 driven MPN *in vivo*. The results from this experiment will be crucial in not only augmenting the existing knowledge on the mechanism and biology of the disease, but also will facilitate the development of novel therapeutic intervention for these patients.

3.2.1 Editing efficiency of Cas9 expressing mutCALR cell lines

Before establishing the screen, we generated stable BaF/3 Wildtype and BaF/3 mutCALR cell lines (Homozygous and Heterozygous) expressing pCas9 and EGFP. Constitutive expression of Cas9 enables efficient gene targeting efficiency for high-throughput screening.

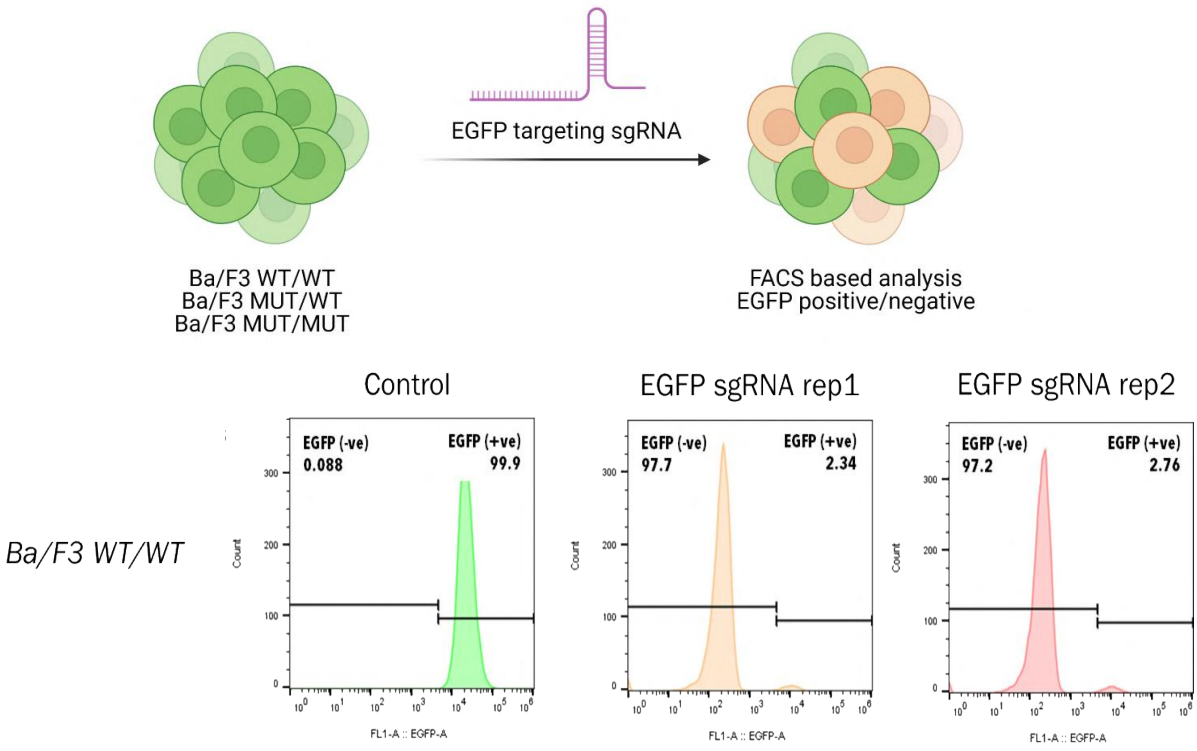

Figure 12: Editing efficiency of stably Cas9 expressing cell line

We transduced our three cell lines with a pLenti-Cas9-blasticidin vector carrying lentiviral particles. We then selected for infected cells with blasticidin for a week (1.25 ug/ml).

The expression of the Cas9 was validated by western blotting. All the three cell lines showed constitutive expression of Cas9, which was consistent with expression of β-actin control. To further assess the editing potential of the cell lines, we cloned EGFP targeting sgRNA into a pLentiguide-puro vector. We generated lentiviral particles carrying the EGFP targeting sgRNA. We transduced all the three cell lines individually with the lentivirus and passaged the cells till day 5 post-transduction. We assessed the percentage of EGFP positive and negative cells via flow-cytometry. From our FACS analysis, we saw that all the three cell lines showed an editing efficiency of 93-97% (Figure 12). We used these cell lines for establishing our CRISPR-Cas9 *in vitro* screen.

3.2.2 Guide RNA representation of the BRIE library and BRIE screen pipeline

The aim was to establish a CRISPR screen of 1000X coverage, wherein there would be at least 1000 cells being targeted by one sgRNA. In order to achieve a 1000X coverage, it is necessary to maintain a uniform number of gRNAs for each gene at the library amplification step. We used the BRIE gRNA library, which is a murine genome wide gRNA targeting library comprising of 78,639 sgRNAs targeting 19,674 genes. BRIE library has been designed with a better algorithm that optimizes the sgRNA targeting efficiency and minimizes the off-target effects of CRISPR-cas9 (Doench *et al.*, 2016).

For a 1000X coverage, it is important to have 'N' number of bacterial colonies that carry specific gRNA at the amplification step (which is 1000 competent cells/gRNA). In this case, we required 1000 competent cells/gRNA x 78,639 sgRNAs = N = 78,639,000 bacterial colonies. The reason as to why we considered enough coverage at BRIE library amplification step was to ensure equal distribution of guide RNAs. Post-amplification, the pooled library that we generated was of 1200X coverage. We further confirmed the distribution of the gRNAs in our pooled library using next-generation sequencing (NGS). We analyzed the sequencing files, plotted the cumulative fraction of reads on y-axis and cumulative fraction of sgRNAs plus genes independently on x-axis. We evaluated the gini-coefficient for the data to distinguish an inequality in the data distribution. Gini-coefficient ranges from 0 representing equality in a distribution to 1 representing inequality in a distribution. The gini-coefficient for evaluating the read disparity in sgRNAs is 0.178 and in Genes is 0.121 (Figure 13). This denotes that the library has equal representation of genes (99%) and sgRNAs (99.3%) with adequate coverage.

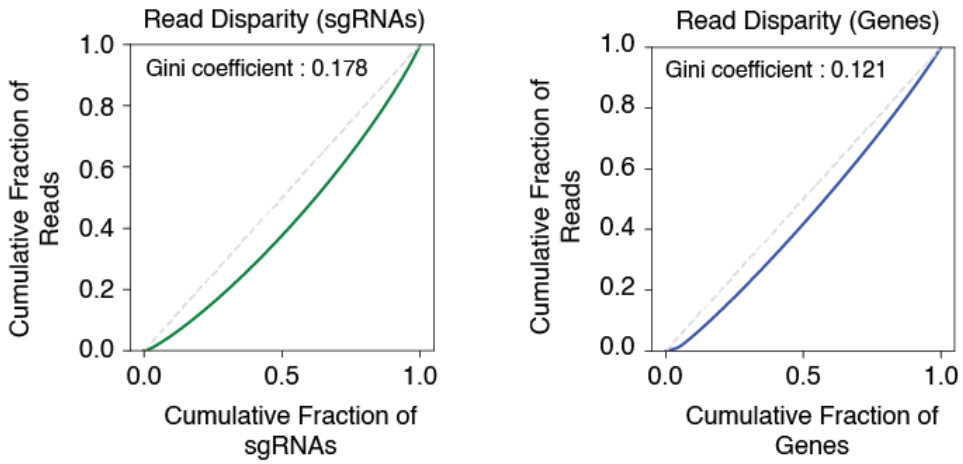

Figure 13: Quality control of the amplified BRIE library used in the genetic perturbation screen using CRISPR-cas9.

Once the library was quality controlled, we generated lentiviral particles of the library using lipofection. Cas9 positive BaF/3 wildtype and mutCALR homozygous and heterozygous cells (30 x10^7) were infected at MOI of 0.3 – 0.5 and selected on puromycin & blasticidin for 5 days (Figure 14). We achieved a coverage of 1000x for the screen.

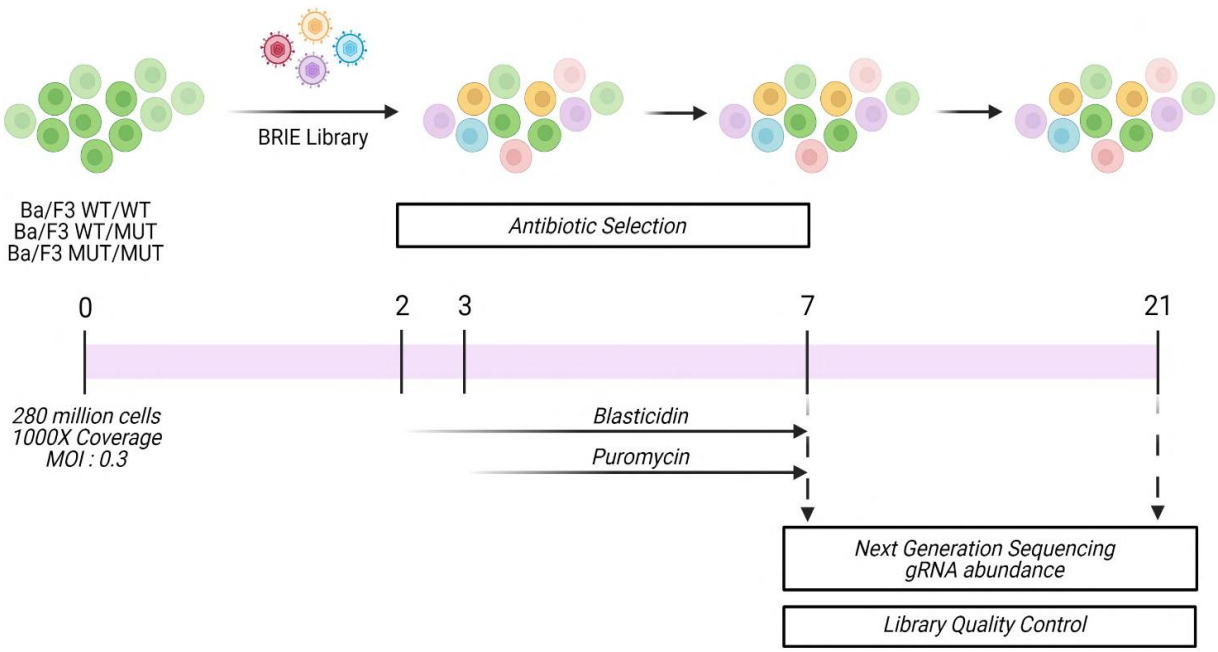

Figure 14: BRIE-Screen pipeline in Ba/F3 cell lines: Wildtype, Heterozygous & Homozygous

The cells were split every three days and we had two replicates per each condition. 100 million cells were passaged on day 7 and day 21 from all the flasks. The representation of individual gRNAs was determined by NGS at the end of puromycin selection on day 7 and day 21.

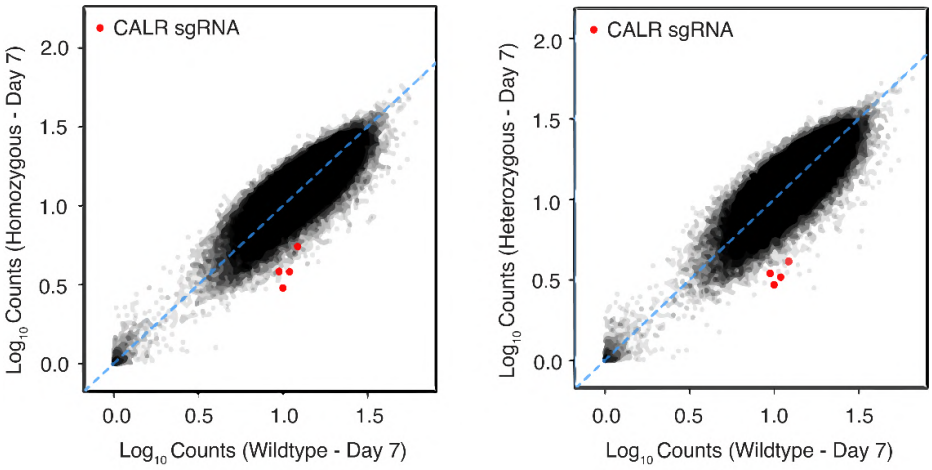

Figure 15: Drop-out of CALR control guide-RNA in both Homozygous and Heterozygous cell lines.

We compared the enrichment and depletion of sgRNA at day 7 in wildtype and mutCALR mutant cell lines. On day 7, we saw that in both the mutant cell lines the positive control gRNAs targeting the CALR gene dropped out, indicating the essentiality of the CALR gene for mutCALR cell viability (Figure 15).

We used a web-interface tool called Pin-APL-Py to analyze for quality control, read alignment and enrichment/depletion analysis of CRISPR/Cas9 screens. The sequencing files were submitted to the web application and it processed the number of reads identified per each condition (Spahn *et al.*, 2017).

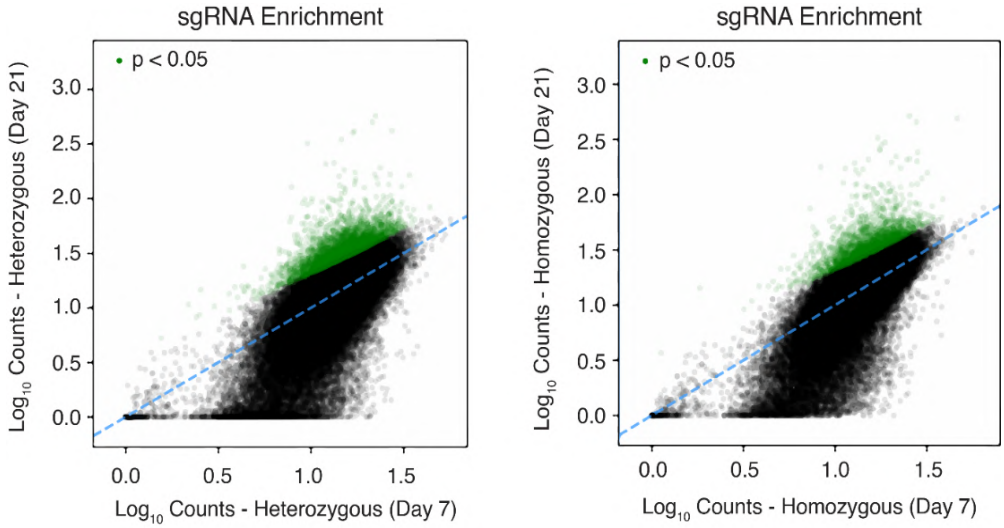

Figure 16: sgRNA enrichment statistics in both Homozygous and Heterozygous cell lines

The analysis output from the application identified list of genes and gRNAs that were significantly enriched and depleted in the CRISPR-Cas9 screen. We further confirmed these results by running the Mageck pipeline which is another CRISPR-screen statistical based analysis algorithm (Li *et al.*, 2014).

We further looked at genes that were depleted at day 21 vs day 7 in all the cell lines (Figure 16). CALR gene ranked number 1 in the list of genes that depleted at an early time-point in both the cell lines. The list of genes that were depleted at an early time-point at day 7 were annotated as early penetrance synthetic lethal interaction genes. Most of the genes were common in both mutCALR cell lines (Appendix Tables: 1,2). The list of the significant genes was submitted to EnrichR and the gene-ontology (GO) analysis revealed that the genes were associated with playing a role in ribosome and proteasome machinery.

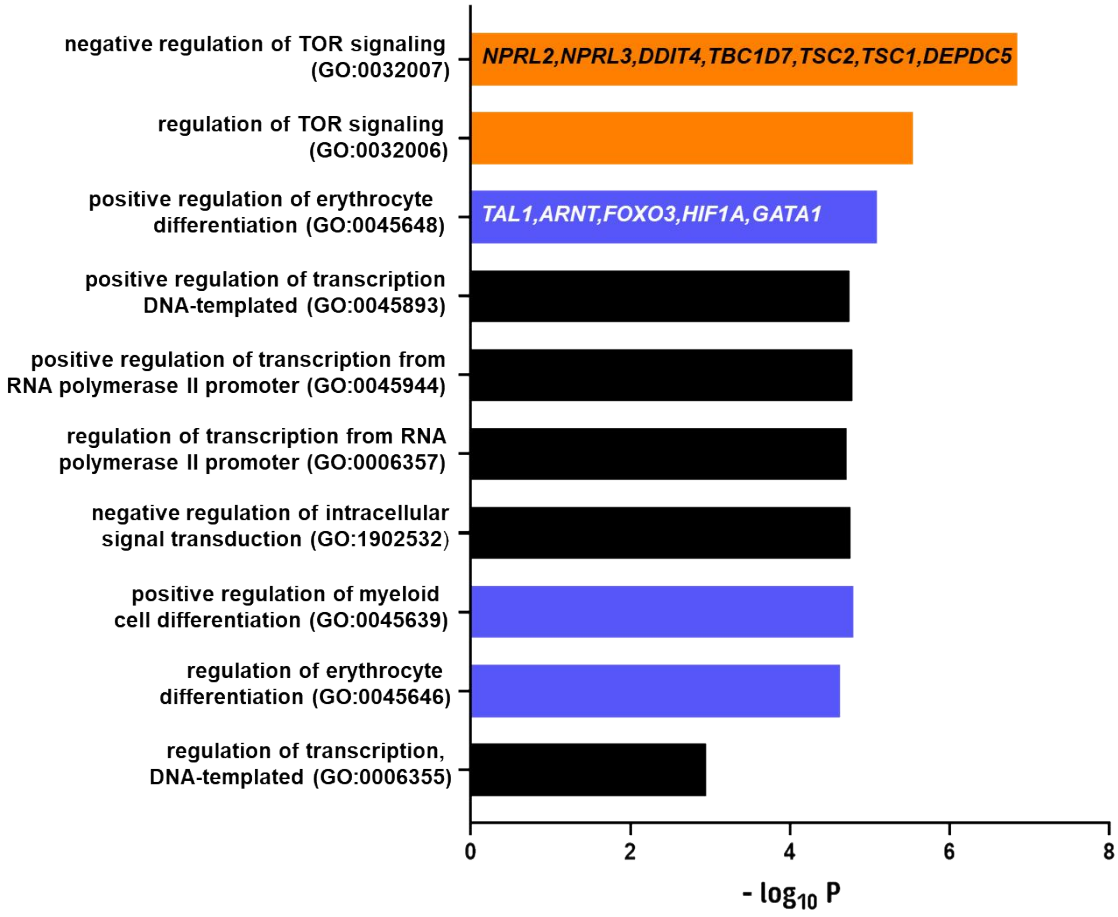

Figure 17: GO analysis of top 25 genes enriched in later time-point in both Homozygous and Heterozygous cell lines (orange: associated with mTOR signaling and blue: associated to erythroid differentiation)

We also analyzed the genes depleted at later time-point (Late synthetic lethal interactions) and submitted the list of these genes to EnrichR and GO analysis. The results from the submission revealed the association of the genes in MHC class 1 processing, mRNA splicing and protein response to misfolded protein (Appendix Tables: 3,4). Their association to mutCALR MPN disease progression is something that needs to be investigated.

We were particularly interested in the tumor suppressor gene cohort that was enriched at day 21 in the mutCALR cell lines (Figure 16). There were 45 genes that were significantly enriched in the mutCALR cell lines (Appendix: Table 5,6). The top 30 genes were associated with negatively regulating the mTOR signaling pathway and positively regulating erythroid differentiation.

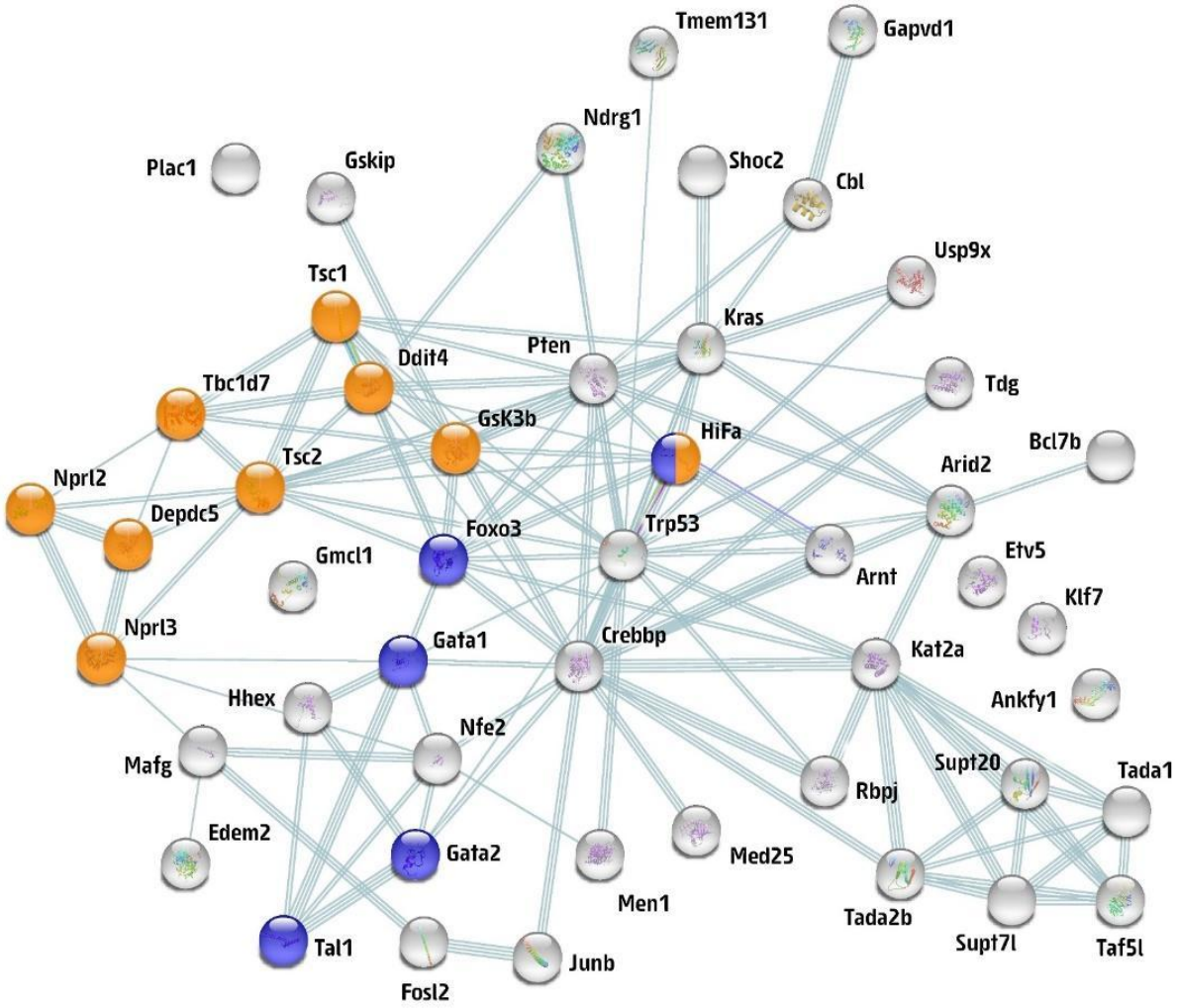

Figure 18: StringDB analysis of top 25 genes enriched in later time-point in both Homozygous and Heterozygous cell lines (orange: associated with mTOR signaling and blue: associated to erythroid differentiation)

We performed a gene-ontology analysis and negative regulation of mTOR ranked higher in the list. We further constructed a network map with StringDB to look at the dependency of genes that ranked significantly in both the cell lines. The components annotated in orange are components that are a part of mTOR signaling. The components annotated in blue are associated with playing a role in erythroid differentiation (Figure 17,18).

We selected the list of TSGs associated with the mTOR pathway and performed a functional validation. To validate both the list of potential candidates of tumor suppressor genes and synthetic lethal partners, individual CRISPR knock-outs cell lines were generated, and competition assays were performed (Figure 19).

For validating the synthetic lethal interactions, the wild-type pCas9 expressing cell lines and mutant mCherry positive pCas9 expressing cell line can be transduced with pLenti-guide Puro vector with guide-RNA targeting the gene. The cells can be combined in a 1:1 ratio and a competition assay can be performed.

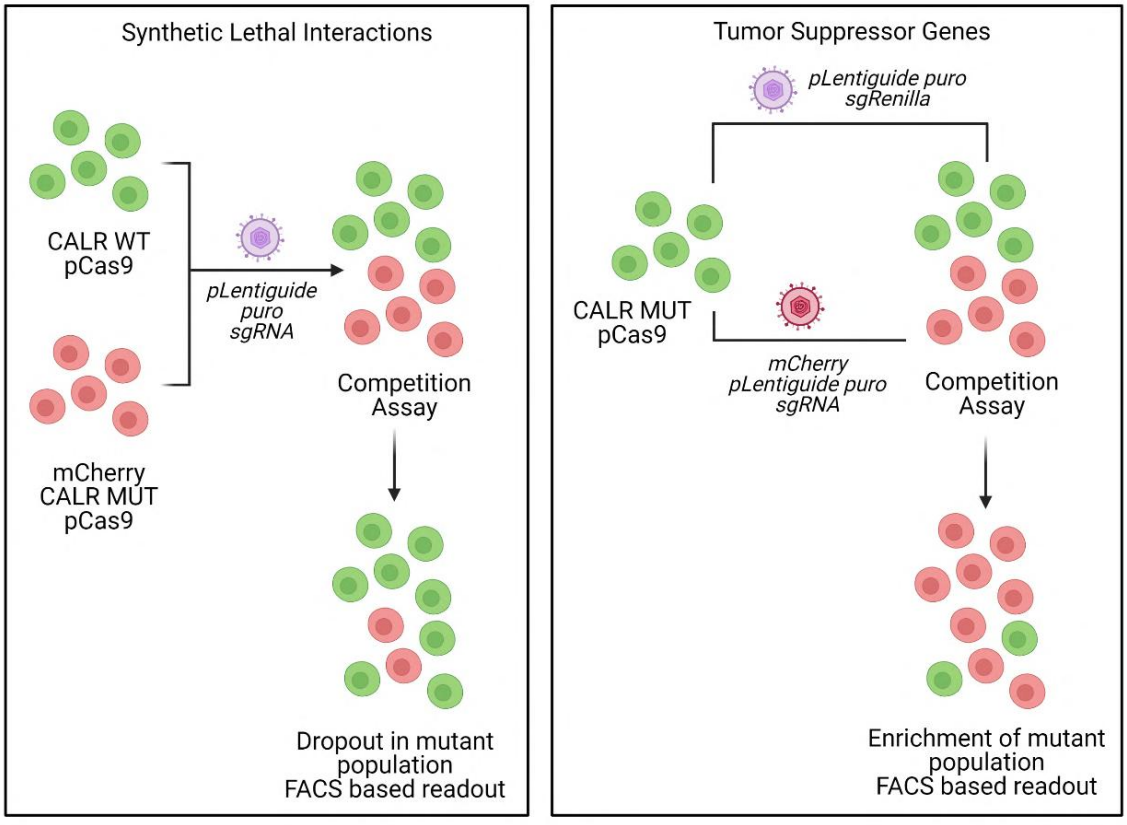

Figure 19: Competition assay setup to validate sgRNAs from tumor suppressor genes and synthetic lethal interaction cohorts

If the gene is a potential synthetic lethal partner, the number of mCherry positive cells will reduce over the time, which can be monitored by FACS based analysis.

For validating tumor suppressor genes, the mutCALR cell lines were transduced separately, 1) pLenti-guide Puro with sgRenilla plasmid and 2) mCherry positive pLenti-guide Puro with sgRNA targeting the gene of interest. A competition assay was performed and the reduction or increase in the population of mCherry positive cells was analyzed by timed analysis. If the gene of interest is a tumor suppressor, then it would give the cells the advantage of outgrowing the inherent population of cells transduced with sgRenilla.

We looked at the TSC2/TSC1 axis that ranked higher in our TSG cohort. We transduced the cell lines with a sgRNA targeting TSC2 according to our schematic plan. We cloned the TSC2 sgRNA1 and sgRNA2 into a mCherry-pLenti-guide-puro vector. Post transduction, we performed a competition assay and profiled for the mCherry positive cell over a period. The mCherry positive cells outgrow in the heterozygous competition setup by day 12 significantly but at a slower rate in the homozygous cell line. This shows the existence of a regulatory axis that could confer a proliferative advantage and worsen disease progression in mutant clones.

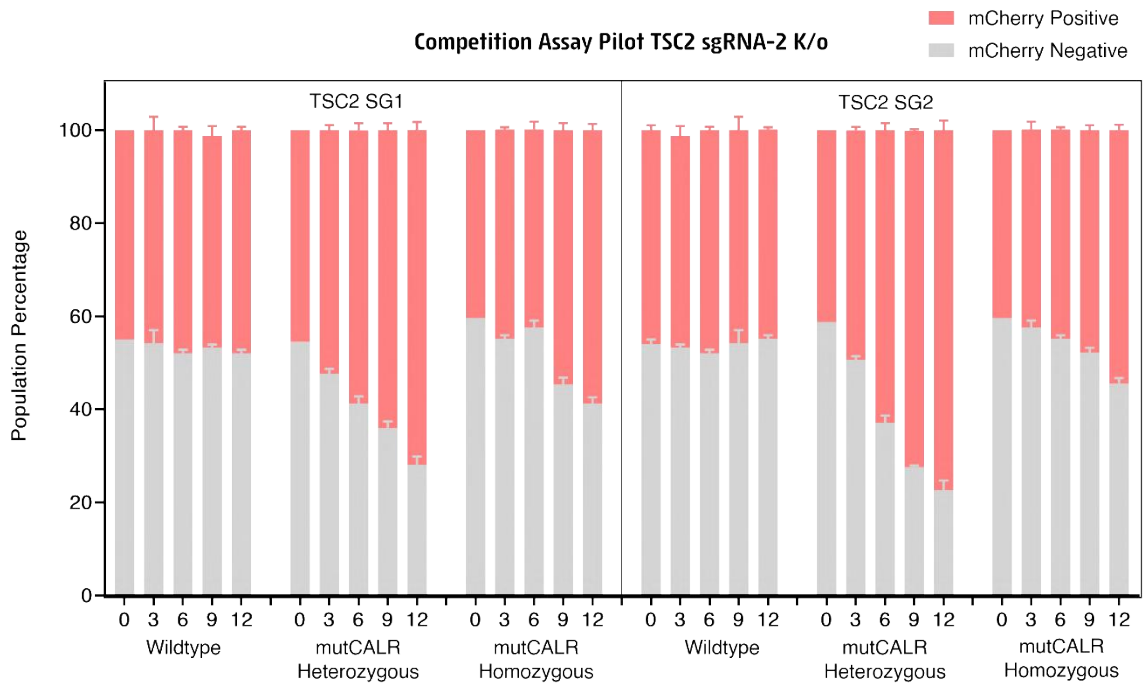

Figure 20: Competition Assay validating that the knockout of TSC2 with sgRNA1 and sgRNA2 in BaF/3 mutCALR Heterozygous and Homozygous cell lines

3.2.3 Negative regulators of mTOR pathway and their role in mutCALR driven MPN progression

Growth factors play a major role in activating the downstream signaling networks that activate the mTOR signaling pathway.

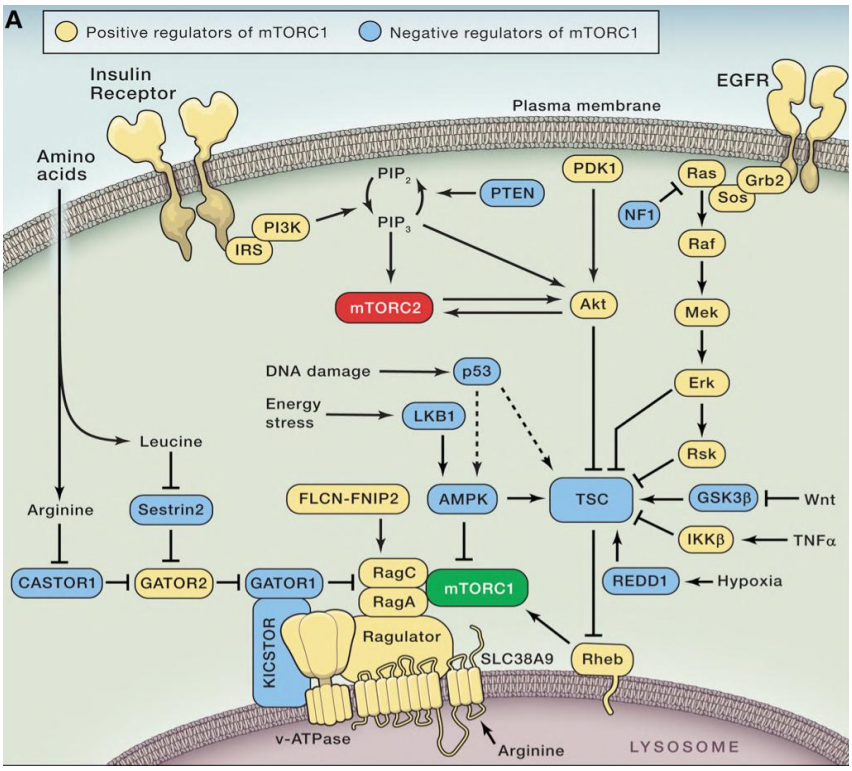

Figure 21: Snapshot of mTOR signaling pathway from (Saxton and Sabatini, 2017)

Two complexes mTORC1 and mTORC2 play a major role in promoting various processes driving key mechanisms and complexes annotated in yellow are positive regulators of mTOR signaling and those annotated in blue are negative regulators of the mTOR (Figure 21).

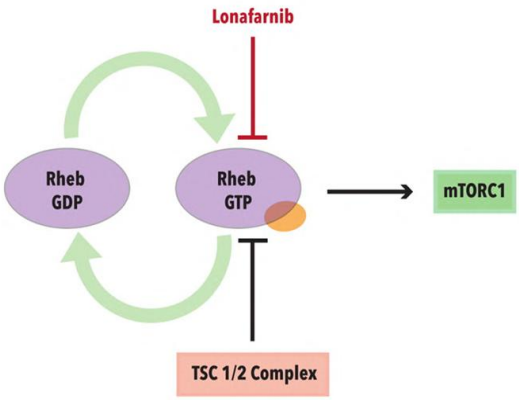

Figure 22: Interaction dynamics of TSC1/2 complex, mTORC1 and Rheb

The key components of TSGs identified from the BRIE screen list are associated with negatively regulating mTOR. We screened for small molecules that would target the positive regulators of mTOR. As TSC1/TSC2 axis was an interest, we looked for active Rheb inhibitors (Figure 22).

Lonafarnib, a farnesyl inhibitor, acts on mTORC1 and Rheb. There is a regulatory network that exists between these components. We performed a viability assay with the wildtype and human del52 overexpressed BaF/3 cell line.

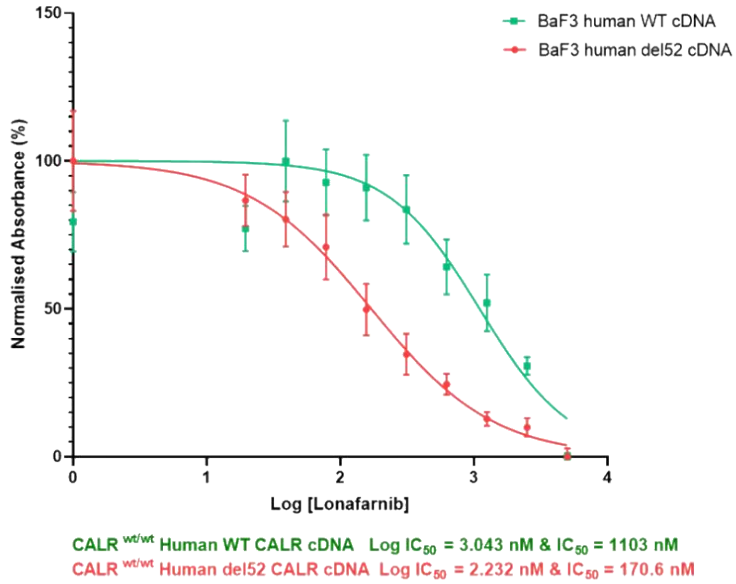

Figure 23: Cell viability assay depicting the effect of Lonafarnib on mutant cell line growth

From the luminescence values, we could see that the mutant cell line was more susceptible to the drug in comparison to the wildtype cell line (Figure 23). We also performed a similar assay with Rapalogs that are active inhibitors of mTORC1 complex (Appendix: Table 7). Lonafarnib fared well in comparison to other Rapalogs. The results have been annotated in the table below.

4. DISCUSSION

4.1 GENERAL DISCUSSION

Somatic mutations in CALR, JAK2, MPL drive the oncogenic signaling pathway of the three classical MPN subtypes (Klampfl *et al.*, 2013; Nangalia *et al.*, 2013). Since the discovery of CALR mutations, an emphasis has been laid in understanding the mechanism of disease progression. Calreticulin (CALR) is a molecular chaperone and is one of the major MPN driver mutations that is acquired in a mutually exclusive manner in comparison to JAK2 and MPL mutations. Two main mutations: del52 (a 52-bp deletion) and ins5 (a 5-bp insertion) account to around 80% in both ET and PMF patients. JAK-STAT signaling pathway is central to the oncogenic disease pathogenesis. MutCALR associates with the thrombopoietin receptor and is cycled to the cell surface as a complex. It serves as a *bona fide* tumor antigen that can be targeted via immunotherapy. Patients with CALR mutations have better prognosis and lower risk of thrombosis (Pietra *et al.*, 2016). With the current line of therapies that are focused at reducing the side-effects, there is a need for developing efficacious MPN-targeted therapies against mutant CALR. In this thesis, we describe a murine transgenic model that recapitulates MPN phenotype. We provide a proof of concept of an antibody-based immunotherapy intervention to target CALR positive MPN in mice. We also map mutCALR gene dependencies that would arguably provide insights into how mutCALR driven MPN gene networks look like and aid in the development of small molecule-based inhibitors for treating CALR positive MPN.

Mouse Models

In a pre-clinical setting, a relevant transgenic model serves as a platform to screen and understand mechanisms of therapeutic interventions. So far, there have been four disease models that have been established by various groups.

In this thesis, we describe a knock-in murine model that expresses mutCALR oncoprotein with human mutant del52 C-terminus. The gene is under the expression of an endogenous promoter and the use of vavCre mice restricts the expression of the transgene to the hematopoietic cell lineage. We generated a homozygous and heterozygous variant of the mice. The splenocytes from both the mice confirm the expression of the mutant protein. The disease is worse in the homozygous mice and both the mice have elevated platelet counts. Homozygous mice develop splenomegaly, have increased amounts of stem cells and megakaryocytes in the bone marrow. We transplanted the mutant stem cells from homozygous mice in a competitive BMT. The mutant cells outgrow the wildtype cells which was further confirmed by the chimerism percentage. Our mice have all the characteristics mimicking

human MPN. We would like to see how we can model it to assess the success of potential therapeutic interventions. This would give us insights into developing efficient MPN targeted therapies.

mutCALR mouse models have already been established by many research groups. Increased platelet numbers are a characteristic of MPN phenotype. Two transgenic models that were established with one expressing human mutCALR (del52) under MHC-I promoter and the other expressing murine mutCALR have a slight increase in platelet numbers in comparison to our transgenic mouse model (Li et al., 2018, Shide et al., 2020). The next mutCALR models used a similar knock-in strategy like our transgenic model and they also express hybrid murine-human mutCALR. The peripheral blood parameters of these transgenic mice were concomitant with our mutCALR murine model. These mice develop a phenotype reiterating human MPN and the disease was also much severe in our mutCALR homozygous mice (Li et al., 2018, Balligand et al., 2020, Shide et al., 2020, Benlabiod et al., 2020). mutCALR stem cells also show clonal fitness in a competitive bone transplant as previously reported by Benlabiod et al., 2020. Transgenic mice harboring homozygous mutation for mutCALR don't survive past embryogenesis (Li et al., 2018, Balligand et al., 2020, Shide et al., 2020, Benlabiod et al., 2020).

None of these models have explored the option of studying the implications of targeted therapies against mutCALR driven MPN. Herein, we provide a proof of concept that mutCALR is a *bona fide* tumor antigen that can be targeted with monoclonal antibodies raised against the mutant C-terminus. We further assess the applicability of immunotherapeutic interventions and assess the challenges that would be potentially faced during administration at clinics.

Transcriptome network of hematopoietic stem cells

We further wanted to analyze the transcriptome of the mutant stem cells and dissect the regulatory gene-sets that would be enriched or depleted in the mutant cell population. To test this, we sorted hematopoietic stem cells and performed full length mRNA sequencing. GSEA revealed key significant gene-sets that can be categorized into oncogenic signaling, cell cycle control, inflammation, and metabolism. In oncogenic signaling, there was a significant enrichment of genes associated with K-ras, Mtorc1, p53 and JAK-STAT signaling. A similar gene-signature identified in mutCALR positive patients. We also see an enrichment of genes that are *bona fide* STAT5 targets. Many key pathways are known to feed into the JAK-STAT signaling pathway. The prominence of their role in the exacerbation of the disease is yet to be elucidated. P53 signaling is another pathway that is commonly seen to be deregulated in MPN. There is a correlation between levels of p53 and JAKV617F in MPN progression (Zhao *et al.*,

2013; Chen *et al.*, 2014). Chronic inflammation is another hallmark of MPN (Uras *et al.*, 2019). We also identified gene-sets associated with TNFα, IFNα and IFNγ signaling to be significantly upregulated. NFKB is considered as the master regulator of inflammation. It would be interesting to see the cytokine profile of plasma isolated from the bone marrow. This would further give information on different cytokines that aid in MPN progression. Inflammatory cytokines are also known to drive the niche architecture in remodeling the micro-environment and promoting fibrosis. Cholesterol homeostasis significantly ranked higher in mutant stem cells. CALR is a molecular chaperone and the mutation in the exon 9 region of the gene, leads to the loss negatively charged C-terminus and hence impairment of calcium binding. ER luminal calcium plays a crucial role in cholesterol sensing and because of the dysregulated calcium signaling, this could impact the cholesterol homeostasis (Wang *et al.*, 2017). Further, gene-sets associated with G2M checkpoints and E2F targets were significantly downregulated in the mutant stem cell pool. It is already known that JAKV617F patients have impaired replication fork machinery that interferes with intra-S checkpoint during cell division (Chen *et al.*, 2014). It would be interesting to explore the role of G2M checkpoints and E2F targets in promoting mutCALR driven MPN progression. Our group identified a greater number of pathways from our transcriptome profiling of stem cells in comparison to the single-cell RNA-seq data published in (Prins *et al.*, 2020).

Assessing success of immunotherapies against mutant CALR epitopes

A paper published by (Morten Orebo Holmström *et al.*, 2018; Holmström, Hasselbalch and Andersen, 2020) identified a spontaneous T-cell response in MPN patients against a PD-L1 derived epitope. This paved a way to further hypothesize that both JAKV617F and mutCALR epitopes are recognized by T-cells. There is a study that is underway that measures the Immunological response to vaccination in patients with CALR-mutant MPN vaccinated with a CALR exon 9 mutated peptide (Holmström *et al.*, 2019). MutCALR, because of the loss of K-DEL sequence is assumed to be secreted out. This was also identified in patients with mutCALR positive MPN (Pecquet *et al.*, 2019). The information on the pathophysiological role of secreted antigen needs to be evaluated. It could potentially interfere with therapeutic interventions by acting as a decoy epitope. Further, it could lead to the activation of JAK-STAT signaling pathway in mutant clones and niche cells. A study mapping the mutational landscape in MPN patients elucidated putative targets for immunotherapy. This also laid a foundation towards exploring the development of personalized anti-tumor responses in MPN patients (Schischlik *et al.*, 2018).

In comparison to patients with JAKV617F mutations, CALR mutations have better prognosis. The current treatment options for MPN patients have their own drawbacks. There is a need to develop targeted therapies that would circumvent key challenges faced by the current line of treatments. Allogenic stem-cell transplant is the last option in patients with worse disease prognosis but the morbidity associated with the procedure has its own complications (Braun and Zeiser, 2020). mutCALR interacting with MPL receptors as a complex serves as a cancer antigen. We generated a mouse model that develops MPN phenotype. To test the hypothesis, that immunotherapy can be used as a form of targeted therapy against mutant clones. We administered anti-mutCALR mAb against human del52 sequence in homozygous mice.

The antibody could effectively target the stem cells and multipotent progenitors in both spleen and bone marrow compartment. The vavCre mice were unaffected by the treatment. This further confirms the specificity of the treatment towards mutCALR. The treatment brought down the levels of platelets in the first six hours and this relapsed to thrombocythemic phase during the 18hr window. This shows that the mAb needs to be administered frequently at regular intervals for the half-life of the antibody to persist in the system and for the treatment to show some efficacy. The treatment didn't show much change in the levels of megakaryocytes. The mutant megakaryocyte that is the major culprit, shedding the enormous amount of platelets, is either hidden in the niche or the antibody needs to further tackle the amount of platelets in the periphery, deplete them to be able to target the megakaryocyte mutant clone.

The mechanism of action is something that needs to be investigated. We assume that the antibody immunodepletes the mutant clone either via ADCC (antibody dependent cell mediated cytotoxicity), CDC (complement dependent cytotoxicity) or ADCP (antibody dependent cell mediated phagocytosis) (Lu *et al.*, 2018; Van Erp *et al.*, 2019). We performed cell-surface staining to identify the levels of mutCALR. We could identify the presence of the antigen on lineage negative cells, megakaryocytes and LSKs.

Another factor influencing the antibody-effector function dynamics is the presence of a secreted antigen acting as a decoy epitope. We know that mutCALR is secreted in patients, this was also proved in analyzing cell culture supernatants. In the paper, we show that mutCALR is not only on the cell surface but is secreted out into the extracellular milieu of the mouse plasma. We also wanted to see if we could use these mice to profile the pathophysiological role of the secreted antigen. We see that the amount of the secreted antigen is in correlation with the amount that is seen to be secreted in patients. This led us to postulate that the secreted antigen might act as a sink for potential therapeutics, interfering with the efficacy of potential regimes. We further show that sCALR (secreted CALR) forms

immune complexes and could be cleared out via unknown mechanisms. This confirms that although the anti-mutCALR antibody binds secreted CALR, it is still able to reduce platelet counts and target the bone marrow stem cells.

For developing a successful therapeutic intervention against mutCALR, one must be aware of the potential challenges: the platelets and sCALR. Another approach to improve efficacy is to profile the epitopes of cell-surface mutCALR and sCALR. One could use a dual targeting combination treatment focused on clearing not only mutCALR cells but sCALR with the same efficacy. We show that our mouse model can be used as a platform to assess the success of immunotherapeutic interventions raised against human mutCALR epitopes.

Mapping cancer dependencies that aid in driving MPN progression

The advent of high throughput technologies has revolutionized ways to understand mechanisms of disease progression. It laid a foundation to aiding in the development of new therapeutics and charting out gene interaction networks. Despite the current treatment regimens to combat cancer in general, many therapies don't make it to clinics at the end of the day. It is necessary to find new ways to engineer new drugs or make use of existing drugs to augment the target treatment stratification. Identification of vulnerabilities that can be defined as genetic dependencies can help in building a cancer dependency map that can guide in classifying new drug targets and reveal ways to kill cancer cells with better precision (McDonald *et al.*, 2017; Tutuncuoglu and Krogan, 2019).

Cancer cells accumulate many mutations over a period that break important regulatory circuits. The ability of cancer cells to evade death by being able to adapt and activate certain gene circuits attributes to the characteristic of the cancer cell to acquire a dependency on one pathway. One can leverage this by deactivating each gene individually in a cancer cell to identify this dependency. Gene-gene dependencies can be categorized into synthetic lethal interactions that are detrimental for cancer cell's survival or tumor suppressor genes that exacerbate the disease progression ('Mapping Out Cancer Dependencies', 2017; Wang *et al.*, 2020). CRISPR-Cas9 technology has transformed genome editing. It has helped in understanding disease pathogenesis better. We can currently establish genome-wide genetic perturbation screens that target genes individually in many cancer cells in a moment (Ran *et al.*, 2013; Zhou *et al.*, 2014; Hartenian and Doench, 2015). The cohort of genes identified in this manner can be used for constructing network maps that would be unique to that cancer/oncogene.

In mutCALR driven MPN, not much is known about the regulatory networks that aid in the mutant clone's survival or death. It's necessary to chart a mutCALR driven MPN dependency map that would open more avenues to target and identify new drug targets. To achieve this objective, we established a genome-wide CRISPR-Cas9 screen using the BRIE library *in vitro*. We profiled the DNA on day 7 and day 21. We saw a drop out of CALR control guide RNA in mutCALR cell lines signifying its essentiality for a clone's survival. From the screen, we identified a high penetrance synthetic lethal interaction that is associated with ribosome and proteasome machinery. In the list of tumor suppressor genes, enriched at a later time-point we see core components of negative regulation of mTOR and positive regulators of erythroid differentiation to be significantly ranked high.
We further pursued the mTOR signaling network. Our hematopoietic stem cell transcriptome data also shows the enrichment of Mtorc1 signaling in mutCALR LSKs. This also proves a dependency that exists between mutCALR and mTOR framework. From the genetic perturbation screen data, we see TSC1/TSC2 complex, DEPDC5, NPRL2/3, DDIT4 are genes of mTORC1 signaling that ranked significantly higher. We generated single guide-RNA knockouts of the genes to validate them *in vitro*. We see that the knock-out of TSC2 gene with two different guide-RNAs gives a proliferative advantage to mutCALR cells aiding in their viability. Homozygous cell line has a slower growth advantage in comparison to heterozygous cell line by day 12.

From available literature search, we looked for active inhibitors of mTORC1 signaling with a particular focus on the TSC1/TSC2 axis. We identified that the knockout of this axis releases the control of keeping mTORC1 phosphorylated. A hyper-phosphorylated mTORC1 can drive the expression of downstream targets. The control of this modification is monitored by Rheb in its active form. Rheb cycles between an active and inactive form, TSC1/TSC2 complex controls the Rheb cycling. We screened for small molecules that are inhibitors of Rheb or mTORC1 (Inoki *et al.*, 2003; Long *et al.*, 2005; Sato, Umetsu and Tamanoi, 2008). We identified Lonafarnib, a farnesyl-transferase inhibitor and few rapalogs and performed a dose-response assay. Interestingly, our mutant cells were more susceptible to drugs in comparison to wildtype cells.

It is well known that many pathways seep into mutCALR driven MPN axis and this is further confirmed by our transcriptome data. Many studies cite synergistic targeting of the JAKV617F cell lines in combination therapy of ruxolitinib and mTOR drugs. The proposed mechanism of action of dependency is something that isn't really explored (Vannucchi *et al.*, 2011; Bartalucci, Guglielmelli and Vannucchi, 2013; Bartalucci *et al.*, 2017). A genetic perturbation screen provides a plethora of information and there are still other gene-gene dependencies that are

yet to be investigated. The *in vitro* data and validation can only be supplemented with promising *in vivo* data. Our mouse model provides a platform that can be used for screening validated drug targets of mTOR and identifying the after-effects of knock-out TSC2 in LSKs. There are still many unanswered questions, such as if this would impact the niche dynamics and worsen disease progression. This can be followed up with an *in vivo* screen and treating the animals with inhibitors of positive regulators of mTOR.

4.2 CONCLUSION AND FUTURE PROSPECTS

Our study shows that hybrid murine-human mutCALR (del52) expressing mice reiterate human MPN. These mice show all the classical MPN hallmarks. mutCALR associates with the thrombopoietin receptor and is presented on the cell surface as a complex and is a *bona fide* tumor antigen. Herein, we assess the applicability of naked antibody therapeutics in the form of a monoclonal antibody (mAb) against human mutCALR epitope. The anti-mutCALR mAb effectively targets LSKs in both spleen and bone-marrow compartment.

We also dissected cancer gene dependencies of mutCALR driven MPN by establishing a genome-wide genetic perturbation screen *in vitro* using CRISPR-Cas9 technology. We identified that there exists a regulatory axis that exists between mTOR and mutCALR. We observed that knock-out of negative regulator of mTOR signaling, TSC2 boosts the proliferative potential of mutCALR cells *in vitro* in a competition assay. However, the use of mTOR inhibitors against positive regulators of mTOR signaling, RheB and mTORC1 limits the proliferative potential of mutCALR murine cells *in vitro* in a viability assay.

In summary, mutCALR mice serve as a relevant model to assess and understand the molecular mechanisms behind potential immunotherapeutic interventions to target mutCALR driven MPN. mutCALR transgenic model can also be used for evaluating the success of gene therapy and for profiling small molecule therapeutic intervention.

4.2.1 Immunotherapeutic development and beyond

There are many crucial questions that still need to be addressed. The effect of monoclonal antibody against the mutant stem cell pool in a competitive bone marrow transplant would be important. Will the co-existence of wildtype and mutant cells in the niche impact or add to the list of existing challenges faced by immunotherapy?

We do see that the amount of sCALR increases over a period in the periphery and this is correlated with the increasing mutant chimerism percentage. What is the pathophysiological role of sCALR in the extracellular milieu? The antibody effectively reduces the amount of sCALR and clears it out of the system via formation of immune complexes. It doesn't constitute an antibody sink as the stem cells are effectively targeted in our study. Another important question that still needs to be dissected is the mechanism of immune depletion. Is it by ADCC, CDC or ADCP? This is something that will need to be addressed.

For the treatment to show efficacy long-term, the mAb needs to be administered at regular intervals. This can be circumvented with a use of subcutaneous osmotic pumps that will release the antibody at a constant flow-rate, thereby maintaining its half-life in the circulatory system. This will not only eliminate the mutant stem cell from the niche but will also effectively target the mutant megakaryocyte clone that is responsible for such high platelet shedding. The use of osmotic pumps would be a representative of how the patient is administered with antibody clinics in a drip-wise infusion.

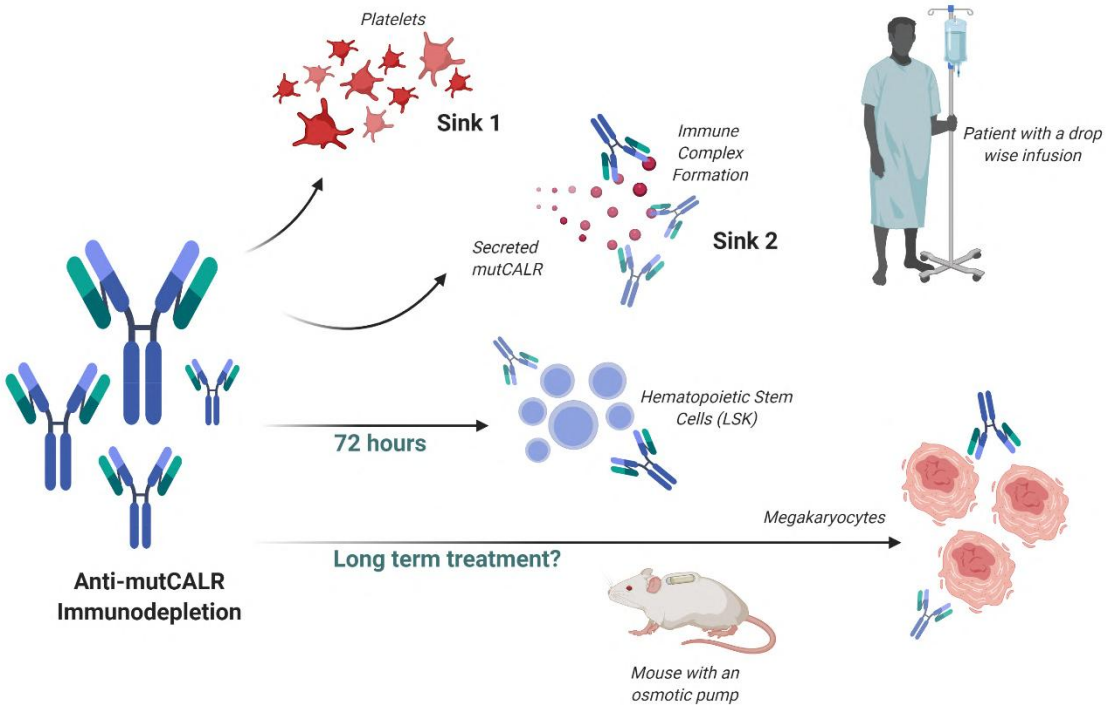

Figure 24: Challenges faced by potential anti-mutCALR immunotherapeutic pipelines

Efficacy of direct targeting of the tumor can be improved with the use of radio-immunotherapy, antibody-drug conjugates, and immunotoxins. For radio-immunotherapy, monoclonal antibodies can be conjugated to radioisotopes of Iodine-131 or Yttrium-90. The radioisotopes are delivered to the targets and efficiently can eliminate the tumor population. One of the demerits of this technology are the ability of the radioimmunotherapy agents to kill nearby cells in the vicinity. Another strategy is the use of antibody drug conjugates and immunotoxins, single chain variable fragments (scFv) against the mutant protein can be coupled to cytotoxic drugs or immunotoxins. These immunotherapy agents are endocytosed upon the binding of scFv to the mutant protein sitting on the surface in a complex with the thrombopoietin receptor. The cytotoxic drug or the toxin are delivered into the cell via receptor mediated endocytosis, thereby killing the tumor cell.

An effective way to improve efficacy is to explore the option of T-cell engaging therapies wherein the induction or enhancing the activity of tumor-specific T cells to recognize and kill tumor cells. Immune checkpoint inhibitors, stimulatory agonists and cellular therapies comprise this category. Tumor cells evade immune surveillance mechanisms and T-cells that have been raised against neo-antigens may be rendered ineffective in the tumor microenvironment. The tumor cells escape from targeting of these anti-tumor T-cells by activating immune checkpoints and blocking of these checkpoints can enhance the ability of anti-tumor cells to detect and kill the mutant cancer cell. Bi-specific T-cell engagers or Bi-specific antibodies can also stimulate and improve the specificity of T cells. They are constructed with a scFv binding to two different antigens and other being able to activate the T-cell receptor. CART is another form of therapy that uses a chimeric antigen receptor that is cloned into a construct comprising scFv that can recognize the mutant antigen and is coupled with an intracellular domain that can activate T-cell plus a co-stimulatory domain. The manufactured and re-engineered T-cells with the CAR construct can be injected into patients, aiding in accentuating the efficacy of treating mutCALR driven MPN.

4.2.2 Mapping cancer dependencies and beyond

To confirm the relevance of the differentially expressed genes for the oncogenic function of mutated CALR, a low-complexity *in vivo* screen using the CRISPR-Cas9 technology will be performed. A library of guide-RNAs (gRNAs against the target identified from the *in vitro* screen will be generated and respective validation experiments will be performed.

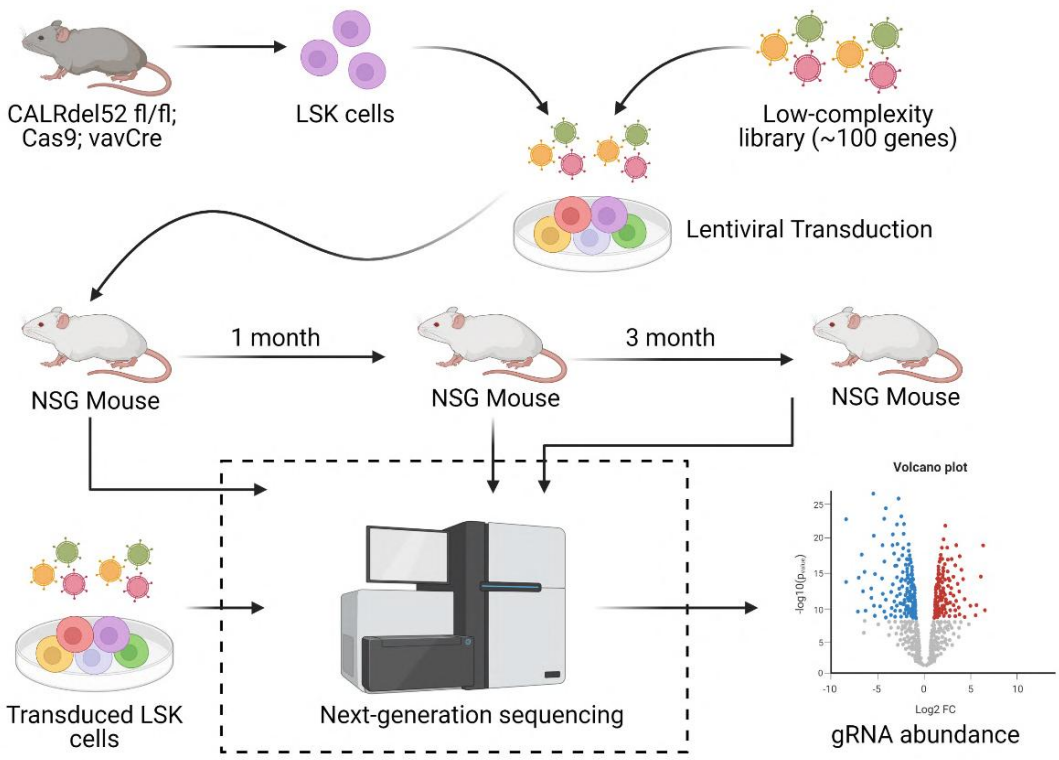

Figure 25: *in vivo* screen to functionally validate genes from BRIE *in vitro* screen

Lineage negative cells from CALRdel52fl/fl;Cas9;vavCre mice will be obtained and will be transduced with lentiviral pools expressing gRNAs (at least 3 gRNAs against every target gene) against the upregulated/downregulated genes. The transduced cells will be selected with the appropriate selection marker and part of the sample will be collected as a reference for basal gRNA composition.

The rest of the cells will be transplanted into NSG mice and samples will be collected from mice at early phase and late phase, 1 month and 6 months post transplantation, respectively. Hematopoietic progenitors from at least 3 mice per time point will be analyzed. Next-generation sequencing will be performed to identify the composition of the gRNAs in the different samples and bioinformatics tools will be used to visualize the changes in the gRNA composition over time.

The *in vitro* CRISPR screen has allowed for the identification of differentially expressed genes in the presence of CALR-del52. The genes that are most relevant for the CALR-del52 driven oncogenic program will be identified by the *in vivo* CRISPR-Cas9 screen. This subset will be enriched in genes that represent the best targets. Analyses of the individual candidate genes in detail may lead to identification of novel therapeutic interventions within the context of CALR mutant proteins.

5. MATERIALS AND METHODS

5.1 Cell line and reagents

Ba/F3-MPL cell lines were generated as previously described (Nivarthi *et al.*, 2016). Ba/F3 cells were maintained with 5% WEHI-3B conditioned media as murine IL-3 supplement. Mycoplasma testing was conducted biweekly.

5.2 Cloning and lentiviral transduction

sgRNAs were cloned into pLentiguide-puro vector and mCherry-pLentiguide-puro vector. Lentiviral particles were generated as suggested in (Doench *et al.*, 2016).

gRNA list:

S.No	gRNA Name	Sequence
1	EGFP	GAGCTGGACGGCGACGTAAA
2	TSC2 sg1	TGAACCACATGGCTATGACG
3	TSC2 sg2	CTGATCCTAGCACACATGTG

5.3 Genome-wide CRISPR-Cas9 screen

5.3.1 Virus production

Genome wide BRIE CRISPR library virus was amplified and the lentivirus produced using standard transduction protocols as suggested by the distributor (Pooled Library #73633). Lenti-X HEK-293T cells were seeded at 40% confluency in DMEM (10% FBS) in 12cm dishes. After 24 hours, the cells were transfected using Lipofectamine® 2000 with the amplified library, pVSVG and psPAX2 lentiviral packaging plasmids. The medium was changed after 6 hours. The lentivirus was harvested at 54 hours and filtered through a 0.45 µm filter.

5.3.2 Screen setup

Ba/F3 wt/wt, Ba/F3 wt/mut and Ba/F3 mut/mut stably expressing pCas9 were kept on selection with blasticidin at 25ng/ul before starting with the screen. The cells were infected at a MOI of 0.3-0.5 with a screen coverage of 1000x. Two biological replicates were performed for each screen. 300 million cells were seeded into 6 well plates at a seeding density of 5 million cells/well in 3ml of media supplemented with the virus. Polybrene was added at the final concentration of 8 µg/mL. The cells were spin-infected at 2,000 rpm, 37 °C, for 1 hours, pooled and transferred to T-150 flasks. On second day, the media was changed, and they were selected with 1,25 µg/mL of puromycin on day 3. 100 million cells were pelleted on day 7 and the cells were kept in culture for 20 days after puromycin selection and split every 2–3 days to

avoid confluency. 100 million cells were pelleted on day 21. The DNA was extracted from the pellets using the QIAGEN Blood & Cell Culture Maxi Kit, according to the manufacturer's protocol.

5.3.3 sgRNA amplification and sequencing

Amplification and sequencing of the samples was pursued according to (Doench *et al.*, 2016)

5.3.4 Screen analysis, pathway construction, statistical analysis and data visualization

The analysis was performed according to Mageck pipeline (Li *et al.*, 2014) and Pin-APL-Py, a web-interface analysis tool (Spahn *et al.*, 2017). Gene ontology enrichment analysis was performed submitting the top 50 genes to EnrichR and the pathway map was constructed using StringDB. All data analytics and visual representations of the screen were made from processing files through R-script, PinAPLPy interface (Spahn *et al.*, 2017) and using the Mageck pipeline (Li *et al.*, 2014).

5.4 Cell viability assay

Wildtype and mutCALR Ba/F3 cells were seeded at 5,000 cells/well in RPMI media into 96-well plates. Desired concentrations of mTOR drugs were added in serial dilutions to make up the volume to 100ul with cells. After 72 hours, cell viability was measured by performing CellTiter-Glo luminescent Cell Viability Assay where luminescence was measured.

5.5 Competition assay

Cell lines were transduced with pLentiguide-mCherry-sgRNA constructs and the fluorescence positive cells were sorted by SH800Z Cell Sorter (Sony). mCherry positive cell lines were mixed 1:1 with their non-fluorescent control cells and were seeded every 3rd day till day 12. Cell samples at each time point were analyzed by flow cytometry.

6. LIST OF FIGURES

7. REFERENCES

1. Achyutuni, S. et al. (2021) ' Hematopoietic expression of a chimeric murine-human CALR oncoprotein allows the assessment of anti-CALR antibody immunotherapies in vivo ', American Journal of Hematology. doi: 10.1002/ajh.26171.
2. Andrikovics, H. *et al.* (2014) 'Distinct clinical characteristics of myeloproliferative neoplasms with calreticulin mutations', *Haematologica*. doi: 10.3324/haematol.2014.107482.
3. Araki, M. *et al.* (2016) 'Activation of the thrombopoietin receptor by mutant calreticulin in CALR-mutant myeloproliferative neoplasms', *Blood*. doi: 10.1182/blood-2015-09-671172.
4. Balligand, T. *et al.* (2020) 'Knock-in of murine Calr del52 induces essential thrombocythemia with slow-rising dominance in mice and reveals key role of Calr exon 9 in cardiac development', *Leukemia*. doi: 10.1038/s41375-019-0538-1.
5. Bartalucci, N. *et al.* (2017) 'Inhibitors of the PI3K/mTOR pathway prevent STAT5 phosphorylation in JAK2V617F mutated cells through PP2A/ CIP2A axis', *Oncotarget*. doi: 10.18632/oncotarget.18073.
6. Bartalucci, N., Guglielmelli, P. and Vannucchi, A. M. (2013) 'Rationale for targeting the PI3K/Akt/mTOR pathway in myeloproliferative neoplasms', *Clinical Lymphoma, Myeloma and Leukemia*. doi: 10.1016/j.clml.2013.07.011.
7. Benlabiod, C. *et al.* (2020) 'Calreticulin del52 and ins5 knock-in mice recapitulate different myeloproliferative phenotypes observed in patients with MPN', *Nature Communications*. doi: 10.1038/s41467-020-18691-3.
8. Bowman, R. L., Busque, L. and Levine, R. L. (2018) 'Clonal Hematopoiesis and Evolution to Hematopoietic Malignancies', *Cell Stem Cell*. doi: 10.1016/j.stem.2018.01.011.
9. Braun, L. M. and Zeiser, R. (2020) 'Immunotherapy in Myeloproliferative Diseases', *Cells*. doi: 10.3390/cells9061559.
10. Chachoua, I. *et al.* (2016) 'Thrombopoietin receptor activation by myeloproliferative neoplasm associated calreticulin mutants', *Blood*, 127(10), pp. 1325–1335. doi: 10.1182/blood-2015-11-681932.
11. Chen, E. *et al.* (2014) 'JAK2V617F promotes replication fork stalling with disease-restricted impairment of the intra-S checkpoint response', *Proceedings of the National Academy of Sciences of the United States of America*. doi: 10.1073/pnas.1401873111.
12. Curto-Garcia, N., Harrison, C. and McLornan, D. P. (2020) 'Bone marrow niche dysregulation in myeloproliferative neoplasms', *Haematologica*. doi: 10.3324/HAEMATOL.2019.243121.
13. Doench, J. G. *et al.* (2016) 'Optimized sgRNA design to maximize activity and minimize off-target effects of CRISPR-Cas9', *Nature Biotechnology*. doi: 10.1038/nbt.3437.

14. Elf, S. *et al.* (2015) 'Physical Interaction Between Mutant Calreticulin and the Thrombopoietin Receptor Is Required for Hematopoietic Transformation', *Blood*. doi: 10.1182/blood.v126.23.lba-4.lba-4.
15. Van Erp, E. A. *et al.* (2019) 'Fc-mediated antibody effector functions during respiratory syncytial virus infection and disease', *Frontiers in Immunology*. doi: 10.3389/fimmu.2019.00548.
16. Fleischman, A. G. *et al.* (2011) 'TNFα facilitates clonal expansion of JAK2V617F positive cells in myeloproliferative neoplasms', *Blood*. doi: 10.1182/blood-2011-04-348144.
17. Fouad, Y. A. and Aanei, C. (2017) 'Revisiting the hallmarks of cancer', *American Journal of Cancer Research*.
18. Han, L. *et al.* (2016) 'Calreticulin-mutant proteins induce megakaryocytic signaling to transform hematopoietic cells and undergo accelerated degradation and Golgi-mediated secretion', *Journal of Hematology and Oncology*. Journal of Hematology & Oncology, 9(1), pp. 1–14. doi: 10.1186/s13045-016-0275-0.
19. Hanahan, D. and Weinberg, R. A. (2011) 'Hallmarks of cancer: The next generation', *Cell*. doi: 10.1016/j.cell.2011.02.013.
20. Hartenian, E. and Doench, J. G. (2015) 'Genetic screens and functional genomics using CRISPR/Cas9 technology', *FEBS Journal*. doi: 10.1111/febs.13248.
21. Holmström, Morten Orebo *et al.* (2018) 'Spontaneous T-cell responses against the immune check point programmed-death-ligand 1 (PD-L1) in patients with chronic myeloproliferative neoplasms correlate with disease stage and clinical response', *OncoImmunology*. doi: 10.1080/2162402X.2018.1433521.
22. Holmström, M. O. *et al.* (2018) 'The calreticulin (CALR) exon 9 mutations are promising targets for cancer immune therapy', *Leukemia*, 32(2), pp. 429–437. doi: 10.1038/leu.2017.214.
23. Holmström, M. O. *et al.* (2019) 'High frequencies of circulating memory T cells specific for calreticulin exon 9 mutations in healthy individuals', *Blood Cancer Journal*. doi: 10.1038/s41408-018-0166-4.
24. Holmström, M. O., Hasselbalch, H. C. and Andersen, M. H. (2020) 'Cancer immune therapy for Philadelphia chromosome-negative chronic myeloproliferative neoplasms', *Cancers*. doi: 10.3390/cancers12071763.
25. Inoki, K. *et al.* (2003) 'Rheb GTpase is a direct target of TSC2 GAP activity and regulates mTOR signaling', *Genes and Development*. doi: 10.1101/gad.1110003.
26. Iurlo, A., Cattaneo, D. and Gianelli, U. (2019) 'Blast transformation in myeloproliferative neoplasms: Risk factors, biological findings, and targeted therapeutic options', *International Journal of Molecular Sciences*. doi: 10.3390/ijms20081839.
27. Kallam, A. *et al.* (2019) 'Phase II multi-center study of ruxolitinib phosphate for the

treatment of relapsed or refractory diffuse large B-cell lymphoma (DLBCL) and peripheral T-cell lymphoma (PTCL).', *Journal of Clinical Oncology*. doi: 10.1200/jco.2019.37.15_suppl.e19063.

28. Klampfl, T. *et al.* (2013) 'Somatic Mutations of Calreticulin in Myeloproliferative Neoplasms', *New England Journal of Medicine*. doi: 10.1056/nejmoa1311347.
29. Li, B., Rampal, R. K. and Xiao, Z. (2019) 'Targeted therapies for myeloproliferative neoplasms', *Biomarker Research*. doi: 10.1186/s40364-019-0166-y.
30. Li, J. *et al.* (2018) 'Mutant calreticulin knockin mice develop thrombocytosis andmyelofibrosis without a stemcell self-renewal advantage', *Blood*. doi: 10.1182/blood-2017-09-806356.
31. Li, W. *et al.* (2014) 'MAGeCK enables robust identification of essential genes from genome-scale CRISPR/Cas9 knockout screens', *Genome biology*. doi: 10.1186/s13059-014-0554-4.
32. Long, X. *et al.* (2005) 'Rheb binds and regulates the mTOR kinase', *Current Biology*. doi: 10.1016/j.cub.2005.02.053.
33. Lu, L. L. *et al.* (2018) 'Beyond binding: Antibody effector functions in infectious diseases', *Nature Reviews Immunology*. doi: 10.1038/nri.2017.106.
34. M.H., E. *et al.* (2017) 'Ruxolitinib for the management of myelofibrosis: Results of an international physician survey', *Leukemia Research*.
35. 'Mapping Out Cancer Dependencies' (2017) *Cancer discovery*. doi: 10.1158/2159-8290.CD-NB2017-119.
36. Marty, C. *et al.* (2016) 'Calreticulin mutants in mice induce an MPL-dependent thrombocytosis with frequent progression to myelofibrosis', *Blood*. doi: 10.1182/blood-2015-11-679571.
37. Masarova, L., Bose, P. and Verstovsek, S. (2019) 'The Rationale for Immunotherapy in Myeloproliferative Neoplasms', *Current Hematologic Malignancy Reports*. doi: 10.1007/s11899-019-00527-7.
38. McDonald, E. R. *et al.* (2017) 'Project DRIVE: A Compendium of Cancer Dependencies and Synthetic Lethal Relationships Uncovered by Large-Scale, Deep RNAi Screening', *Cell*. doi: 10.1016/j.cell.2017.07.005.
39. Menden, M. P. *et al.* (2017) 'A cancer pharmacogenomic screen powering crowd-sourced advancement of drug combination prediction', *bioRxiv*. doi: 10.1101/200451.
40. Nangalia, J. *et al.* (2013) ' Somatic CALR Mutations in Myeloproliferative Neoplasms with Nonmutated JAK2 ', *New England Journal of Medicine*. doi: 10.1056/nejmoa1312542.
41. Nangalia, J. *et al.* (2019) 'Myeloproliferative neoplasms', in *Molecular Hematology*. doi: 10.1002/9781119252863.ch7.
42. Nivarthi, H. *et al.* (2016) 'Thrombopoietin receptor is required for the oncogenic function of

CALR mutants', *Leukemia*. doi: 10.1038/leu.2016.32.

43. Pecquet, C. *et al.* (2019) 'Calreticulin mutants as oncogenic rogue chaperones for TpoR and traffic-defective pathogenic TpoR mutants', *Blood*. doi: 10.1182/blood-2018-09-874578.
44. Picelli, S. *et al.* (2014) 'Full-length RNA-seq from single cells using Smart-seq2', *Nature Protocols*. doi: 10.1038/nprot.2014.006.
45. Pietra, D. *et al.* (2016) 'Differential clinical effects of different mutation subtypes in CALR-mutant myeloproliferative neoplasms', *Leukemia*. doi: 10.1038/leu.2015.277.
46. Prins, D. *et al.* (2020) 'The stem/progenitor landscape is reshaped in a mouse model of essential thrombocythemia and causes excess megakaryocyte production', *Science advances*, 6(48), pp. 1–13. doi: 10.1126/sciadv.abd3139.
47. Ran, F. A. *et al.* (2013) 'Genome engineering using the CRISPR-Cas9 system', *Nature Protocols*. doi: 10.1038/nprot.2013.143.
48. Reap, L. *et al.* (2020) 'Myeloproliferative Neoplasms with Subsequent Development of Chronic Myelogenous Leukemia: A Case Series', *Clinical Hematology and Research*. doi: 10.36959/831/380.
49. Rieger, M. A. and Schroeder, T. (2012) 'Hematopoiesis', *Cold Spring Harbor Perspectives in Biology*. doi: 10.1101/cshperspect.a008250.
50. De Roeck, L. *et al.* (2018) 'Coexisting driver mutations in MPN: clinical and molecular characteristics of a series of 11 patients', *Hematology*. doi: 10.1080/10245332.2018.1498182.
51. Sato, T., Umetsu, A. and Tamanoi, F. (2008) 'Characterization of the Rheb-mTOR Signaling Pathway in Mammalian Cells: Constitutive Active Mutants of Rheb and mTOR', *Methods in Enzymology*. doi: 10.1016/S0076-6879(07)38021-X.
52. Saxton, R. A. and Sabatini, D. M. (2017) 'mTOR Signaling in Growth, Metabolism, and Disease', *Cell*. doi: 10.1016/j.cell.2017.02.004.
53. Scanlon, T. C., Dostal, S. M. and Griswold, K. E. (2014) 'A high-throughput screen for antibiotic drug discovery', *Biotechnology and Bioengineering*. doi: 10.1002/bit.25019.
54. Schischlik, F. *et al.* (2018) 'Mutational Landscape of the Transcriptome Offers a Rich Neoantigen Resource for Immunotherapy of Myeloproliferative Neoplasms', *Blood*. doi: 10.1182/blood-2018-99-118049.
55. Shide, K. *et al.* (2020) 'Calreticulin haploinsufficiency augments stem cell activity and is required for onset of myeloproliferative neoplasms in mice', *Blood*. doi: 10.1182/blood.2019003358.
56. Soret, J. and Kiladjian, J. J. (2016) 'The role of ruxolitinib in the treatment of myeloproliferative neoplasms', *Bulletin du cancer*. doi: 10.1016/S0007-4551(16)30143-6.
57. Spahn, P. N. *et al.* (2017) 'PinAPL-Py: A comprehensive web-application for the analysis

of CRISPR/Cas9 screens', *Scientific Reports*. Springer US, 7(1), pp. 1–8. doi: 10.1038/s41598-017-16193-9.

58. Steensma, D. P. *et al.* (2005) 'The JAK2 V617F activating tyrosine kinase mutation is an infrequent event in both "atypical" myeloproliferative disorders and myelodysplastic syndromes', *Blood*. doi: 10.1182/blood-2005-03-1183.
59. Stein, B. L., Crispino, J. D. and Moliterno, A. R. (2011) 'Janus kinase inhibitors: An update on the progress and promise of targeted therapy in the myeloproliferative neoplasms', *Current Opinion in Oncology*. doi: 10.1097/CCO.0b013e32834d1b22.
60. Tefferi, A. (2010) 'Novel mutations and their functional and clinical relevance in myeloproliferative neoplasms: JAK2, MPL, TET2, ASXL1, CBL, IDH and IKZF1', *Leukemia*. doi: 10.1038/leu.2010.69.
61. Tefferi, A. and Vardiman, J. W. (2008) 'Classification and diagnosis of myeloproliferative neoplasms: The 2008 World Health Organization criteria and point-of-care diagnostic algorithms', *Leukemia*. doi: 10.1038/sj.leu.2404955.
62. Tutuncuoglu, B. and Krogan, N. J. (2019) 'Mapping genetic interactions in cancer: A road to rational combination therapies', *Genome Medicine*. doi: 10.1186/s13073-019-0680-4.
63. Uras, I. Z. *et al.* (2019) 'CDK6 coordinates JAK2V617F mutant MPN via NF-kB and apoptotic networks', *Blood*. doi: 10.1182/blood-2018-08-872648.
64. Vannucchi, A. M. *et al.* (2011) 'Inhibitors of PI3K/Akt and/or mTOR Inhibit the Growth of Cells of Myeloproliferative Neoplasms and Synergize with JAK2 Inhibitor and Interferon', *Blood*. doi: 10.1182/blood.v118.21.3835.3835.
65. Wang, T. *et al.* (2020) 'Systematic mapping of cancer cell target dependencies using high-throughput drug screening in triple-negative breast cancer', *Computational and Structural Biotechnology Journal*. doi: 10.1016/j.csbj.2020.11.001.
66. Wang, W. A. *et al.* (2017) 'Loss of Calreticulin Uncovers a Critical Role for Calcium in Regulating Cellular Lipid Homeostasis', *Scientific Reports*. doi: 10.1038/s41598-017-05734-x.
67. Zhao, W. *et al.* (2013) 'The Role Of p53 In JAK2V617F-Induced Myeloproliferative Neoplasms', *Blood*. doi: 10.1182/blood.v122.21.4103.4103.
68. Zhou, Y. *et al.* (2014) 'High-throughput screening of a CRISPR/Cas9 library for functional genomics in human cells', *Nature*. doi: 10.1038/nature13166.

APPENDIX

1) Mageck Analysis of top 50 early synthetic lethal genes in mutCALR heterozygous cell line at Day 7

Gene ID	Z-Score	Adj.P value	Rank
Calr	7.7548e-06	3.4721e-05	1
Gm3336	2.1659e-05	8.5964e-05	2
Dio3	2.5114e-05	0.00010033	3
Klk7	3.073e-05	0.0001214	4
Gm20877	3.1153e-05	0.00012284	5
Adipor2	5.374e-05	0.00019659	6
Arrdc2	6.5034e-05	0.00022964	7
Zfhx3	7.1476e-05	0.00025406	8
Plrg1	7.534e-05	0.0002713	9
Slc12a5	7.6211e-05	0.00027322	10
Scmh1	7.8561e-05	0.00028232	11
Hrh2	7.9451e-05	0.00028471	12
Serinc3	0.00011952	0.00043461	13
Ltv1	0.00012556	0.00045951	14
Rfxank	0.00014738	0.0005529	15
Zfp872	0.00016157	0.00061564	16
Zfp367	0.00016265	0.00061755	17
Osbpl2	0.00017579	0.0006688	18
Zswim5	0.00018095	0.00069226	19
Olfr706	0.00018119	0.00069274	20
Tnfrsf8	0.00018471	0.00070472	21
Ttc28	0.00019941	0.00075596	22
Gga2	0.00021938	0.00083498	23
Hapln3	0.00022528	0.00085845	24
Rasa3	0.00022601	0.00086036	25
Sele	0.00023594	0.0008982	26
Prrt2	0.0002435	0.00092645	27
Plekha5	0.00026512	0.0010098	28
Snap47	0.00027622	0.0010462	29
Rgs2	0.00027896	0.0010538	30
Npffr2	0.00028119	0.0010601	31

Olfr3	0.00029079	0.0010945	32
Defb25	0.00029339	0.0011046	33
Erich4	0.00032027	0.0011942	34
Med23	0.00032644	0.00122	35
Tmem28	0.0003355	0.0012444	36
Aurkaip1	0.00036396	0.0013359	37
Vmn2r83	0.00037666	0.0013805	38
Zfp58	0.00042687	0.001551	39
Spdl1	0.0004344	0.0015782	40
Apcs	0.00045203	0.0016424	41
Pla2g2d	0.00047708	0.0017411	42
Fcgr1	0.00049923	0.0018148	43
Slc25a2	0.00050556	0.001833	44
Edn2	0.00052729	0.0019092	45
Onecut2	0.00055586	0.0019973	46
Ccdc55	0.0005775	0.0020797	47
Gm5592	0.0006277	0.0022482	48
Arcn1	0.00063266	0.0022684	49
Hs6st1	0.00064734	0.002323	50

2) Mageck Analysis of top 50 early synthetic lethal genes in mutCALR homozygous cell line at Day 7

Gene ID	Z-Score	Adj. Pvalue	Rank
Hrh2	5.1046e-06	2.0354e-05	1
Prrt2	6.2792e-06	2.5143e-05	2
Gm3336	1.4634e-05	5.9624e-05	3
Dio3	2.5114e-05	9.8416e-05	4
Acacb	4.2778e-05	0.00015301	5
Arrdc2	4.388e-05	0.00015684	6
Tmem28	4.6662e-05	0.00016929	7
Aurkaip1	5.4049e-05	0.00019755	8
Osbpl2	7.534e-05	0.00027178	9
Rgs2	9.3084e-05	0.00033931	10
Apcs	0.00010019	0.00036517	11
Fam26d	0.00010908	0.00039773	12

Plrg1	0.00012556	0.00046143	13
Slc12a5	0.00014114	0.00051794	14
Olfr706	0.00015008	0.00055386	15
Zfhx3	0.00015833	0.00058451	16
Chrm4	0.00017579	0.00064677	17
Clps	0.00019736	0.00072291	18
Med23	0.00022601	0.00082253	19
Zswim5	0.00023399	0.00085078	20
Spdl1	0.00025311	0.00092502	21
Rasa3	0.00027622	0.0010014	22
Arcn1	0.00028492	0.0010289	23
Klk7	0.00029863	0.0010821	24
Gm20877	0.00031513	0.0011362	25
Tnfrsf8	0.00032006	0.0011487	26
Ccdc117	0.00032522	0.0011669	27
Utp11l	0.00032644	0.0011717	28
Trpc7	0.00034272	0.0012325	29
Onecut2	0.00035933	0.0012919	30
Wdr77	0.00037666	0.0013498	31
Calr	0.00038503	0.0013824	32
Setd6	0.00039295	0.0014063	33
Defb25	0.00039477	0.0014097	34
Taldo1	0.00040861	0.0014624	35
Tomm20l	0.00041209	0.0014743	36
Snap47	0.00042687	0.0015299	37
Adamts5	0.00044637	0.0015921	38
Zfhx2	0.00044823	0.0016003	39
Itln1	0.0004568	0.0016309	40
Rasal1	0.00045751	0.0016333	41
Vmn2r31	0.00046804	0.0016759	42
Atg16l1	0.00047708	0.0017147	43
Lgr4	0.0004782	0.0017186	44
Gart	0.00048256	0.0017353	45
Slc25a2	0.00048571	0.0017497	46
Cdk17	0.00049049	0.0017655	47
Sele	0.00049059	0.001766	48

Olfr1290	0.00049734	0.0017866	49
Scgb1c1	0.00049899	0.0017914	50

3) Mageck Analysis of top 50 late synthetic lethal genes in mutCALR heterozygous cell line at Day 21

Gene ID	Z-Score	Adj. Pvalue	Rank
Spdl1	1.9733e-06	7.4231e-06	1
Calr	4.5012e-06	1.7001e-05	3
Lrr1	9.9226e-06	3.7116e-05	4
Gart	1.2211e-05	4.4299e-05	5
Cdc37	1.2385e-05	4.4778e-05	6
Alg1	1.4869e-05	5.5793e-05	7
Ptpn2	1.5054e-05	5.6751e-05	8
Ireb2	1.7246e-05	6.2977e-05	9
Ccdc86	1.8866e-05	7.1118e-05	10
Ppat	2.1375e-05	7.6386e-05	11
Sh2b3	2.4026e-05	8.357e-05	12
Ctc1	2.5114e-05	8.8359e-05	13
Pmvk	2.9368e-05	0.00010321	14
Skp2	3.073e-05	0.00010704	15
Polr1c	3.0941e-05	0.00010799	16
Gm10471	3.1758e-05	0.00010895	17
Med10	3.2804e-05	0.0001123	18
Arcn1	3.9407e-05	0.00012955	19
Canx	4.1077e-05	0.0001329	20
Tomm20	5.2521e-05	0.00017648	21
Hnrnpl	5.3143e-05	0.00017887	22
Trpm7	5.4658e-05	0.00018558	23
Hus1	5.6046e-05	0.00018797	24
Prpf3	5.8179e-05	0.00019516	25
Zc3h18	6.1657e-05	0.00020857	26
Hist1h2bn	6.4411e-05	0.00021766	27
Ddx42	7.093e-05	0.00024065	28
Rpl23	7.534e-05	0.00025885	29
Cul3	7.9614e-05	0.00027705	30

Eif1ad	8.2751e-05	0.00028519	31
Ccdc55	8.4197e-05	0.00029142	32
Olfr1148	8.4442e-05	0.0002919	33
Gm21319	8.7543e-05	0.00030123	34
Haus2	9.2494e-05	0.00031824	35
Anapc2	9.5561e-05	0.00033212	36
Pnn	9.9081e-05	0.00034218	37
Polr3b	0.00010025	0.00034505	38
Ppan	0.00010025	0.00034505	39
Kdsr	0.00011517	0.00039534	40
Zcchc9	0.0001158	0.00039582	41
Uggt1	0.00011692	0.00040013	42
Peo1	0.00011752	0.00040252	43
Cars2	0.00012322	0.0004236	44
Wdr77	0.00012556	0.00043365	45
Rps24	0.00012954	0.00044467	46
Oip5	0.00012976	0.00044563	47
Nsl1	0.00014234	0.000494	48
Rpl7l1	0.00015067	0.00052848	49
Spc24	0.00015373	0.00053997	50

4) Mageck Analysis of top 50 late synthetic lethal genes in mutCALR homozygous cell line at Day 21

Gene ID	Z-Score	Adj. Pvalue	Rank
Spdl1	2.0878e-06	6.4653e-06	1
Cpne9	1.2596e-05	4.2862e-05	2
Cox6c	1.5014e-05	5.5314e-05	3
Utp11l	2.5114e-05	8.5964e-05	4
Tex16	2.7388e-05	9.1711e-05	5
Skp2	3.2804e-05	0.00011039	6
Ddah1	5.0999e-05	0.00017025	7
Pet2	6.8406e-05	0.00023203	8
Pom121	7.534e-05	0.00025981	9
Nprl2	9.3954e-05	0.0003326	10
Rnf181	9.8672e-05	0.00035463	11

Rhbdf1	0.00012556	0.00045568	12
Trpm7	0.00013401	0.00048921	13
Puf60	0.00014701	0.00053422	14
Diexf	0.00015451	0.000562	15
Nadk	0.0001621	0.00059169	16
Mfap1a	0.00017579	0.00064629	17
Zc3h18	0.00018207	0.00066736	18
Wbscr22	0.00019822	0.00072483	19
Lrr1	0.00020691	0.00075452	20
Alg1	0.00021043	0.00076841	21
Polr1c	0.00022028	0.0008005	22
Arl4a	0.00022601	0.0008254	23
Gfpt1	0.00022851	0.00083881	24
Arcn1	0.00023128	0.00085174	25
Cdh9	0.00027622	0.0010222	26
Uchl3	0.0002788	0.0010323	27
Btbd9	0.00028265	0.0010428	28
Acacb	0.00028801	0.0010653	29
Pdik1l	0.00030711	0.0011305	30
Rad21	0.00031572	0.0011626	31
Lrrc47	0.00032316	0.0011879	33
4933402N03Rik	0.00032413	0.0011908	34
Wbscr16	0.00032644	0.0012004	35
Zwilch	0.00032773	0.0012057	36
Ercc2	0.00033636	0.001233	37
Gm10471	0.00033997	0.0012483	38
Cux1	0.00035438	0.001301	39
Ccdc116	0.00037143	0.0013503	40
Mslnl	0.00037666	0.0013694	41
Lsm5	0.0003778	0.0013738	42
2010107E04Rik	0.00039798	0.0014465	43
Hrh2	0.00040573	0.0014705	44
Clec4a1	0.00041969	0.0015193	45
Csgalnact1	0.00042687	0.0015457	46
Zfp40	0.00046066	0.0016621	47
Entpd7	0.0004682	0.0016898	48

Eif5	0.00047542	0.001719	49
Olfr733	0.00047708	0.0017272	50

5) Mageck Analysis of top 25 genes enriched in mutCALR heterozygous cell line at Day 21

Gene ID	Z-Score	Adj. Pvalue	Rank
Med25	5.4623e-11	2.3946e-07	1
Pten	6.0773e-10	2.3946e-07	2
Hif1a	8.5395e-10	2.3946e-07	3
Arnt	1.3132e-08	2.3946e-07	4
Gsk3b	1.7465e-08	2.3946e-07	5
Tsc1	2.4912e-08	2.3946e-07	6
Rbpj	3.4562e-08	2.3946e-07	7
Shoc2	4.1296e-08	2.3946e-07	8
Arid2	2.5897e-07	2.3946e-07	9
Nprl2	2.7731e-07	2.3946e-07	10
Gata1	1.336e-06	1.6762e-06	11
Tsc2	3.6108e-06	1.1254e-05	12
Nprl3	4.1228e-06	1.1733e-05	13
Tal1	5.42e-06	1.4607e-05	14
Gskip	7.1071e-06	2.179e-05	15
Plac1	1.8952e-05	7.0639e-05	16
Foxo3	2.1008e-05	7.6865e-05	17
Mslnl	2.5114e-05	9.1711e-05	18
Depdc5	3.0282e-05	0.00010895	19
4930430A15Rik	3.7876e-05	0.00013002	20
Acat2	5.2559e-05	0.0001827	21
Tbc1d24	5.4049e-05	0.00018701	22
Wscd1	6.2206e-05	0.00021335	23
Rhbdf1	7.534e-05	0.00025741	24
Mapk1	7.8855e-05	0.0002713	25

6) Mageck Analysis of top 60 genes enriched in mutCALR homozygous cell line at Day 21

Gene ID	Z-Score	Adj.P value	Rank
Pten	4.4381e-17	2.3946e-07	1
Tsc1	1.0512e-14	2.3946e-07	2
Tsc2	3.5222e-14	2.3946e-07	3
Depdc5	4.4128e-14	2.3946e-07	4
Nprl2	9.7495e-14	2.3946e-07	5
Gsk3b	1.3756e-13	2.3946e-07	6
Gata1	3.5566e-13	2.3946e-07	7
Arnt	5.8007e-13	2.3946e-07	8
Nfe2	9.9314e-13	2.3946e-07	9
Hif1a	1.5252e-12	2.3946e-07	10
Gata2	2.6388e-12	2.3946e-07	11
Shoc2	4.1259e-12	2.3946e-07	12
Med25	4.2733e-12	2.3946e-07	13
Nprl3	2.9765e-10	2.3946e-07	14
Foxo3	5.2665e-10	2.3946e-07	15
Gapvd1	8.304e-10	2.3946e-07	16
Etv5	2.1376e-09	2.3946e-07	17
Supt20	4.1322e-09	2.3946e-07	18
Arid2	4.9062e-09	2.3946e-07	19
Tal1	6.4796e-09	2.3946e-07	20
Rbpj	7.1105e-09	2.3946e-07	21
Tada1	2.5515e-08	2.3946e-07	22
Crebbp	4.4322e-08	2.3946e-07	23
Tbc1d24	4.4939e-08	2.3946e-07	24
Tada2b	7.2679e-08	7.1837e-07	25
Supt7l	9.8044e-08	7.1837e-07	26
D930015E06Rik	7.732e-07	3.5918e-06	27
Ndrg1	8.187e-07	4.0707e-06	28
Junb	9.0828e-07	4.0707e-06	29
Hhex	1.1007e-06	5.0286e-06	30
Usp9x	1.2778e-06	5.5075e-06	31
Sh2b3	1.5119e-06	5.9864e-06	32
Tmem131	1.5556e-06	5.9864e-06	33
Tbc1d7	1.6437e-06	5.9864e-06	34
Edem2	1.7331e-06	6.4653e-06	35

Trp53	2.2372e-06	9.3387e-06	36
Ankfy1	3.3508e-06	1.5086e-05	37
Klf7	3.4044e-06	1.5086e-05	38
Ddit4	3.4722e-06	1.5086e-05	39
Gskip	4.8307e-06	1.8438e-05	40
Zfp296	5.1379e-06	1.9875e-05	41
Fosl2	5.5271e-06	2.1312e-05	42
Mafg	5.6772e-06	2.179e-05	43
Gmcl1	5.6959e-06	2.179e-05	44
Xpnpep1	6.0443e-06	2.3227e-05	45
Men1	6.5718e-06	2.5143e-05	46
Plekha2	6.9674e-06	2.6101e-05	47
Nudcd2	1.1599e-05	4.9088e-05	48
Zmynd19	1.18e-05	5.0046e-05	49
Pdcd10	1.5808e-05	6.8724e-05	50
Pfkl	1.7333e-05	7.3513e-05	51
Plac1	1.7405e-05	7.3513e-05	52
Cbl	2.4135e-05	9.5064e-05	53
Kras	2.7766e-05	0.00010991	54
Cyp4a29	3.9815e-05	0.00014391	55
Taf5l	4.586e-05	0.00016546	56
Kat2a	5.1812e-05	0.00018223	57
Tdg	5.69e-05	0.00019803	58
Bcl7b	6.6892e-05	0.00022868	59
Usp34	7.2658e-05	0.00025047	60

7) Dose-response results for mTOR inhibitors

S.No	Drug Name	Fold Change IC50 (nM)
1	Lonafarnib	957
2	AZD8055	8
3	CC-223	81
4	INK-128	6
5	SAR245	3
6	AZD2014	64

7	Rapamycin	850
8	Torin	300

SUPPLEMENTARY INFORMATION

Competitive bone marrow transplantation

Total bone marrow cells from vavCre mice (F1 CD45.1/CD45.2 - 1.8 million cells) and CALRdel52 mice (CD45.2 - 0.2 million cells) were mixed and 2 million cells from the mix were injected intravenously (tail vein) into recipient mice (CD45.1) that were lethally irradiated (2x – 5.5 Grey) a day before (as depicted in Figure 2A). To directly compete LSK cells, total bone marrow total bone marrow cells from vavCre mice (F1 CD45.1/CD45.2) and CALRdel52 mice (CD45.2) were mixed such that the ratio of the wildtype to LSK cells was 80:20. 2 million cells from the mix were injected intravenously (tail vein) into recipient mice (CD45.1) that were lethally irradiated (2x – 5.5 Grey) a day before (as depicted in Figure 2E).

Flow cytometry

Single cell suspension of cells was pelleted (300 g, 5 minutes) and resuspended in FACS buffer (PBS, 1% FCS). The cells were stained with appropriate antibodies and fixed in 1% PFA. Acquisition of samples was performed on LSRFortessa™ (BD). Analysis was performed using FlowJo™ software (BD). The antibodies and compensation particle sets used for FACS are listed in supplementary table 2. To detect mutCALR on the cell surface the cells were stained with anti-mutCALR antibody (Dianova) followed by staining with a secondary antibody – anti-mouse IgG2a-HRP (Southern Biotech).

Western blot

Western blotting was performed using standard protocols. The antibodies used for western blotting are listed in supplementary table 3. Clarity™ Western ECL Blotting Substrates (Bio-Rad, #1705061) was used for the chemiluminescence detection method.

RNA-sequencing

Total bone marrow cells were isolated from vavCre and CALRdel52$^{fl/fl}$;vavCre (mutCALR^{Hom}) mice. Lineage negative cells were depleted using the Easy Sep Mouse Progenitor Isolation kit. The isolated/deleted cells were stained for lineage negative, Sca-1 and c-kit markers. 1200 LSK cells per each mice/group were sorted into the lysis buffer using FACSAria (BD). Full length mRNA sequencing was performed as previously described in Picelli *et al*. (Picelli *et al.*, 2014). The data was processed with an established RNA-seq analysis pipeline from Bioconductor packages, including DeSeq2.

Histology

Mouse tissue samples were fixed in 4% paraformaldehyde (PFA) overnight at 4°C and embedded in paraffin after dehydration in ascending concentrations of ethanol. For histological

analysis, 2-4 µm-thick paraffin sections were prepared and stained with hematoxylin and eosin. Reticulin staining was performed with the Polysciences Reticulin Stain Kit (No. 25094).

Statistics

All graphs were made using the software Graphpad Prism™. The values represent Mean±SEM. Significance was calculated using two-way anova test, unless otherwise specified. The statistical significance of the blood parameters of the cohort were calculated using multiple t-test. * - $p < 0.05$, ** - $p < 0.01$, *** - $p < 0.005$ and **** - $p < 0.001$.

SUPPLEMENTARY FIGURES

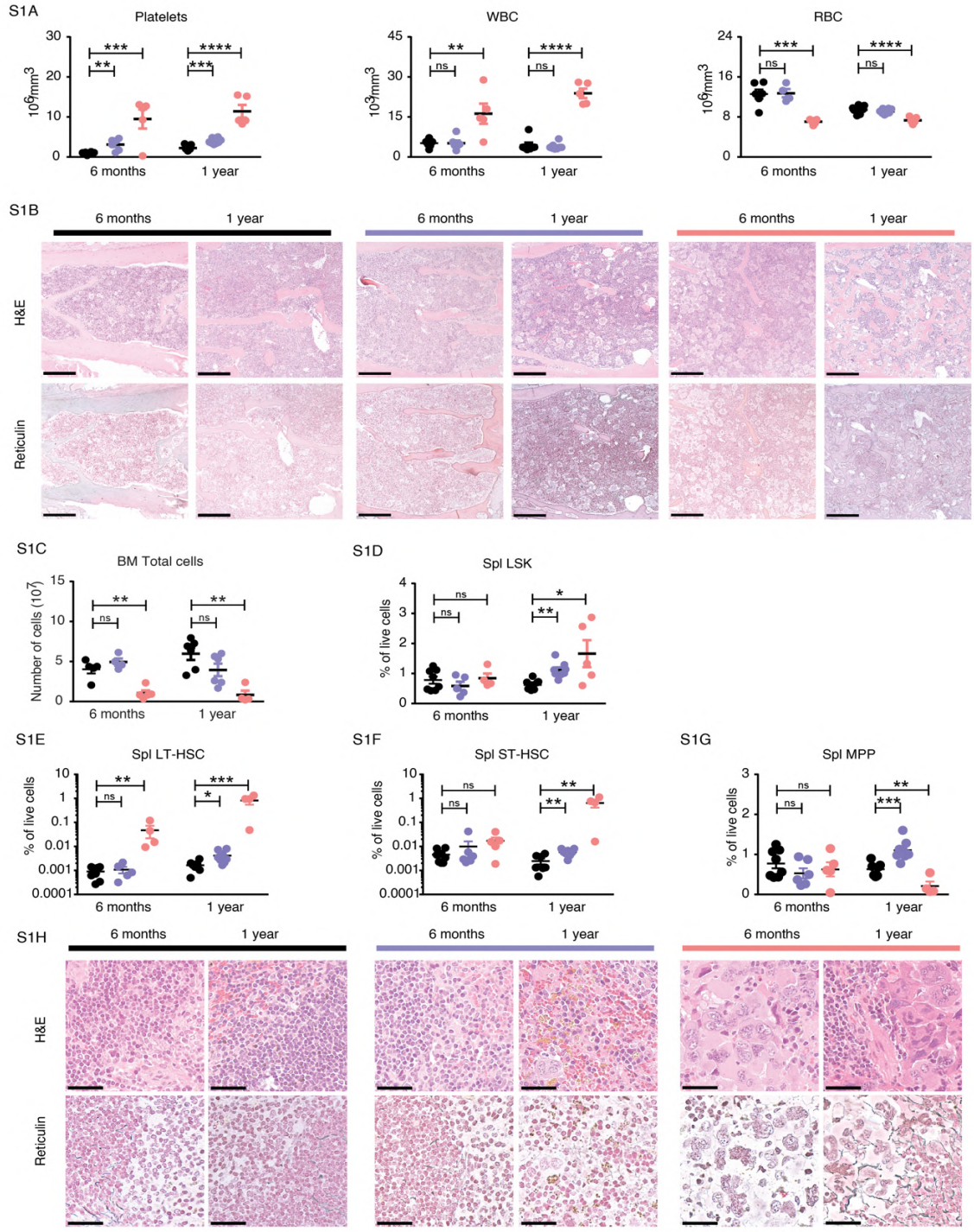

Supplementary Figure 1

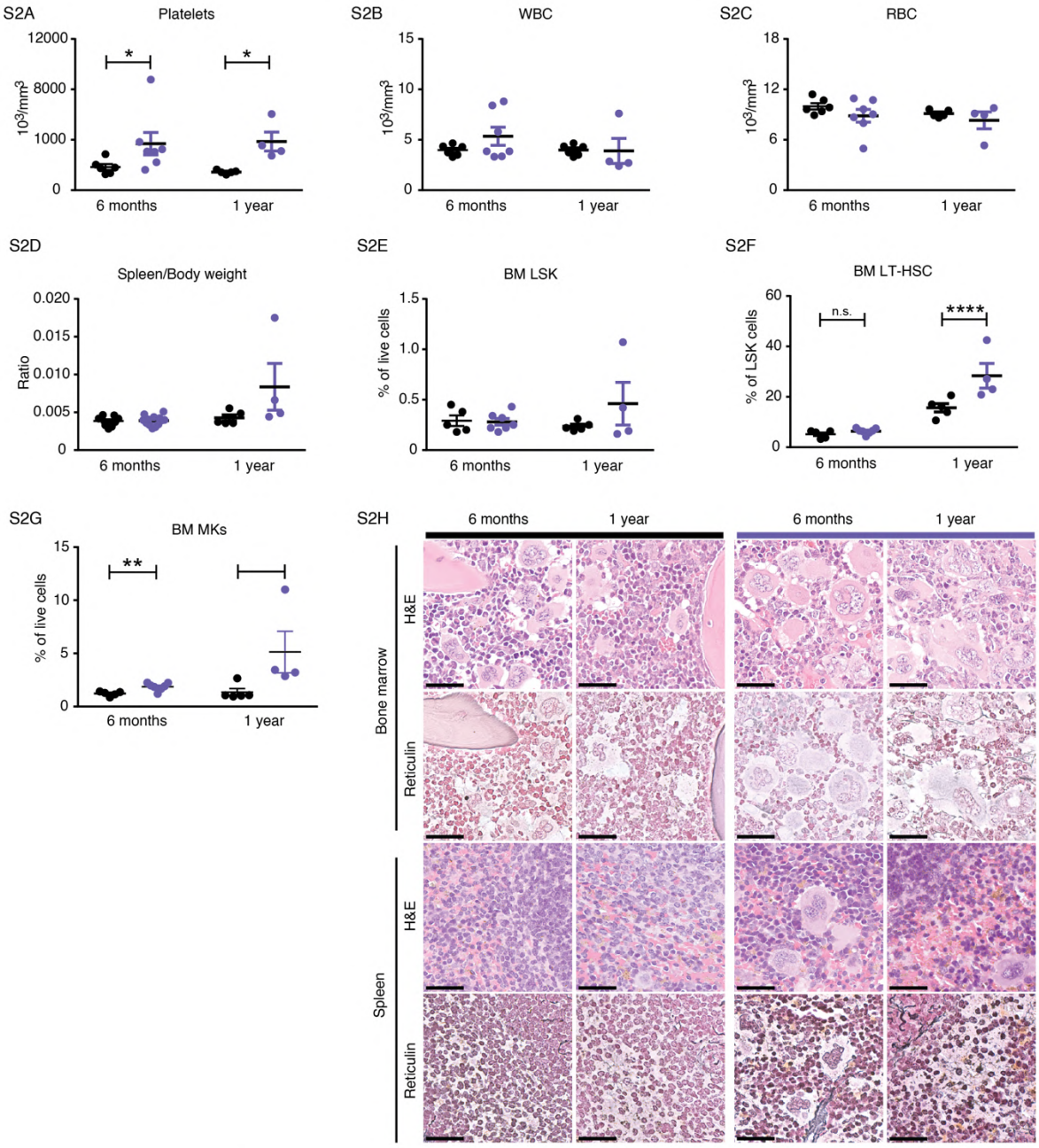

Supplementary Figure 2

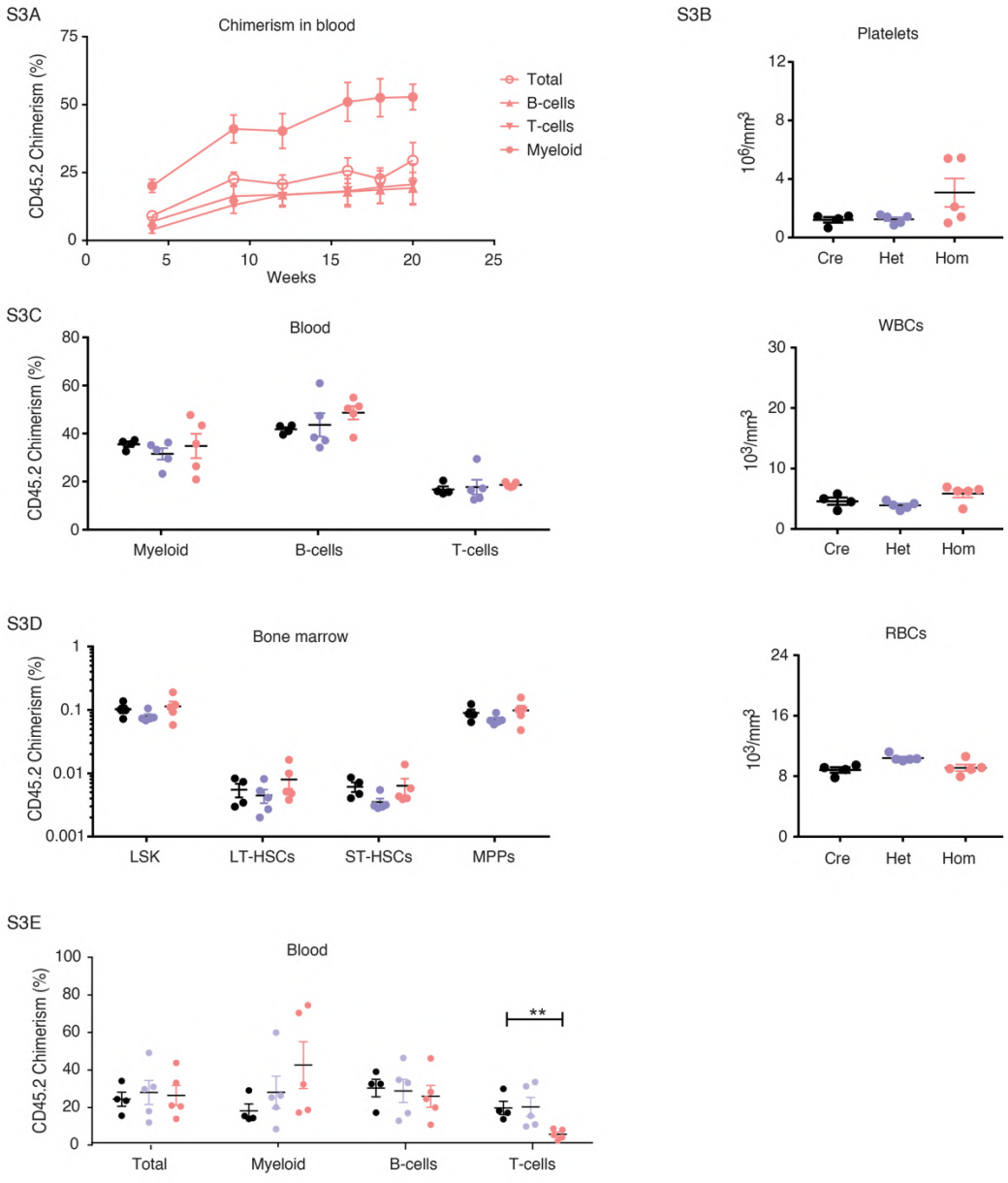

Supplementary Figure 3

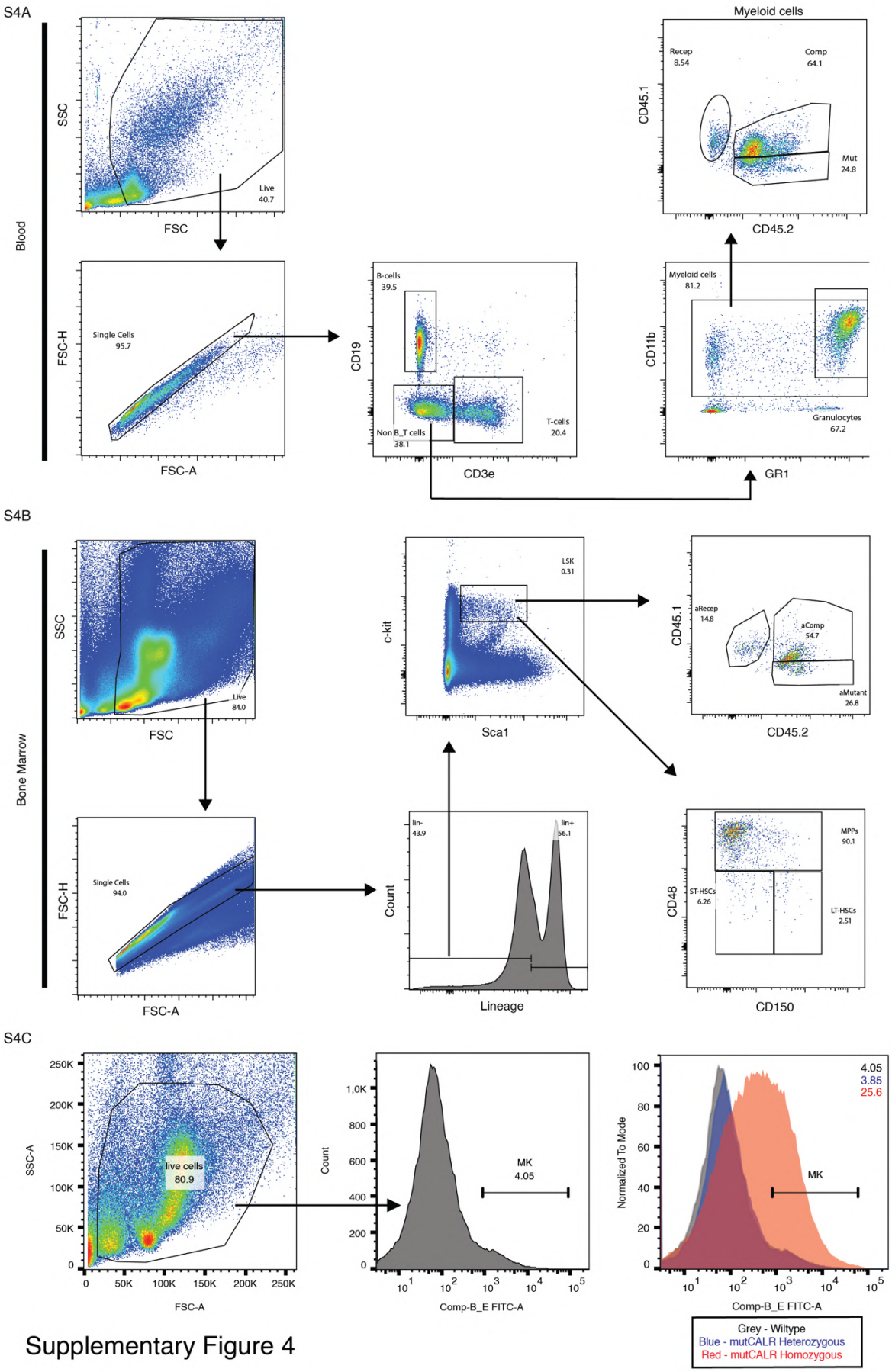

Supplementary Figure 4

S5A

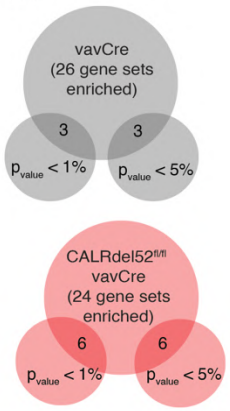

S5B

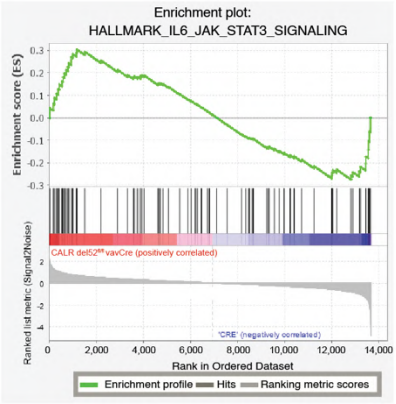

Supplementary Figure 5

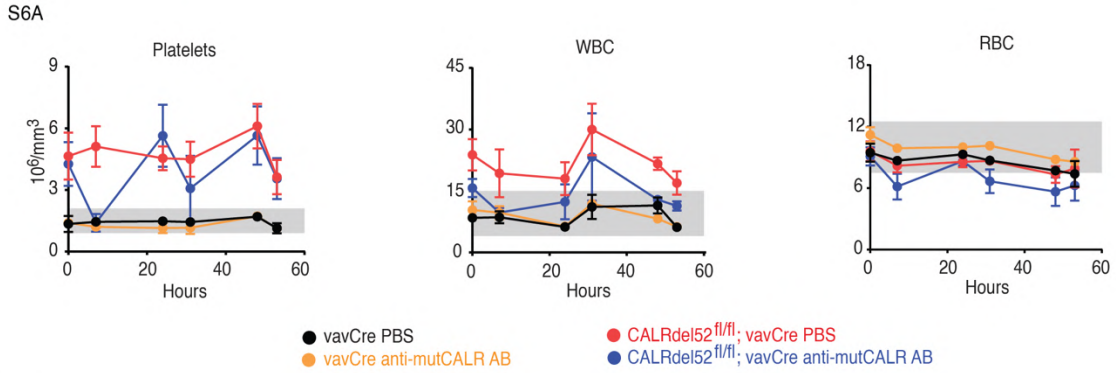

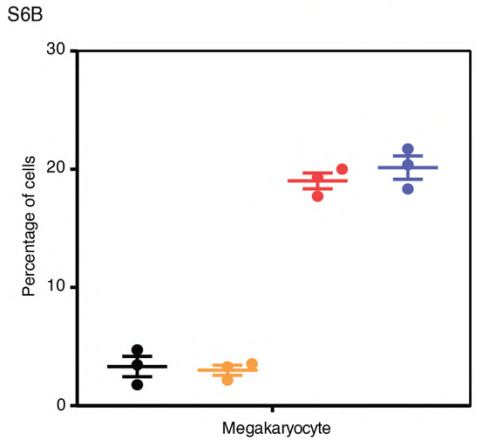

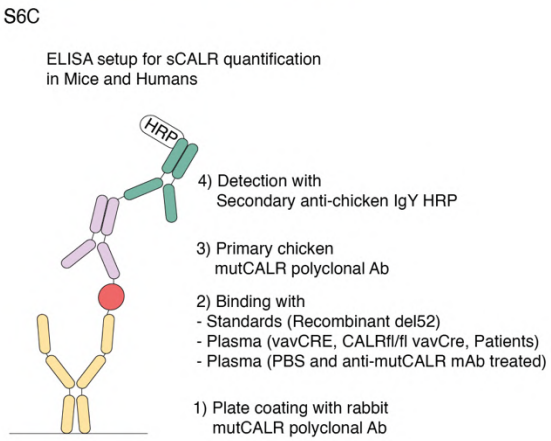

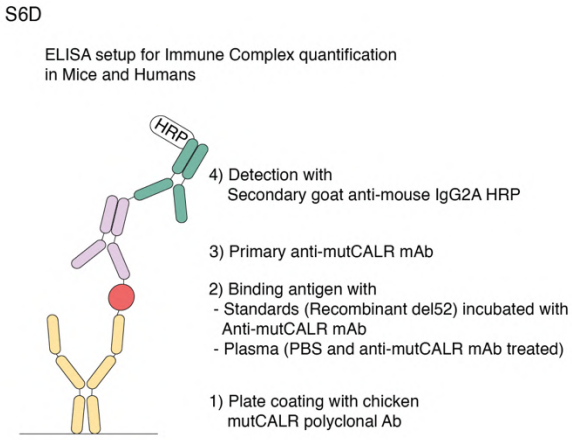

Supplementary Figure 6

SUPPLEMENTARY FIGURE LEGENDS

Supplementary Figure 1: Level of Platelets, WBC and RBC in wild type (black), mutCALR^{het} (blue) and mutCALR^{hom} (red) mice at 6 months and 1 year of age (A). (B) Histopathological analysis of the sternum at 6 months and 1 year of age, by H&E and reticulin staining. Black bar corresponds to 200 μm. Total bone marrow cells in transgenic mice at 6 months and 1 year of age (C). Percentage of different populations in the spleen of transgenic mice LSK cells (D), LT-HSCs (E), ST-HSCs (F) and MPPs (G). (H) Histopathological analyses of spleens of transgenic mice at 6 months and 1 year of age, by H&E and reticulin staining. Black bar corresponds to 50 μm.

Supplementary Figure 2: Peripheral blood values of Platelets (A), WBC (B) and RBC (C) at 6 months and 1 year of age, in wildtype (black) and germline heterozygous (purple) mice. (D) Spleen to body weight ratio at 6 months and 1 year of age. Percentage of LSK cells (E), LT-HSCs (F) and megakaryocytes (G) in the bone marrow. (H) Histopathological analysis of the sternum and spleen. Black bar corresponds to 50 μm.

Supplementary Figure 3: (A) Percentage of mutCALR^{hom} cells in different lineages in peripheral blood post-transplant. (B) Peripheral blood values of platelets, WBC and RBC at end point of competitive bone marrow transplant. Percentage of different lineages in peripheral blood (C) and bone marrow (D). (E) Percentage of CD45.2 mutant cells in different lineages in peripheral blood.

Supplementary Figure 4: Gating strategies for congenic mouse model: (A) Blood: Live cells were gated based on the forward and sideward scatter and doublets were excluded from the analysis. B-cell (CD19) and T-cell (CD3e) gates were defined. CD19^{-} and CD3e^{-} double negative cells were analysed for the expression of CD11b (myeloid cells) and GR1 (granulocytes). All the gated lineage populations were assessed for the expression of CD45.1 and CD45.2 to define the cells from recipient, competing and mutant mice. (B) Bone marrow: Live cells were gated based on the forward and sideward scatter and doublets were excluded from the analysis. Lineage negative cells (lineage antibody cocktail) were gated and analysed for the expression of Sca1 and c-kit to define LSK cells. The LSK cells were further categorized into LT-HSCs, ST-HSCs and MPPs based on the expression of CD150 and CD48. All the gated lineage populations were assessed for the expression of CD45.1 and CD45.2 to define the cells from recipient, competing and mutant mice. (C) Gating strategy used to define megakaryocytes by CD41 staining.

Supplementary Figure 5: (A) Number of gene sets identified by the GSEA analysis. (B) Enrichment plot for the IL6-JAK-STAT signalling pathway.

Supplementary Figure 6: (A) Peripheral blood values of Platelets, WBC and RBC and (B) Percentage of megakaryocytes in mutCALR^{hom} mice upon treatment with anti-mutCALR mAb. Schematic representation of the ELISA set up for (C) quantification of soluble CALR (sCALR) in the murine and human plasma, and (D) detection of immunecomplexes in mice treated with mAb.

SUPPLEMENTARY TABLES

1) Antibodies used:

S.No	Antibody	Company	Product number
FACS	CD16/CD32 (FcRg) Fc block	eBioscience	14-0161-86
FACS	Anti-rat compensation particles set	BD Biosciences	552844
FACS	Anti-rat anti-hamster comp. particles set	BD Biosciences	552845
FACS	Anti-mouse comp	BD Biosciences	552843
FACS	CD11b FITC	eBioscience	11-0112-42
FACS	Sca-1 FITC	eBioscience	11-5981-85
FACS	CD41 FITC	eBioscience	11-0411-85
FACS	CD42d PCPeF710	eBioscience	46-0421-82
FACS	CD41 PE	Thermo Fisher	12-0411-83
FACS	CD49b PE	eBioscience	12-5971-83
FACS	CD48 PE	eBioscience	12-0481-82
FACS	CD71 PE	BioLegend	113807
FACS	CD45.1 PE	Invitrogen	12-0453-82
FACS	CD3e PerCP Cy5.5	eBioscience	45-0031-82
FACS	Lin-Biotin cocktail	Invitrogen	88-7774-75
FACS	Streptavidin-PerCP Cy5.5	eBioscience	45-4317-82
FACS	CD34 Alexa Fluor 647	BioLegend	128606
FACS	TER119 APC antibody	eBioscience	17-5921-83
FACS	Gr1 APC antibody	eBioscience	17-9668-82
FACS	CD45.1 APC antibody	BD Biosciences	561873
FACS	c-kit APC H7 antibody	BD Biosciences	560185
FACS	CD45.1 eF780 antibody	eBioscience	47-0453-82
FACS	CD19 PE Cy7 antibody	eBioscience	25-0193-83
FACS	CD150 PE Cy7 antibody	eBioscience	25-1502-82
FACS	CD16/CD32 (FcRg) PE Cy7	eBioscience	25-0161-82
FACS	CD45.2 eF450	Invitrogen	4344415
WB	Calregulin Antibody	Santa Cruz Biotech	#F-4

WB	Anti-HSC70	Santa Cruz Biotech	#B-6
WB, ELISA	Anti-mutCALR (rabbit polyclonal, SAT601)	MyeloPro	
ELISA	Anti-mutCALR (IgY)	MyeloPro	
ELISA	Anti-chicken IgY-HRP	Abcam	Ab6877
ELISA	Anti-mouse IgG2a-HRP	Southern Biotech	0103-05
ELISA, *in vivo*	Anti-mutCALR (mouse monoclonal)	Dianova	DIA-CAL-100

2) Primers used for genotyping mice:

Primer	Supplier	Sequence
Calr del52 - primer F	Sigma	GGGAATAGAGGCCTGTCCAGAGCC
Calr del52 - primer R	Sigma	AGGGTGTTCAGGCCTCAGTCCA
vavCre - primer F	Sigma	TCAGAGTGAAGGACATCTCCCGCACC
vavCre - primer R	Sigma	GTGGCAGAAGGGGCAGCCACACCATT

Sarada Achyutuni

Predoctoral Fellow at CeMM

Vienna, Austria | +4366565249608 | sarada.achyutuni@gmail.com | linkedin.com/in/sarada-achyutuni/ | twitter.com/SaradaAchyutuni

EDUCATION

Medical University of Vienna, Austria — Aug 2017 - Present

Doctor of Philosophy (PhD) in Molecular Signal Transduction

- *PhD Dissertation : Mutant calreticulin driven MPN (Myeloproliferative neoplasms) targeted therapies*
- *Intended graduation date : August/September 2021*
- *Clubs/Activities:*
  a) Member, Scientific Graphic Design Club, CeMM – collaborated with 9 fellow enthusiasts and developed key scientific graphics and illustrations for over 10+ important institute and advisory board meetings.
  b) Member, Social Media Working Group, CeMM - work collaboratively with 12 diverse research groups to implement communication strategies for better outreach online and on social media platforms.

Birla Institute of Technology and Science, Pilani, Rajasthan, India — July 2014 - May 2016

Master of Engineering (M.E) in Biotechnology

- *Master's Project : Role of lncRNAs (Long non-coding RNAs) in epithelial to mesenchymal transition associated to hepatocellular carcinoma*
- *Graduated with CGPA of 8.51/10 in First Class Honors*
- *Scholarships:*
  a) BITS Institute 50% Fee Waiver Scholarship awardedamong 16 applicants
  b) GATE Scholarship Recipient

National Institute of Technology - Warangal, Telangana, India — July 2010 - May 2014

Bachelor of Technology (B.Tech) in Biotechnology

- *Bachelor's Dissertation : Study of β-catenin WNT signaling pathway in different cellular systems*
- *Graduated with CGPA of 8.32/10 in First Class with Distinction*
- *Clubs/Activities:*
  a) General Secretary, Amateur Radio & Robotics Club 2013, NITW - Collaborated with club panel members and provided an over-all direction for the club events
  b) Event Manager, Technozion 2012, NITW - Led a team of 25 volunteers, organized and managed the FoxHunt event for technical fest at the University

WORK EXPERIENCE

Predoctoral Fellow at CeMM - Center for Molecular Medicine, Vienna, Austria — Aug 2017 - April 2021

Principal Investigator : Robert Kralovics ; Post-Doc Supervisor : Harini Nivarthi

- *Established a genome-wide CRISPR-Cas9 Screen in murine cell lines to identify synthetic lethal interactions and tumor suppressor genes that regulate Mutant CALR (MutCALR) driven MPN regulatory networks.*
- *Implementation and assessment of immunotherapeutic pipelines for pre-clinical testing of monoclonal antibodies in vivo in a transgenic murine model against mutCALR driven MPN in a private partnership with Myelopro Diagnostics and Research.*
- *Establishment of an RNA-sequencing pipeline for profiling murine hematopoietic stem cells from the bone marrow to analyze the transcriptome and differentially expressed genes.*
- *DOE for cell-based assays to identify and probe potential gene interactions and drug-based interactions.*
- *Attended 10+ Workshops and presented talks in 30+ scientific meetings, 2+ institute recess & to Nobel laureates in scientific advisory board meeting in CeMM 2019*

Junior Research Fellow at Rajiv Gandhi Center for Biotechnology (RGCB), India — Jan 2016 - May 2017

Principal Investigator : Dr. Priya Srinivas

- *Managed, designed, and validated experiments to analyze the role of DNA damage in the progression of BRCA1 defective breast cancer*
- *Characterized the association and co-expression of Ezrin with BRCA1 in GTD cell lines using proximity ligation assays and immunohistochemistry.*
- *Validated and quantified the expression of ERM proteins in GTD progression.*
- *Performed data analytics to create a comprehensive pipeline to understand the key role of genes and miRNA transcribed from Chromosome 17 in cancer.*

Graduate Teaching Assistant at Birla Institute of Technology & Science, India — Mar 2014 - Dec 2015

Project Management

- *Demonstrated effective leadership by managing and training all new undergraduate students and researchers.*
- *Designed and organized study material for coursework and laboratory lectures.*
- *Catalogued and managed the undergraduate grading system portal for assignments and examinations.*

PUBLICATIONS

1. "Hematopoietic expression of a chimeric murine-human CALR oncoprotein allows the assessment of anti-CALR antibody immunotherapies in vivo" - American Journal of Hematology, 2021
2. "Gene expression signatures: A tool for analysis of breast cancer prognosis and therapy"- Critical Reviews of Oncology, 2020
3. "BRCA1 promoter hypermethylation in human placenta: a hidden link with β-hCG expression" - Carcinogenesis, 2020
4. "The prodigious network of chromosome 17 miRNAs regulating cancer genes that influence the hallmarks of cancer" - Seminars in Oncology, 2017

LICENSES & CERTIFICATIONS

Data Analytics and Visualization Tools - *Certified by IBM*
Drug Development and Product Management Specialization - *University of San Diego*
Design and Interpretation of Clinical Trials - *John Hopkins University*
Project Management and Other Tools for Career Development -*University of California, Irvine*
Climate Reality Leader - *Trained by Al Gore, Climate Reality Leadership Corps*
Certified Amateur Radio Operator - *Ministry of Communications, India*

TECHNICAL SKILLS

Pooled CRISPR-Cas9 genetic screens and knockout cell line generation, Library Preparation, RNA-sequencing & Transcriptome Analysis, Immunoassays, Phagocytosis Assays, ELISA's, NK cell assays (ADCC) and Complement Assays (CDC), PBMC isolation and Magnetic bead separation of Immune Cells, Bacterial and Mammalian expression systems, Lentivirus & Retrovirus Production, Florescence Activated Cell Sorting (FACS), Fluorescence & Confocal Microscopy, Proximity ligation assays (PLA), Bioreactor & UV-Vis Spectrophotometer Operation, Isolation of DNA, RNA, protein & lncRNA, Cloning & Animal Cell culture Techniques, MTT Assay, Caspase Assay, Cell titer-Glo, LDH Assay, SDS-PAGE, Western Blotting, 2D-PAGE, Real Time PCR, RT-PCR, Conventional PCR, HPLC, LC-MS, FELESA B certification

OTHER SKILLS

Scientific Publications and Communication - *https://orcid.org/0000-0002-0907-3308*
Photography - https://500px.com/saradaachyutuni
IT - *MS Office, Graphpad Prism, Adobe Photoshop & Illustrator, Mini-tab, AutoCAD*
Languages - English (Native), Hindi (Native), Telugu (Native) & German (Elementary)

REFERENCES

- **Robert Kralovics,** PhD Supervisor, Medical University of Vienna. Email : rkralovics@cemm.at
- **Harini Nivarthi,** Post-doc PhD Supervisor, CeMM – Research Center for Molecular Medicine. Email : niv.hari@gmail.com
- **Stefan Kubicek,** PhD Co-Supervisor, CeMM – Research Center for Molecular Medicine. Email : skubicek@cemm.at
- **Priya Srinivas,** Master's Thesis & JRF Supervisor, Rajiv Gandhi Center for Biotechnology. Email : priyasrinivas@rgcb.res.in

PUBLICATIONS

1) Achyutuni, S. *et al.* (2017) 'The prodigious network of chromosome 17 miRNAs regulating cancer genes that influence the hallmarks of cancer', *Seminars in Oncology*. doi: 10.1053/j.seminoncol.2017.11.001.
2) Nivarthi, H. *et al.* (2019) 'PS1436 IFN-A TREATMENT NORMALIZES THE PLATELET COUNTS AND REDUCES QUIESCENT STEM CELLS IN A CALR-DEL52 TRANSGENIC MOUSE MODEL, IN VIVO', *HemaSphere*. doi: 10.1097/01.hs9.0000564020.51112.fa.
3) Nadhan, R. *et al.* (2020) 'BRCA1 promoter hypermethylation in human placenta: A hidden link with β-hCG expression', *Carcinogenesis*. doi: 10.1093/carcin/bgz117.
4) Latha, N. R. *et al.* (2020) 'Gene expression signatures: A tool for analysis of breast cancer prognosis and therapy', *Critical Reviews in Oncology/Hematology*. doi: 10.1016/j.critrevonc.2020.102964.
5) Achyutuni, S. *et al.* (2021) ' Hematopoietic expression of a chimeric murine-human CALR oncoprotein allows the assessment of anti-CALR antibody immunotherapies in vivo ', *American Journal of Hematology*. doi: 10.1002/ajh.26171.